3-22-2018

The Study and Application of Carbon Nanotube Film Heaters for Space Applications

Christopher C. Rocker

THE STUDY AND APPLICATION OF CARBON NANOTUBE FILM HEATERS FOR SPACE APPLICATIONS

THESIS

Christopher C. Rocker, Captain, USAF

AFIT-ENY-MS-18-M-290

DEPARTMENT OF THE AIR FORCE
AIR UNIVERSITY

AIR FORCE INSTITUTE OF TECHNOLOGY

Wright-Patterson Air Force Base, Ohio

AFIT-ENY-MS-18-M-290

THE STUDY AND APPLICATION OF CARBON NANOTUBE FILM HEATERS FOR SPACE APPLICATIONS

THESIS

Presented to the Faculty

Department of Aeronautical and Astronautical Engineering

Graduate School of Engineering and Management

Air Force Institute of Technology

Air University

Air Education and Training Command

in Partial Fulfillment of the Requirements for the

Degree of Master of Science in Astronautical Engineering

Christopher C. Rocker, B.S.M.E.

Captain, USAF

March 9, 2018

AFIT-ENY-MS-18-M-290

THE STUDY AND APPLICATION OF CARBON NANOTUBE FILM HEATERS FOR SPACE APPLICATIONS

Christopher C. Rocker, B.S.M.E.
Captain, USAF

Committee Membership:

Major Ryan P.O'Hara, PhD
Chair

Dr. Bradley Ayres, PhD
Member

Dr. Anthony Palazotto, PhD
Member

Abstract

The purpose of this research was to examine the feasibility of using Carbon Nanotube (CNT) sheets as thin film heaters for space applications. The ability to maintain the temperature of space components has a direct impact on a space vehicle's operation and longevity. Currently etched foil heaters are used to heat satellite batteries. Battery heaters are the focus of this research. However, as this study will show, they have limitations and are susceptible to failure. CNT sheets have many beneficial properties and show potential in replacing the etched foil design. In this study test specimens were created by forming laminate test articles comprised of CNT sheets and an adhesive Kapton® substrate material. These test articles were subjected to a series of tests both in atmosphere and in vacuum. Comparative tests were done on etched foil heaters and specimens made from a new polyimide material from Dupont™. As a secondary study, the effects of CNT grain orientation on heat generation capability was included. It was found that while the CNT articles were not as power efficient as the etched foil design, in the configurations tested, they offered a much higher maximum temperature, a faster response time (how fast the specimens heated up), and mitigated the potential for total heater failure. With respect to the grain orientation study, it was found that using commercial off the shelf (COTS) CNT sheets resulted in no significant change in thermal properties for specimens of the size used in these tests. In conclusion, CNT thin film heaters proved to be a viable alternative to current battery heater technology.

Acknowledgments

I would like to thank my thesis advisor, Major Ryan O'Hara, for all his guidance, support, insight, and most importantly his patience. I would, also, like to thank the amazing staff here at AFIT; contractors, instructors, and military alike. Without all their hard work this research would not have been possible. I would like give special recognition to Jorge Urena for his help in last minute and late night component fabrication and software coding aid.

I would like to thank my parents for their support through this challenging time. Their confidence in me and support never wavered.

Thank you

Christopher C. Rocker

Contents

Page

Page

List of Figures

Figure Page

Figure Page

Figure Page

List of Tables

List of Acronyms

AFIT Air Force Institute of Technology

CNT Carbon Nanotube

CVD Chemical Vapor Deposition

DWCNT Double-walled Carbon Nanotube

GNR Graphene Nanoribbon

IR Infrared

LEO Low Earth Orbit

$LiFePo_4$ Lithium-Iron Phosphate

LiPo Lithium-Ion-Polymer

MWCNT Multi-walled Carbon Nanotube

MWIR Mid-wave Infrared

NiCd Nickel-Cadmium

NiH_2 Nickel-Hydrogen

PTFE Polytetrafluoroethylene

PWM Pulse Width Modulation

SWCNT Single-walled Carbon Nanotube

UV Ultra-Violet

List of Symbols

µ	micro (10^{-6})
Ω	Ohms
A	Amps
C	Temperature in Celsius
I	Current in Amps
P	Power in Watts
R	Resistance in Ohms
$Torr$	Pressure in millimeters of Mercury (mmHg)
V	Voltage in Volts
W	Watts

THE STUDY AND APPLICATION OF CARBON NANOTUBE FILM HEATERS FOR SPACE APPLICATIONS

I. Introduction

1.1 Background

Satellites, especially small satellites (CubeSats, MicroSats, etc.), require heating of critical components for the purpose of preventing damage or excessive wear, improving fuel efficiency, or improving operating speed of on-board processors. Battery packs, optics, and thrusters are a few examples of this. Batteries, in particular, are of great concern for satellite designers as their best operating temperatures are between 0°C-20°C [2] and are prone to rupture if their charging cycle begins below 0°C.

Whilst satellites are in view of the Sun, maintaining minimum temperatures is not particularly difficult. However, when the satellite is in the shadow of the Earth, occluding the Suns energy, components can become cold-soaked and therefore less efficient and/or ill-prepared for pending use. Current satellites use etched foil heaters or cartridge heaters to mitigate these problems [8]. Carbon Nanotube (CNT) film heaters are the next generation solution to this problem and should replace these antiquated methods.

1.2 Problem

While effective, etched foil heaters have their limitations and flaws such as inefficient power consumption, focused (non-uniform) heating, and the potential for electrical shorts [9]. CNT heaters could mitigate these problems but are currently

not being studied widely for such applications. CNT heater development has been explored for application in commercial industry but little research has been done to date applying the technology to satellites. CubeSats are becoming more widely used within the space industry and the need for reliable, cost effective, and efficient heating solutions is increasing. CubeSats are small satellites comprised of one or more 10cmx10cmx10cm blocks.

1.3 Justification

The purpose of this study is to analyze the thermal properties, limitations, and physical characteristics of carbon based thin film heaters and to develop means of utilizing them for space vehicle applications. If successful, CNT heaters may prove to have lower production costs, higher efficiency, longer operational lives, and more uniform heat distribution compared to traditional heaters. Furthermore, the flexibility of the material will allow for effective heating of space components with more complex geometries.

1.4 Assumptions

Several assumptions were made going into this research. For the purposes of the experiments, it was assumed that the CNT film heaters would be operated in a vacuum to simulate on-orbit conditions. Additionally, the heaters must operate without the need for any type of servicing beyond that which can be provided by software. The potential for damage from micrometeorites or other space debris was not considered.

1.5 Scope

The scope of this research focuses on the thermal properties of Multi-walled Carbon Nanotube (MWCNT) film heaters, product development, and their application on satellite components. Thermal properties to be researched include behavior of the CNT sheet under different loads, thermal response time, and heating distribution. Applications studied include the feasibility of using certain substrates, such as Kapton® MT+, to form flexible film heaters, how those film heaters will receive power (electrical contacts), and how they perform under different current loads. Additionally, this research includes the study and comparison of Dupont's™ polyimide film material, RS100, in similar configurations for the same applications as the CNT film heaters.

1.6 Methodology

To approach this problem, research was conducted into contemporary satellite thermal management designs with emphasis on state-of-the-art patch heaters. A multi-tiered analytical approach was then used to answer questions posed. First, experiments utilizing different methods of power application were conducted to establish a baseline of CNT thermal behavior. The difference between using a single point of contact versus a sheet wide conductive strip to apply power was tested. Uniform distribution of current, and thereby heat generation, was the goal.

Next, a study into usable substrates and experiments with flexible printed circuits was conducted. Incorporating the CNT onto a substrate material with printed circuits allowed for testable specimens to be manufactured. Finally, utilizing what was discovered in the first step and the specimens created in the second step, experiments into various current flow patterns through CNT, with respect to grain orientation, were conducted with the resulting properties captured and recorded. Their recorded

characteristics and respective benefits were then analyzed for potential satellite component heating application and compared to existing thin film heaters.

1.7 Research Questions and Hypotheses

1.7.1 Question 1

How can electrical current be applied to CNT sheet and polyimide conductive films such that uniform heating distribution is accomplished? The hypothesis is that Using copper, or similar, conductors spanning the width of the CNT coupon at each end should produce uniform heating when current is applied. If the conductor is narrower than the CNT sheet or polyimide film, the electrons will not flow uniformly to areas that do not lie between the two conductors.

1.7.2 Question 2

What materials can be used to form flexible heaters using CNT sheets or polyimide conductive films? In the past substrate materials such as Kapton® have been used in the fabrication of patch heaters for their low profile design, low mass, and thermal stability. It is speculated that it will work for thin film materials as well. CNT sheets are very flexible as well, barring creases or folds, they should be applicable to Kapton® to form the desired heater shapes.

1.7.3 Question 3

How does the thermal range of CNT compare to those products that are already on the market? With a lower resistance value, and using the same power source as for etched foil heaters, it is predicted that the top of the thermal range should be much higher for CNT.

1.7.4 Question 4

What are the pros/cons of the CNT thin film heaters over existing heating products? Based the design of the etched foil heaters, CNT sheet heaters should be less susceptible to total failure. Also CNT should be able to heat larger areas, using the available on-board power, than the etched foil heaters.

II. Literature Review

2.1 Chapter Overview

2.1.1 Introduction

The need for research into carbon nanotube film heaters will be presented in this section of the study. This review will cover the importance and problem of satellite thermal control, the current mitigation strategies being employed, types of heaters, current technology being implemented, the highest area of interest for potential heater application, current Carbon Nanotube (CNT) technology and research, and finally the current gap in application research. This review also discusses historical research done in this field.

2.1.2 Driving Requirement

Thermal control of satellite components is of paramount importance in the satellite's design. As such, many approaches to thermal management and control have been explored and utilized in current satellites. As this is an ongoing problem for engineers, newer and better methods to manage this are always under development.

"Satellites perform better and last longer when their components remain within certain temperature limits, usually, but not always, near the level at which they were assembled"[10]. Particular interest is given to those components whose performance and durability is most affected by temperature variations. Many components can have very tight temperature tolerances which, if exceeded, can cause damage or degradation to performance. According to both [10] and [11] these components include overboard dump valves for liquids, structure on space telescopes, gyroscopes and accelerometer guidance platforms, pressure transducers, electronic components, infrared reference sources, windows (condensation), solar panels, hydrazine catalyst beds, and batteries.

Batteries on-orbit provide necessary energy storage for operation while in the eclipse of the earth. A typical Low Earth Orbit (LEO) satellite takes approximately 90 minutes to complete one orbit. During that time, the satellite is in total solar eclipse for roughly 30 minutes. While not able to generate its own power from the solar panels during that time, the satellites on-board components still require power to perform their functions. That power comes from the batteries. Most satellites have used Nickel-Cadmium (NiCd) or Nickel-Hydrogen (NiH_2) rechargeable batteries as they are extensively proven, inexpensive, and lightweight[2]. These types of batteries have low energy densities meaning that their power to volume ratios ($\frac{W}{m^3}$) are not as high as other battery technologies. Newer technologies include Lithium-ion, Lithium-Ion-Polymer (LiPo), and Lithium-Iron Phosphate ($LiFePo_4$) to name a few are an improvement on this technology[1]. These Lithium based batteries offer a much higher energy density than their Nickel based counterparts though they are still susceptible to temperature influences. Studies have shown that the internal temperatures of Lithium based batteries greatly affects their discharge profile as can be seen in Figure 2.1[1]. A study of NiCd shows comparable results where the decrease in battery temperature reduces the available capacity, as can be seen in Figure 2.2, and increases the discharging curve as shown in Figure 2.3[2]. While at room temperature, +20°C, the batteries perform normally, below 0°C a notable decrease in performance is observed.

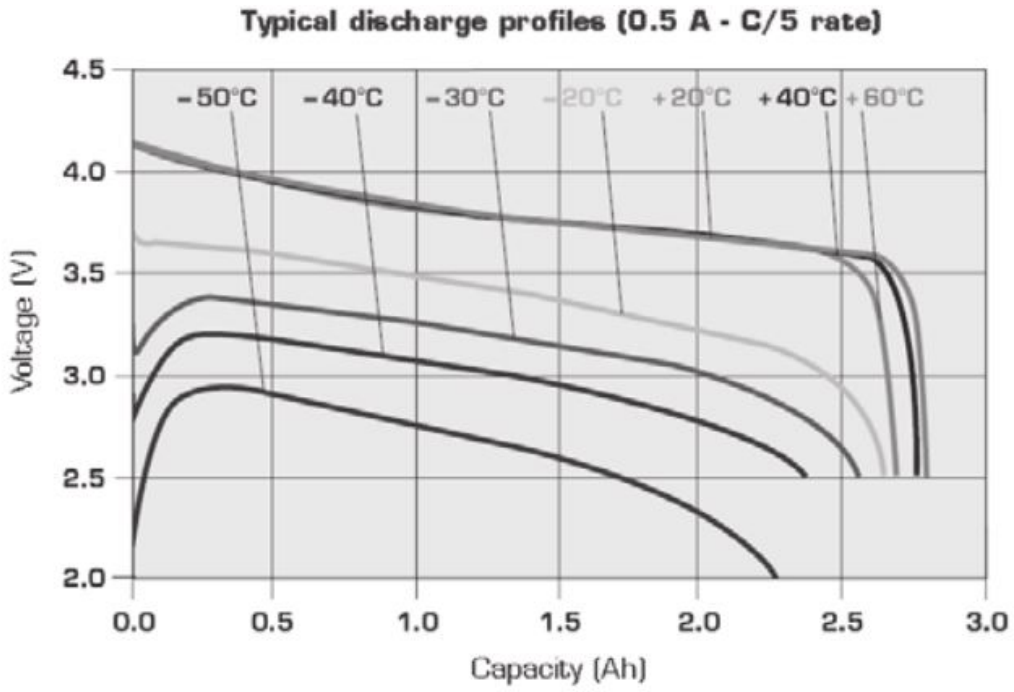

Figure 2.1: Lithium-Ion Capacity versus Temperature [1]

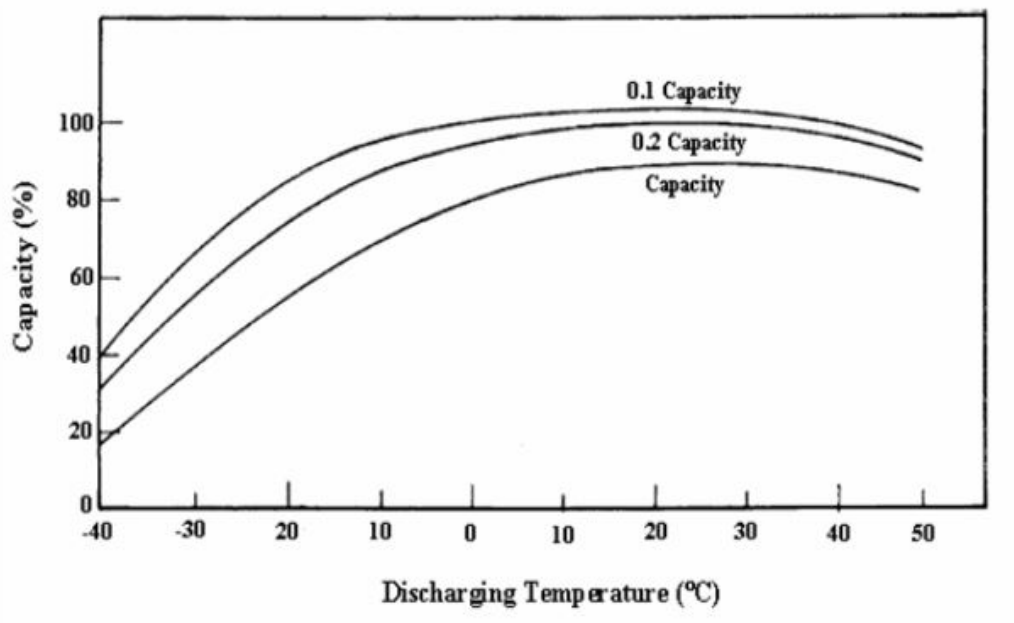

Figure 2.2: Nickel-Cadmium Capacity versus Temperature [2]

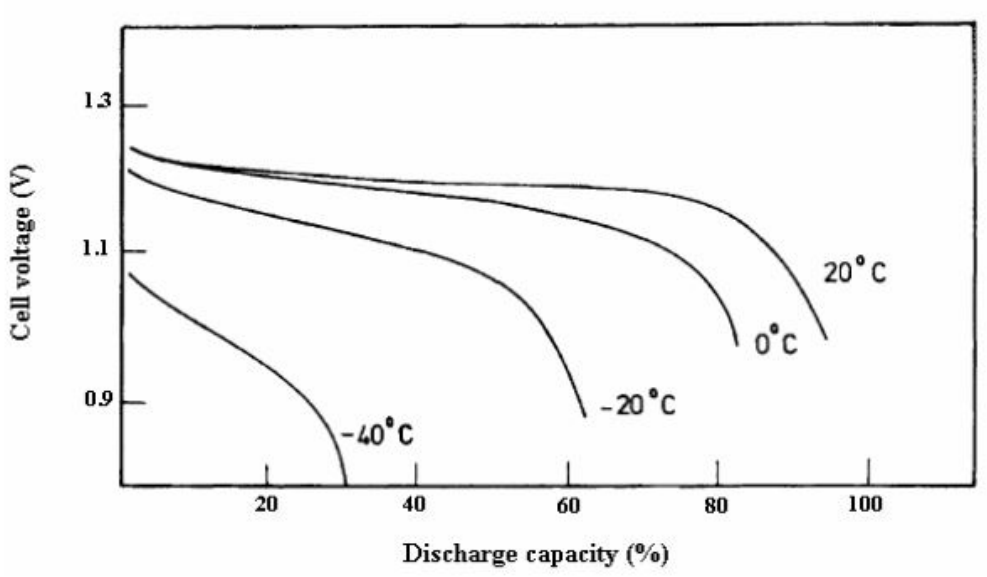

Figure 2.3: Nickel-Cadmium Discharge Curve versus Temperature [2]

Aside from performance, low temperatures present another, more dramatic, risk to the spacecraft. As the temperature lowers, the internal resistance of the battery increases requiring a much greater amount of supplied energy to force the current through[12]. This leads to excessive gassing and loss of electrolytes. For sealed batteries, internal pressure from gassing can exceed the capacity of the relief valve causing the battery to expand and rupture. Different types of batteries have different charging and discharging ranges, however, few are capable of charging below 0°C. The list of recommended charge ranges for the various types of Lithium and Cadmium based batteries is shown in Figure 2.4.

Battery type	Charge temperature	Discharge temperature	Charge advisory
Lead acid	–20°C to 50°C (–4°F to 122°F)	–20°C to 50°C (–4°F to 122°F)	Charge at 0.3C or lessbelow freezing. Lower V-threshold by 3mV/°C when hot.
NiCd, NiMH	0°C to 45°C (32°F to 113°F)	–20°C to 65°C (–4°F to 149°F)	Charge at 0.1C between –18°C and 0°C. Charge at 0.3C between 0°C and 5°C. Charge acceptance at 45°C is 70%. Charge acceptance at 60°C is 45%.
Li-ion	0°C to 45°C (32°F to 113°F)	–20°C to 60°C (–4°F to 140°F)	No charge permitted below freezing. Good charge/discharge performance at higher temperature but shorter life.

Figure 2.4: Recommended temperature charging ranges for various battery types[3]

"...consumer-grade lithium-ion batteries cannot be charged below 0°C (32°F). Although the pack appears to be charging normally, plating of metallic lithium can occur on the anode during a sub-freezing charge. This is permanent and cannot be removed with cycling" [3]. Because of these risks batteries require thermal mitigation. Dissipating excess heat and generating heat when needed will be discussed next.

Methods of thermal mitigation are categorized as passive (environment heating) or active control (dissipation or generation)[13]. Passive control utilizes the sun's energy, or other heavenly body, to either directly or indirectly heat the satellite through the use of surface finishes, reflectors, louvers, and structure. Active control utilizes onboard energy sources to actively generate or dissipate heat. The use of heat sinks and heat pipes to channel heat generated by internal components, such as electronics, to overboard dumps are examples of this. When temperatures drop too low heaters are

used to warm components up to their operating temperature[11].

Satellite heaters come in two main types: electric and radioisotope[11]. Electric heaters can be powered by any source of electrical current such as batteries (chemical energy) or solar panels. Radioisotope power generators utilize the natural decay of radioactive elements, Plutonium-238 for example, to produce heat. These are mainly used on deep space satellites where their distance from the sun makes their collection and use of solar energy impractical.

2.1.3 CubeSat Patch Heater Technology

When it comes to electrical heaters, there are two main types [8, 11]: film (patch) heaters and cartridge heaters. Meseguer[11] tells us that patch heaters are the most commonly used on spacecraft because of their versatility. Patch heaters are very thin, lightweight, and flexible. This allows them to be placed directly on components to which they can apply focused heat. As was discussed in the battery section of the Literature Review, certain spacecraft components require heating of this nature. Being able to control where the heat is applied is a great advantage.

Patch heaters are composed of an electrically resistant conductor, such as etched foil, "sandwiched between two sheets of flexible electrically insulating material, such as Kapton®"[8] allowing the entire heater to remain thin and flexible as shown in Figure 2.5. Patch heaters contain either a single circuit or if redundancy is needed they will contain multiple circuits. Redundancy is often required on spacecraft due to the fact that heater circuits can fail and repair or replacement is often not possible. Another advantage patch heaters offer is their lightweight and low profile design allowing them to be wrapped around the components needing heat without sacrificing space or adding significant mass to the overall spacecraft.

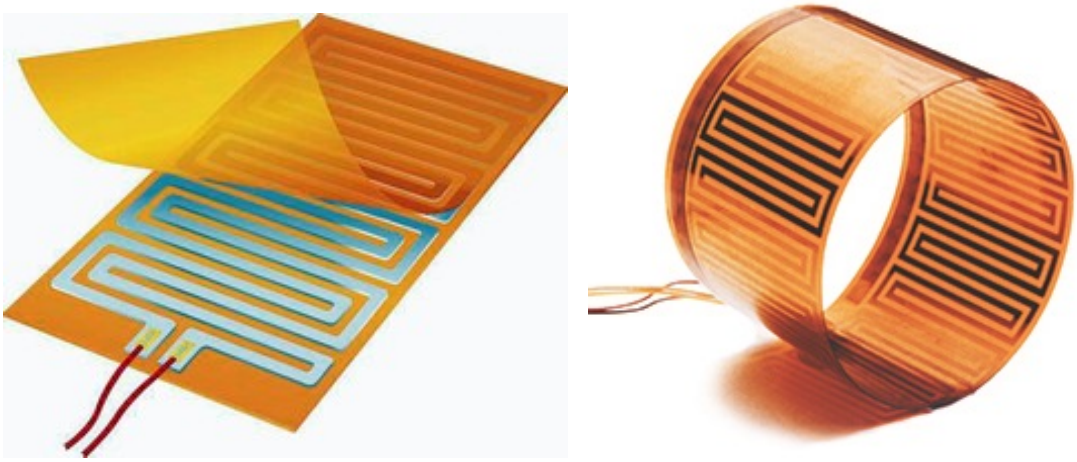

(a) (b)

Figure 2.5: (a) Etched foil heating element between two Kapton® layers [4] (b) Rolled etched foil heater demonstrating flexibility [5]

Etched foil heaters are extensively used and well developed for patch heater application. They are produced for a multitude of commercial uses by companies such as Minco™, Hotwatt™, Tutco™, and BriskHeat™.

2.1.4 Carbon Conductive Polyimide Film

New products by companies such as Dupont™ and Villinger™ that have just recently hit the market show promise as an advancement on the previously mentioned etched foil heater technology. Similar to the premise that is the focus of this thesis, CNT sheet film heaters, these new sheet film heaters use a carbon based electrically conductive layer bonded to a dielectric insulator (polyimide film). This differs from the etched foil heaters by providing a uniform heating surface as opposed to heating 'coils' or lines as can be seen in Figure 2.6 below.

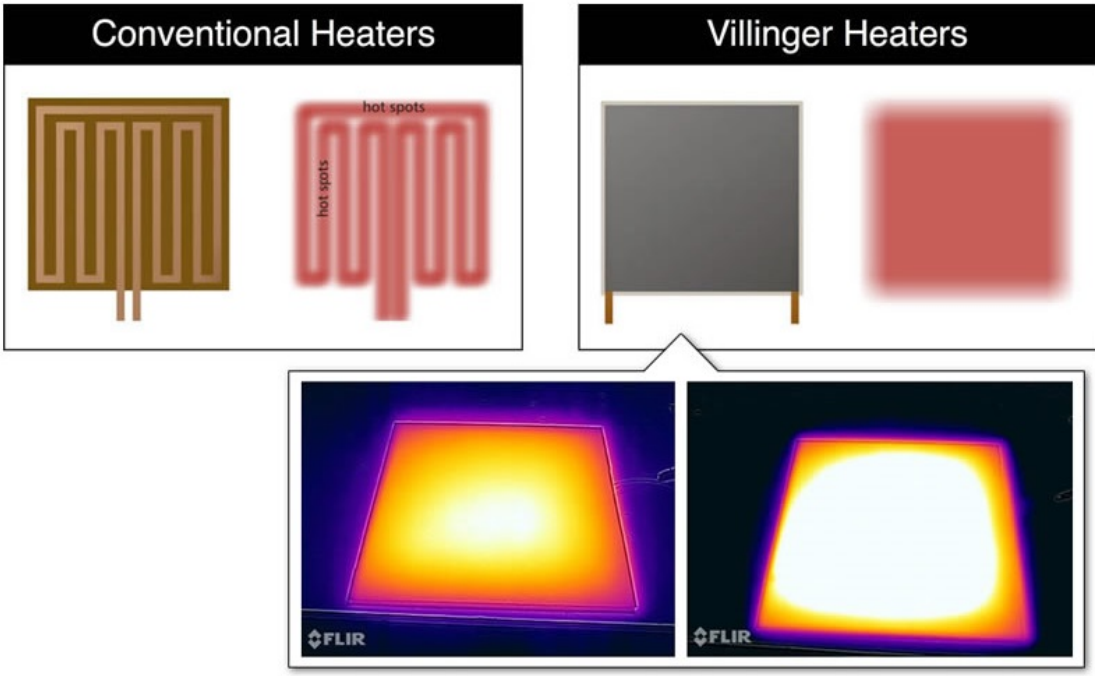

Figure 2.6: Etched foil heaters thermal distribution (upper left) vs Sheet film heaters heating distribution (upper right) [6]

While etched foil heaters are well characterized and widely used, sheet film heaters are a relatively new concept. Dupont^{TM} RS100 sheet film heaters, as well as others, may eventually replace foil heaters as the preferred method as mentioned before. Though the new line of products by Dupont^{TM} and Villinger^{TM} shows promise, it is currently unclear what they are made of and whether or not CNT sheet heaters, the focus of this thesis, are an improvement over them. What is known is that these new materials still maintain the benefits of low weight, high flexibility, and thin profile that are the main advantages of etched foil heaters. Additional benefits of these new thin film heaters are their resistance to radiation and extreme temperatures, high efficiency, durability, and versatility[14]. Currently the product is being marketed for such applications as surface deicing, interior heating for automobiles, aerospace temperature regulation, industrial tube heating, composite curing, wearables (clothing),

and consumer appliances[14]. Throughout the provided literature the application of these film heaters to space hardware was not mentioned specifically, however, a remark that the material has a thermal durability up to 325°C in oxygen-free environments is suggestive. Further research into spacecraft application is required before these can replace etched foil heaters as the preferred method of heat generation. One thing that can be speculated on is that, while the etched foil heaters have only one or two heating 'coils', thin film heater's entire surface is a heating 'coil' and therefore less susceptible to a single point failure. A single break in an etched foil heater would lead to complete heater failure. In this respect, thin film heaters are more desirable for use on critical satellite components such as battery packs.

2.1.5 CNT

Carbon nanotubes were discovered in the early 1990's and have been widely studied for their exceptionally high strength to weight ratio and electrical conduction properties. Only recently has their use as a thin film heater been explored.

As the name implies, a carbon nanotube is a very small tube made out of carbon atoms generally between 0.7 to 50 nm in diameter and 10's of microns in length[15]. Single-walled Carbon Nanotube (SWCNT) consist of a single atomic layer of carbon-carbon bonds arranged in a hexagonal patterned sheet called graphene, shown in Figure 2.7, which is then rolled into a cylindrical tube[7]. The graphene sheets can be rolled in several different orientations with respect to their structure; the most common being zigzag and armchair. The direction in which they are rolled is called their circumferential vector ($\overrightarrow{C}$) and it is a result of its chiral. Being chiral means that the edges of the graphene pattern are not mirror images of one another and therefore can mate together. An example of this would be the Ying-Yang symbol. In Figure 2.7, when a CNT has a Zig-Zag end, it will have a Armchair Graphene Nanoribbon

(GNR). The opposite is true for the Armchair CNT. A GNR is the name of the edge that will actually mate together with the other end to enclose the tube.

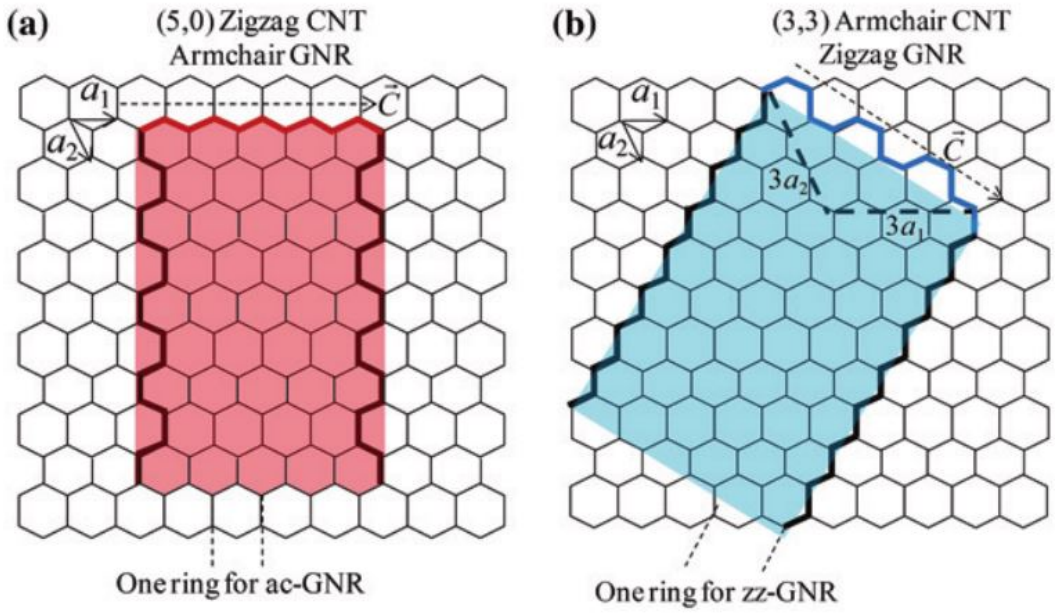

Figure 2.7: a) Zig-Zag CNT with an Armchair GNR b) Armchair CNT with a Zig-Zag GNR[7]

Double-walled Carbon Nanotube (DWCNT) and Multi-walled Carbon Nanotube (MWCNT) are an arrangement of two or more concentric SWCNT as shown in Figure 2.8.

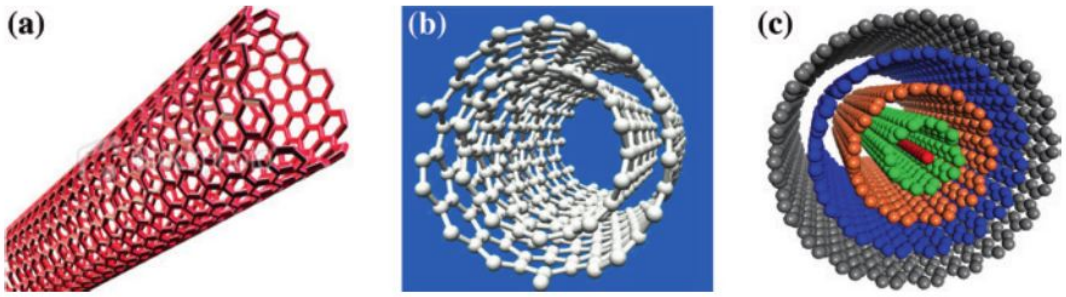

Figure 2.8: a) SWCNT b) DWCNT c) MWCNT [7]

Of particular note is the process of how CNTs are formed and layered into sheets. MWCNTs are often formed through a method called Chemical Vapor Deposition (CVD)[16]. The sheets that were used for this study from Nanocomp Technologies, Inc were produced using this process. The CNTs sheets are composed of synthetic nano-fibers that were layered onto a translating drum and made into a non-woven textile mat [17]. Work done at the Air Force Institute of Technology (AFIT) showed that during this process, the CNTs go from random orientations, similar to a bowl of spaghetti, to having a net alignment in the feed direction of the translating drum as can be seen in Figure 2.9[17].

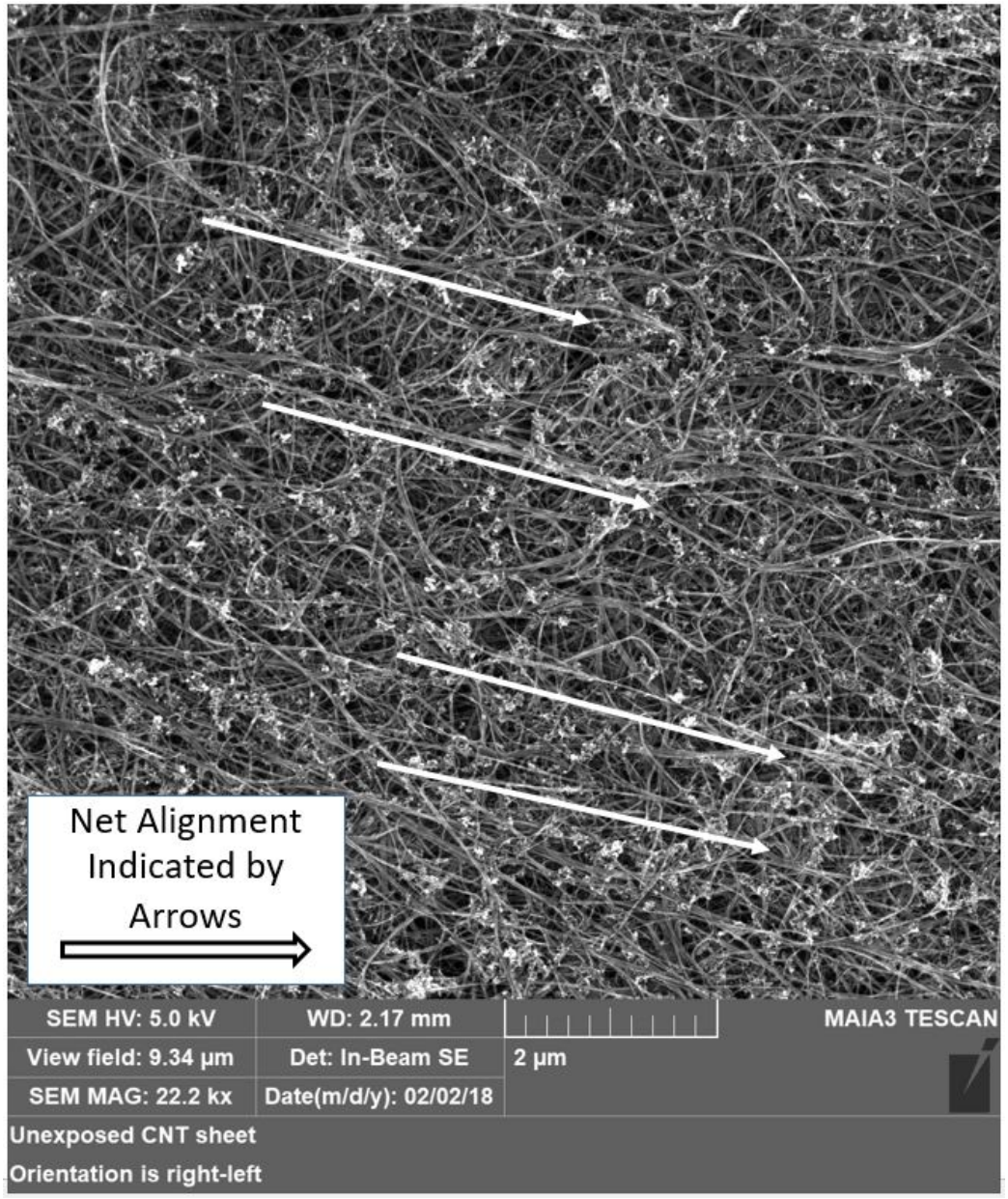

Figure 2.9: Net alignment of the CNT grain as a result of the CVD process

When CNT sheets have a net grain alignment, passing current perpendicular to it yields resistance values several times higher than if the current were passed along the direction of net alignment[9]. This is thought to be due to the increased number of electrical junctions the current has to pass through[9]. This will be of particular

interest during testing outlined later in this document.

While the structures of CNTs are well known, a significant gap in the literature exists pertaining to the their thermal conduction properties. What is known is that CNTs conduct heat by means of coupled vibrations of their carbon atoms with adjacent material. This is known as phonon transport[18]. Though this phenomenon is at a level of study above what this thesis will cover, it will briefly be covered to demonstrate the difference between current methods of heat generation and the new thin film heaters. This phenomenon means that the thermal capabilities of CNT sheets are not dependent on their cross sectional area as is the case with crystalline materials. Crystalline materials, such as metals, conduct heat through movement of electrons causing inelastic collisions. As the cross sectional area of a crystalline material decreases so does its thermal capabilities. Studies have shown that CNT sheets thermal properties are a factor of their temperature[18]. As the temperature of a CNT goes up it transitions from being a diffusive conductor to a ballistic conductor. This transition point is a factor of the individual CNTs length. As the length of each individual CNT in a sheet cannot be controlled during production, the thermal properties of CNT sheets cannot be accurately predicted. Slight variations will occur between theoretical and experimental results as temperature is increased. Despite being difficult to predict, the phonon transport and dispersion properties of a CNT make it capable of very high thermal conductivities even with very small cross sectional areas. The Dupont^{TM} product also behaves as a non-crystalline structure, however, unlike the CNT sheets the materials thermal capabilities are not a factor of its temperature[14].

The phenomenon where phonons and electons generate heat through inelastic collisions is known as Joule heating. CNTs, whose primary means of conduction is through the coupled vibrations of carbon atoms, has led to the coining of a new

term; "Remote Joule Heating"[19]. The author who coined this term, Kamal Baloch, describes this method reminiscent of microwave heating where a high frequency, high energy wave is passed through a substance to excite the water molecules within to generate heat. With CNTs, this energy is passed by means of the coupling of phonons between the CNTs and their neighboring material (substrate). This allows the energy passing through the CNT to be transferred to the paired material directly causing the substrate to heat up while the CNT material remains relatively cool. Experiments conducted determined that approximately 84% of the energy passing through CNTs is transferred directly into the substrate material as opposed to being first absorbed by the CNT structure[19].

2.1.6 Conclusion

The purpose of this literature review was to investigate the need for heaters on board a spacecraft; identify existing heater types being used; characterize the benefits and limitations of each type; and present current theory and existing data on CNTs for possible future use as heaters.

Throughout this literature review, very little was found suggesting that CNT sheet film heaters are being developed on any scale for use on satellites. There is, however, clearly much consideration for the commercial application of etched foil heaters and even some for sheet film heaters. The benefits of the later are promising as is evident by the Kapton® RS film being marketed by Dupont™. Comparative research into CNT sheet film heaters has either not yet been conducted or not widely publicized.

Through this research the application of CNT space heaters will be considered and compared to these existing technologies.

III. Research Methodology

3.1 Chapter Overview

Based on the current research, what is needed to be determined by this study is how the Carbon Nanotube (CNT) film heaters compare to the heating products that already exist. As such, etched foil heaters are being used as the baseline for comparison in this study. To accomplish this comparison, testing needs to performed on the etched foil heaters and on equivalent heaters made from the thin film materials: CNT sheet and RS100. This methodology section is broken down into four main sections to accomplish this. First, it needs to be determined how thin film materials react to electrical current being passed through them. Creating uniform heat distribution is the aim. Second, incorporating what was discovered in the first section, a fabrication process for creating thin film heater specimens will be developed. A repeatable process that produces stable specimens that maintain flexibility and minimizes complexity is the goal. As maintaining batteries above freezing temperatures is of principal interest in the operation of spacecraft, the specimens designed and tested throughout this research will be of a size and configuration suited for such an application. Next, initial testing outside the vacuum chamber needs to be performed on the thin film heaters. This is necessary to characterize their electrical current, or temperature, limits before being placed in the vacuum chamber. The vacuum chamber test plan is dependent on the results of this initial testing. Finally, once all comparable specimens have been successfully fabricated and initial testing completed, testing of all heaters will be conducted in a vacuum similar to that which these heaters may someday be exposed to. Testing in a vacuum is necessary to eliminate any thermal loss due to convection. It also serves to expose any flaws in the manufacturing process that may not be apparent in atmospheric testing. Finally, testing in this manner allows for the

control of environmental variables and as such improves the accuracy of the collected data. This will help in determining how efficient the heaters are when compared to one another as well as the pros/cons of each of the heating methods in a vacuum environment.

This methodology approach will be an iterative process relying on the results of a previous section to guide the steps in the next section. As such, results of each section will be presented in Chapter 4 but certain conclusions drawn from them will be referenced in sections of this chapter as the study progresses. A flowchart of the process can be seen in Figure 3.1.

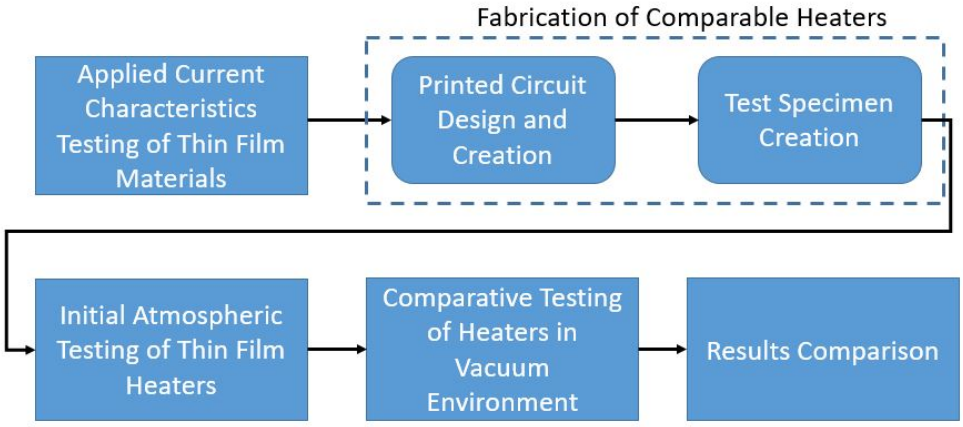

Figure 3.1: Methodology Flow Chart

3.2 Section 1: Applied Current Characteristics Testing of Thin Film Materials

Stated in the introduction to this chapter, this section's focus is on determining the effects of current application on thin film materials. The aim of which is to create uniform heating across the entire surface of the thin film materials.

The polyimide film material, RS100, was purchased from Dupont^{TM} and came

in sheets of size 8.5“ x 11”. These sheets consisted of a layer of dielectric insulator and a layer of electrically conductive carbon based material. Sheets of Multi-walled Carbon Nanotube (MWCNT) were purchased from Nanocomp Tech Inc. of size 300 mm x 300 mm and 0.038 mm thick. Both types of sheets were cut into rectangular coupons 2.16“ x 1.18” (55mm x 30 mm), similar in size to the Minco^{TM} product, using a LPKF Ultra-Violet (UV)-laser shown in Figure 3.2.

Figure 3.2: LPKF UV-laser used for cutting out substrate and thin film materials for specimen creation

This laser has been used by the Air Force Institute of Technology (AFIT) in the past for its precision cutting and rapid prototyping capability. It is suitably designed to handle delicate materials such as the polyimide film and CNT sheet material. The precision of the laser also allows for the addition of tabs with alignment holes (Figure 3.3) which are necessary for proper specimen fabrication demonstrated in the next section.

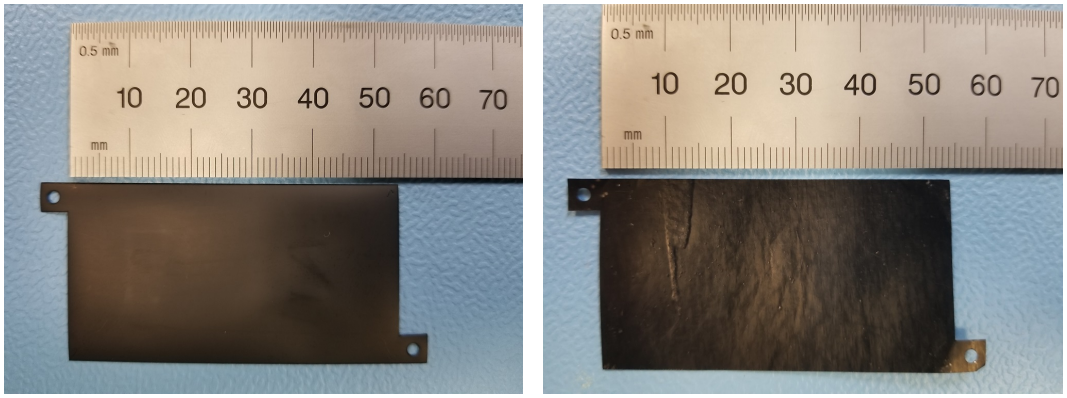

(a) (b)

Figure 3.3: (a) RS100 specimen coupon (b) CNT specimen coupon

The setup for this first phase of testing included the use of a power supply rated up to 16V and 5A, a Mid-wave Infrared (MWIR) camera (Optotherm Inc. Model: MI320), and a computer. 14.7V is the maximum available voltage that a standard CubeSat 8-cell battery pack is capable of supplying so the 16V power supply was deemed sufficient for testing purposes. A diagram of the setup can be seen in Figure 3.4.

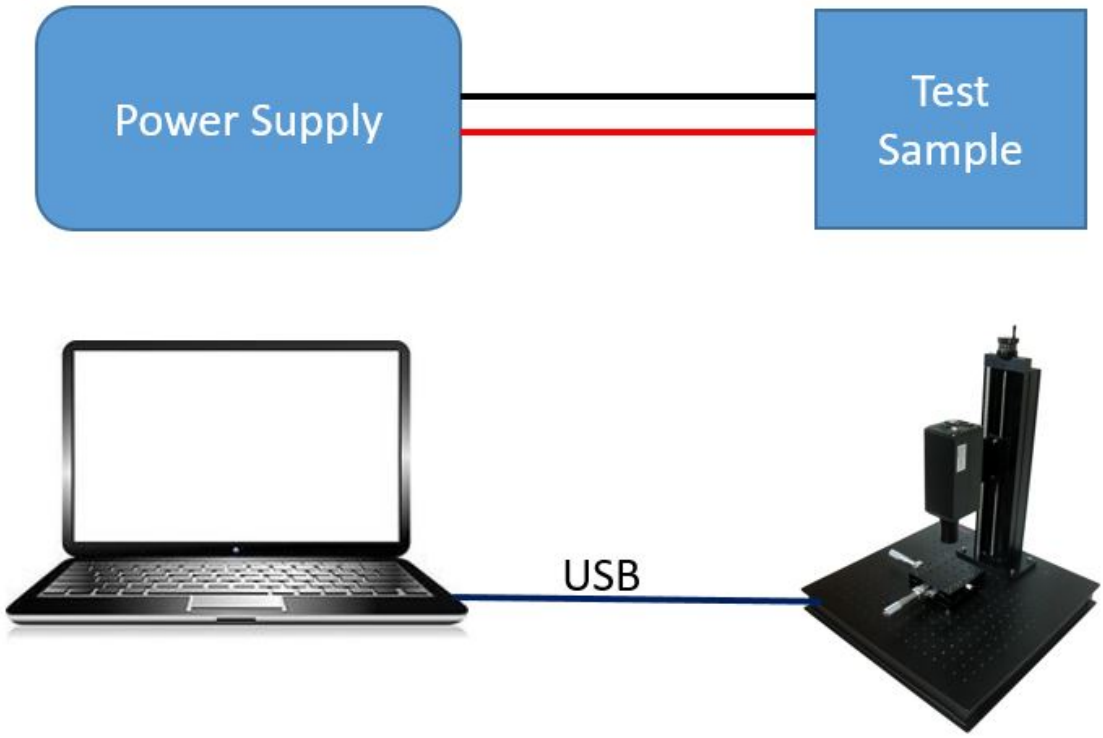

Figure 3.4: Test setup diagram for the applied current characteristics testing

Additional supplies included 20 ga. wire leads, copper strips, binder clips, Printed Circuit Board (PCB) sheets, and alligator clips.

3.2.0.1 Current Application Characteristics Test Plan

To determine how the method of applying power to specimens affected the heating characteristics, the following test plan was used.

First a PCB sheet was fitted with alligator clips that were in turn connected to the power supply. The RS100 specimen was then clipped in-between the two alligator clips as shown in Figures 3.5 and 3.6.

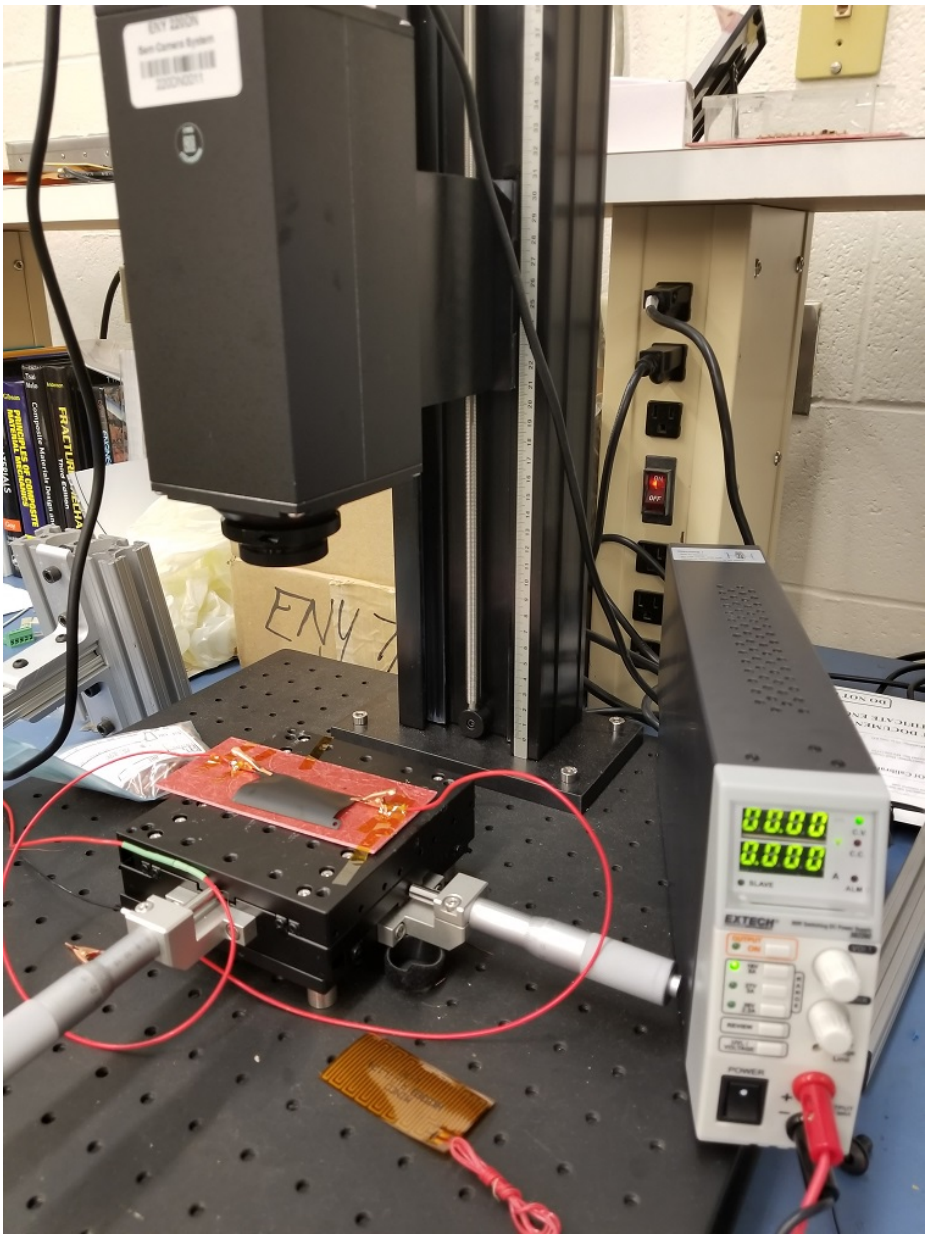

Figure 3.5: Picture of test stand setup for the applied current tests

The IR camera feeds readings to the computer through its USB cable connection and thermal images are captured using screenshots from the computer. The power supply for RS100 is set to 16V. This was used instead of the 14.7V available from a CubeSat battery pack to increase the number of data points. In later testing this will allow any resulting trend from the data to be verified beyond the 14.7V maximum.

Once the power is applied and the specimen's heat output stabilized, a screenshot of the resulting heat distribution is taken from the computer. The first test is run with the alligator clips attached to the upper corners of the RS100 specimen as is shown in Figure 3.6.

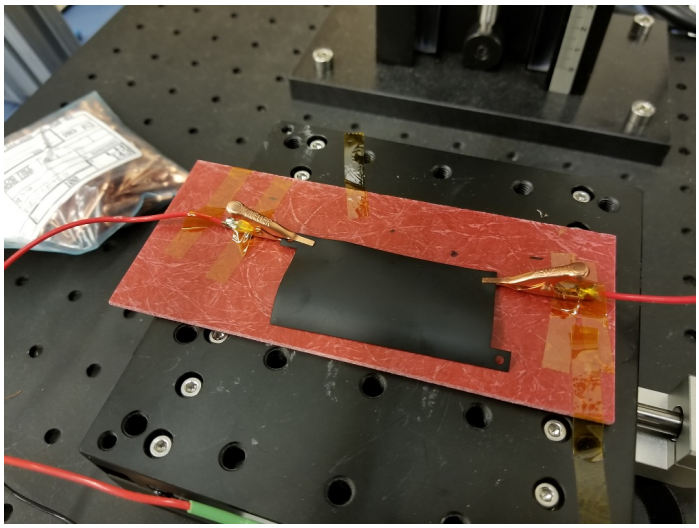

Figure 3.6: Picture of the first point contacts test setup

This process is repeated for the three placement configurations shown in Figure 3.7 for both RS100 and CNT. When applying power to the CNT, however, the voltage on the power supply is turned down. At 16V the RS100 coupon uses 0.11 A as read off the power supply. This equals 1.76 Watts of power usage according to equation 3.1. Through trial and error it was found that a similar power draw for the CNT occurred at 1.5V. Therefore, for the CNT coupon testing, the voltage on the power supply is held at 1.5V to show the heating distribution at 1.76 Watts, the same as the RS100 coupon.

$$P = I * V \tag{3.1}$$

Where P is power in Watts, I is current in Amps, and V is voltage in Volts.

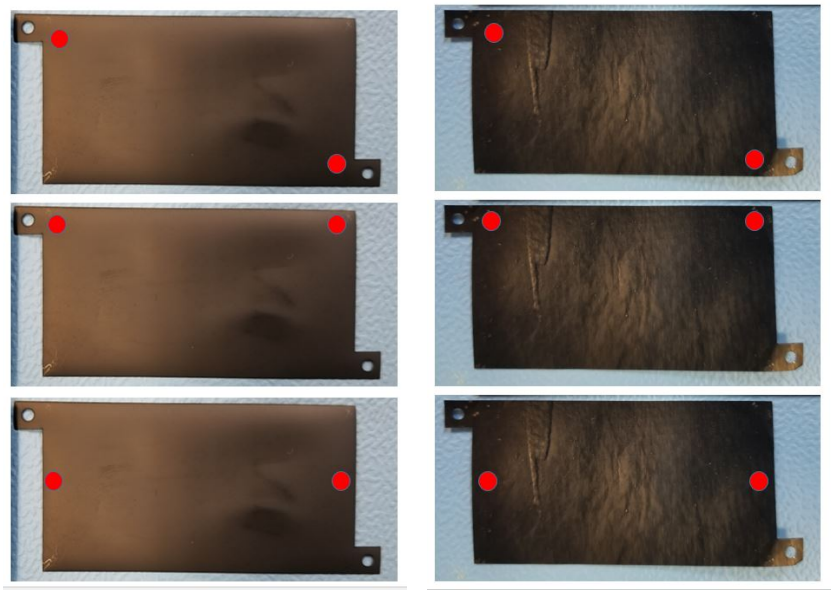

(a) (b)

Figure 3.7: (a) Point contact test attachment points diagram for the testing of the RS100 material (b) Point contact test attachment points diagram for the testing of the CNT material

Next the setup is reconfigured to apply power across the entire width of the specimens using copper strips and binder clips to create a uniform line of contact as is shown in Figures 3.8 and 3.9. The leads coming from the power supply are soldered directly onto the copper strips.

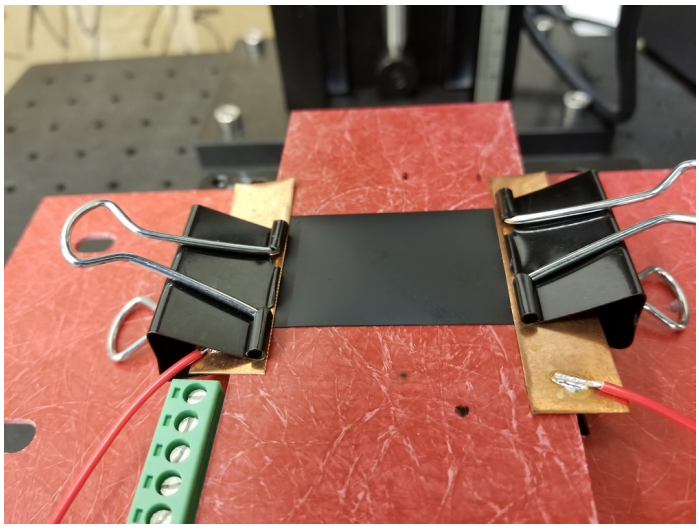

Figure 3.8: Picture of the full width strip contact test setup

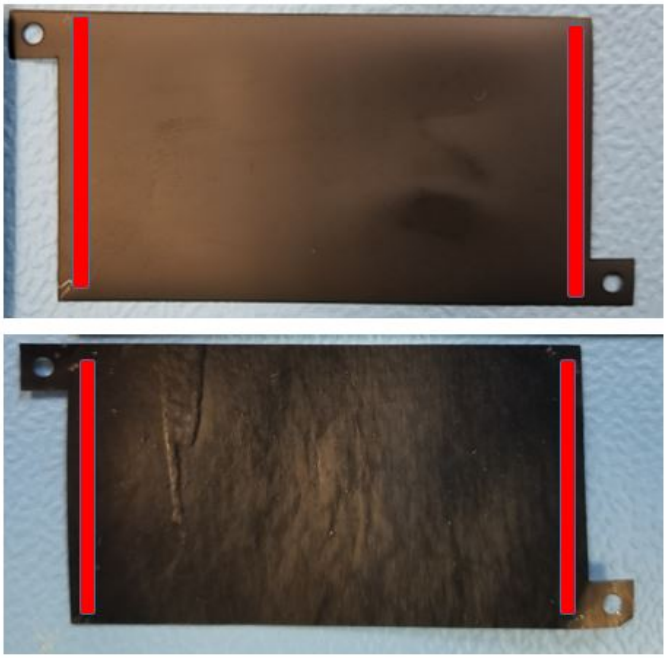

Figure 3.9: Full width contact strip layout diagram for testing the RS100 and the CNT materials

Again, for the RS100 the power supply is set at 16V while for the CNT it is set at 1.5V. Thermal images are captured for both specimens once the temperature

stabilizes.

Using the results from these tests and the conclusions drawn from them will direct the steps in the next section of the methodology.

3.3 Section 2: Fabrication of Comparable Heaters

Before beginning the experiments, three heater types: etched foil, RS100, and CNT must be constructed such that any data collected from the tests would have meaningful and repeatable results. This was accomplished by selecting and/or fabricating heaters with known dimensions, resistances, and current capacities as comparisons. As mentioned before the etched foil heaters are already a commercially available product, however heaters made from the polyimide film material (RS100) and CNT film material are not. To facilitate testing heaters made of RS100 and CNT, specimens were created using the available raw materials listed in Appendix E. First, though, the comparative etched foil heater was prepared.

3.3.1 Etched Foil Heater Fabrication

Etched foil heaters are available from many different vendors. For the purpose of these tests the one chosen was the Minco^{TM} HK5369 R101L12A shown in Figure 3.10. This heater is space qualified and will be used on battery buses on-board AFIT CubeSats, such as the Grissom, in the future. Additionally, Pumpkin Inc. has incorporated these heaters into their battery pack design and will be launching them on several of their own satellites.

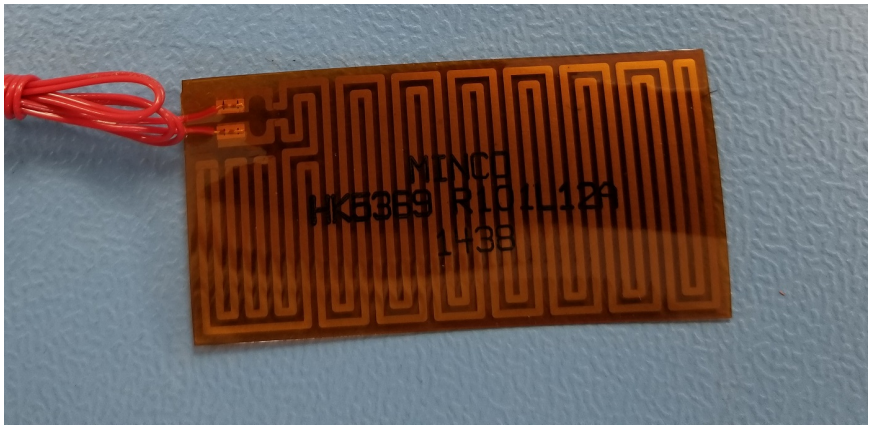

Figure 3.10: Minco^{TM} HK5369 etched foil battery heater used on AFIT CubeSats

This heater has known dimensions of 2.5“ x 1.25” (64mm x 32 mm), a resistance of 101 Ohms (Ω) and a max current rating of 12 Amps (A). To prepare this heater for testing a thin film adhesive, same as the type used in the fabrication of the polyimide film heater, is used. This thin film adhesive is used to create a uniform bond between the test specimen and a 2.0“ x 2.0” (50mm x 50 mm) 11 gauge aluminum heat sink plate as is shown in Figure 3.11. The same size heat sink is used for all three types of heaters and the contact area between the heater and the heat sink is the same for all.

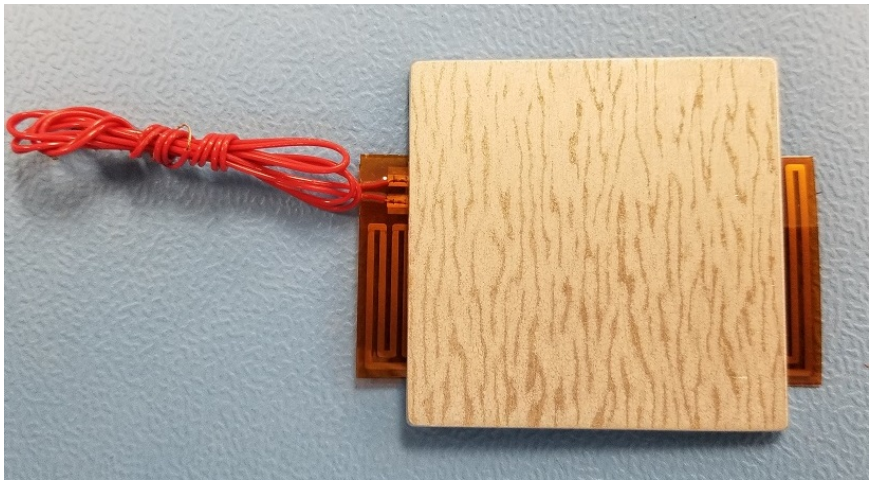

Figure 3.11: Minco^{TM} heater specimen with bonded heat sink plate

To activate the adhesive film and facilitate bonding, the assembly is then heated to 200°C for one hour using simple C-clamps to apply pressure across the entire surface. (Note: The MultiPress S is not used for this task as early attempts to bond the heat sink using the press caused damage to the etcher foil making the specimen unusable)

As will be explained in the next section, substrate material is used to fabricate the thin film heaters made of RS100 and CNT. This substrate provided excess material to clamp the specimen to the custom specimen mount for testing as is shown in Figure 3.37. As the etched foil heater does not require any additional substrate material added to it during fabrication, it could not be suspended in the custom specimen mount in the same way as the other two types of heaters. To facilitate mounting, Kapton® tape tabs are added to either side of the heat sink to create a grip point for the binder clips as can be seen in Figure 3.12.

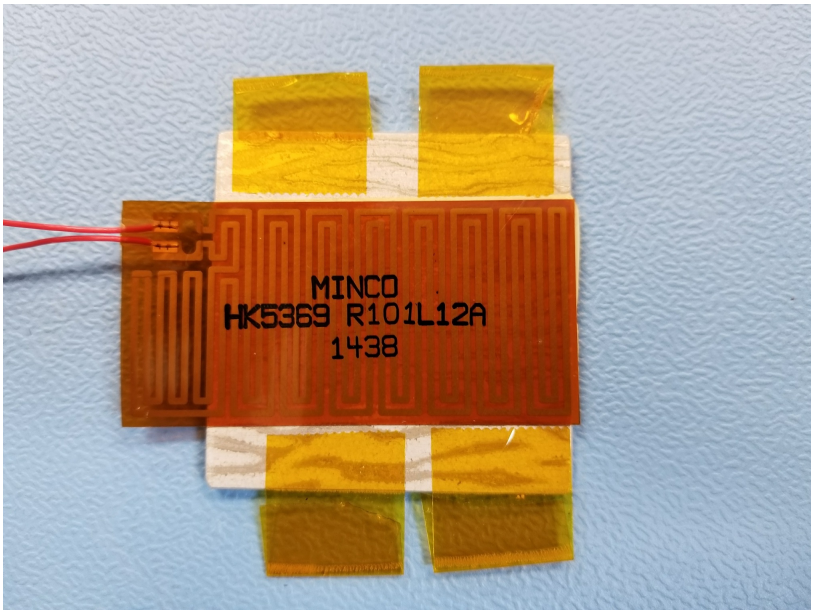

Figure 3.12: Etched foil heater with Kapton® mounting tabs

This allows for comparable mounting while still maintaining thermal isolation from the surrounding mount material. No further steps are needed in the fabrication

of the etched foil heater used for testing.

3.3.2 Thin Film Heater Fabrication

For the fabrication of the thin film heaters a Kapton® substrate material is used; Kapton® MT+. This is used for several reasons. First, its adhesive layer makes it suitable to forming laminates with the thin film materials. Second, etched foil heaters are constructed of Kapton® substrates. Having all the heaters constructed of the same substrate material will permit a more equal comparison for testing in the next section. Finally, Kapton® substrates are a space proven material and are therefore acceptable for the fabrication of heaters used in the space environment.

Results from the previous section, presented in Chapter 4, led to the use of full coupon width electrical contacts being used for the thin film heater fabrication processes described next.

3.3.2.1 Polyimide Film Heater Fabrication

The same coupon design and laser cutting method described in the previous section is used to produce additional test samples of the polyimide film material for this part of the development process. Additionally, Kapton® substrate rectangles, with the adhesive backing, of size 3.5“ x 2.375” (90mm x 60 mm) are also cut out using the laser as is shown in Figure 3.13. Holes are cut in the substrate to allow for coupon alignment and access to the electrical terminal pads which will be explained later.

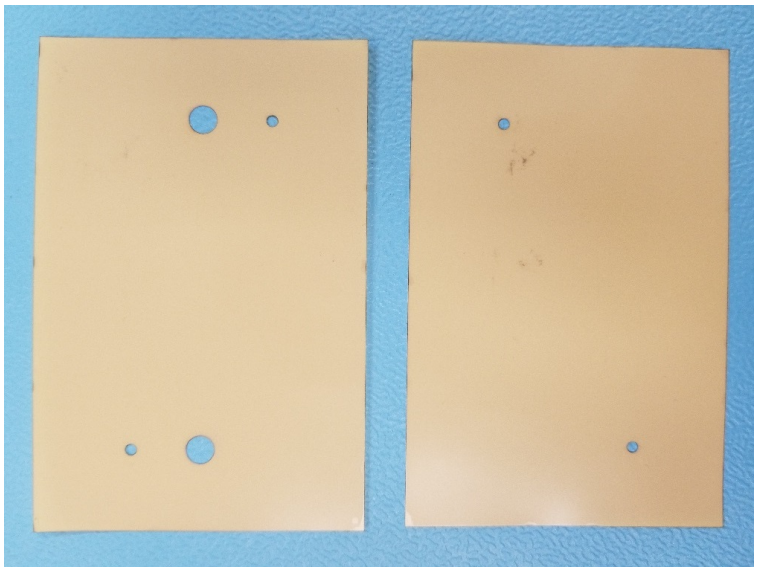

Figure 3.13: Kapton® MT+ adhesive substrate material cut into rectangles for specimen production

Once cut out, the protective film must be removed from the adhesive side of the substrate. This can be accomplished by peeling back a corner of the film from the substrate with a sharp knife or similar instrument. Once started, the film comes off cleanly and easily. Full coupon width electrical contacts and pads, shown in Figure 3.14, can then printed onto the substrate using Voltera flexible conductive ink and the Voltera V-One circuit printer as is seen in Figure 3.15. For proper circuit alignment, the V-One software directs the user to select reference points from the circuit diagram to be printed. It then allows the user to manually position the printer nozzle over the location on the circuit board where that feature is to be placed. After this is accomplished for several reference points, the V-One is then able to orient itself to print the circuit pattern precisely where it is intended by the user. This makes the alignment of the electrical pads with the corresponding holes in the substrate, used later in the assembly process, possible.

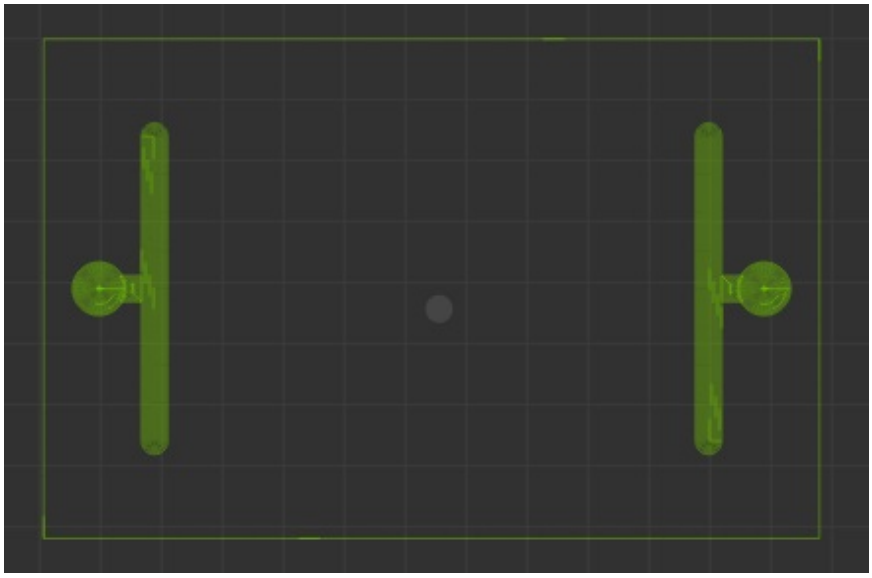

Figure 3.14: Conductive ink pattern on V-One software interface

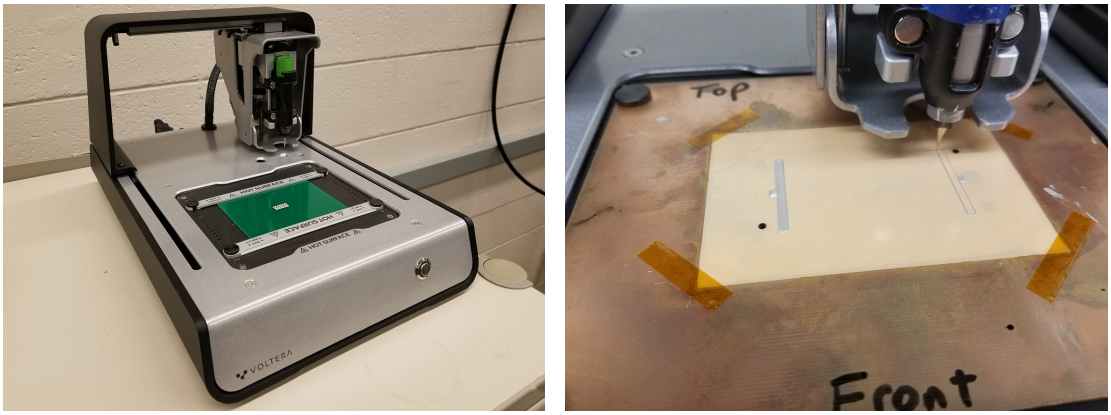

(a) (b)

Figure 3.15: (a) Voltera V-One circuit printer (b) Printed ink circuit being applied to adhesive substrate surface

The conductive ink can then be cured using the V-One or an oven such as the OMegalux seen in Figure 3.16. The oven is used instead of the Voltera V-One's heater in the event that faster specimen production is required and only one V-One is available. The V-One is capable of printing circuits and curing the ink, however it cannot do both processes simultaneously. While the V-One's heater is running, the

ink printing capability is unavailable. Using the oven allows for additional specimens to be printed while others are cured. The specimens cured in the oven are baked for 1 hour at 210°C. These are the same conditions that the V-One's heater provides during its curing process.

Figure 3.16: Omegalux oven used for curing the conductive ink on the adhesive substrate

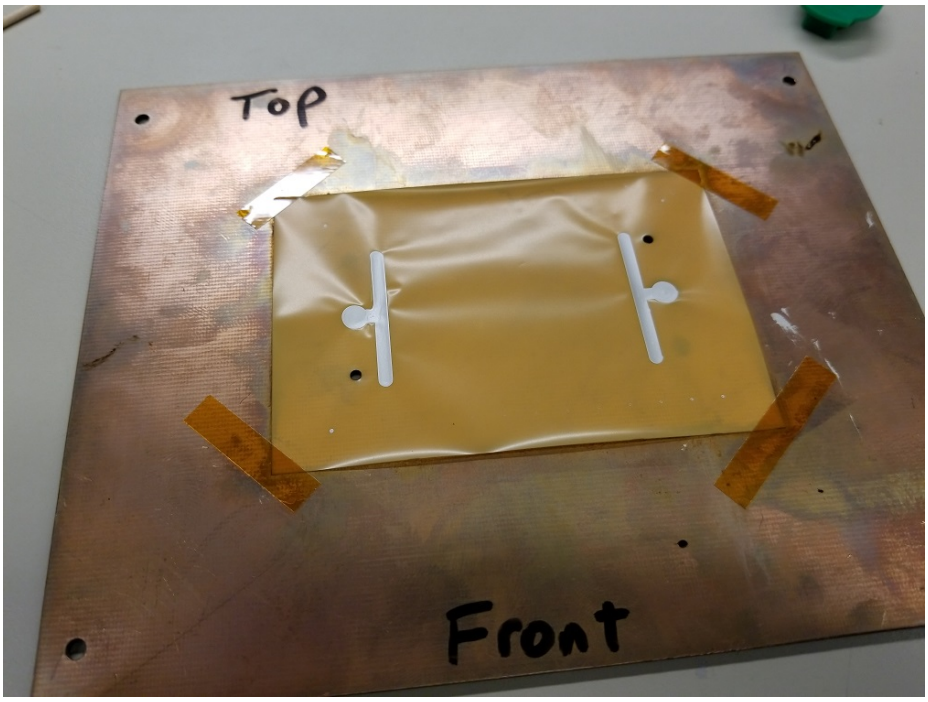

Figure 3.17: Cured conductive ink on adhesive substrate

Once curing is complete as is shown in Figure 3.17, and the substrate is cool, a RS100 coupon is then layered in between the substrate with the printed circuit and another rectangular of adhesive substrate. The conductive side of the RS100 (matte finish side) must be in contact with the printed electrical strips on both ends. This will allow current to pass through the specimen as shown in Figure 3.18. Using the previously mentioned alignment holes to ensure proper positioning, Kapton® tape is used to hold the layers in place on a sheet of Polytetrafluoroethylene (PTFE), used in the pressing process, prior to bonding as shown in Figure 3.19.

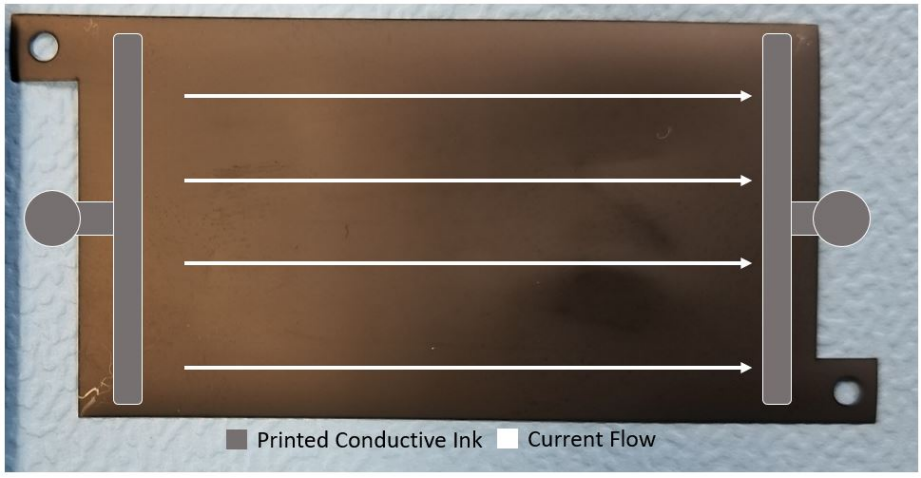

Figure 3.18: RS100 specimen intended current flow design

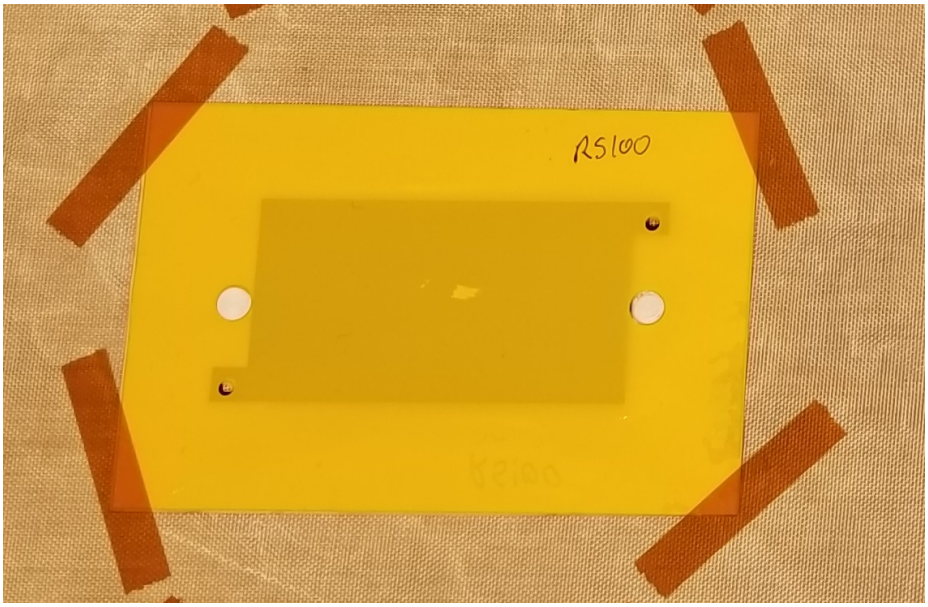

Figure 3.19: Alignment of substrate layers with thin film material pre-pressing process

The layers are then bonded together into a laminate using the LPKF MultiPress S, as seen in Figure 3.20 using the settings in Table 3.1. The press is needed to apply heat to the specimen to activate the adhesive on the substrates while exerting pressure to force out air pockets and bond the materials together.

Figure 3.20: LPKF MultiPress S

Table 3.1: MultiPress S Settings

Temperature (°C)	Pressure (N/cm^2)	Time (mins)
192	153	60

Once cooled, a layer of adhesive film, 2.0“ x 2.0” (50mm x 50 mm), is centered on top of the specimen (Figure 3.21) and a 2.0“ x 2.0” (50mm x 50 mm) 11 gauge aluminum heat sink plate is aligned on top of that (Figure 3.22). The specimens are then again put through the press using the same conditions as before from Table 3.1. Once again the press is used to activate the adhesive, this time the thin film adhesive, and force out any air pockets. The film described is shown in Figure 3.21, the bonded heat sink is shown in Figure 3.22, and the finished specimen can be seen in Figure 3.23.

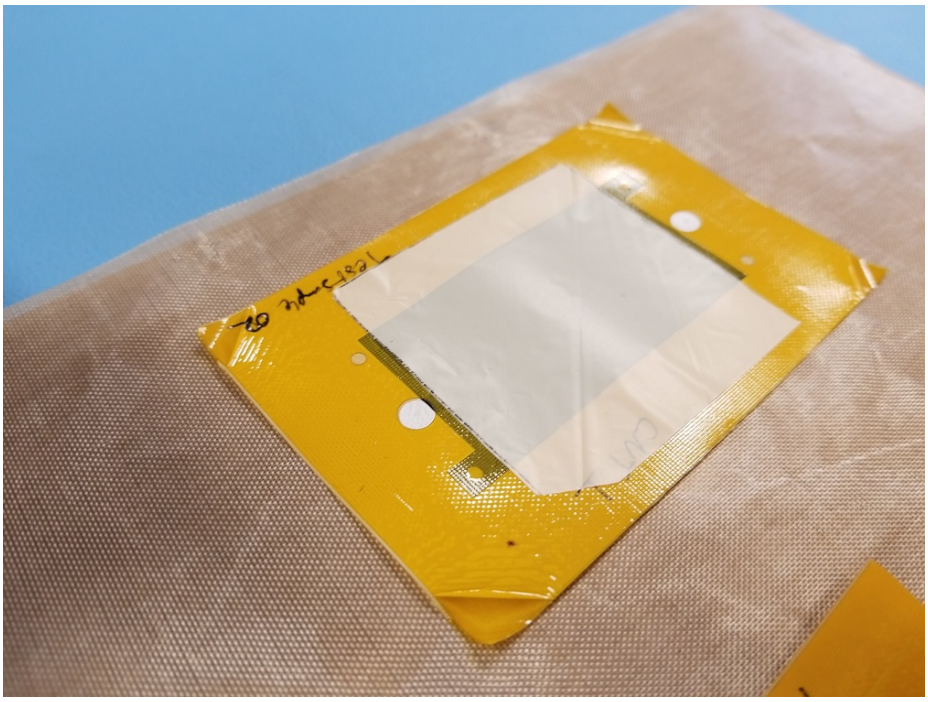

Figure 3.21: Pyralux adhesive film on post-press laminate specimen

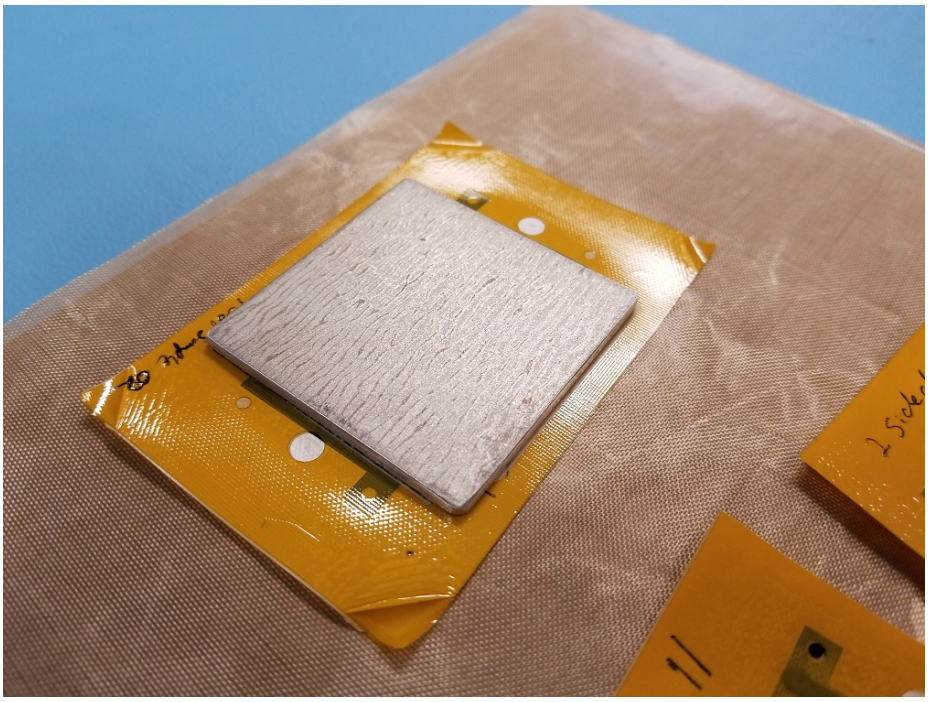

Figure 3.22: Aluminum heat sink plate over Pyralux adhesive film on specimen (pre-press bonding)

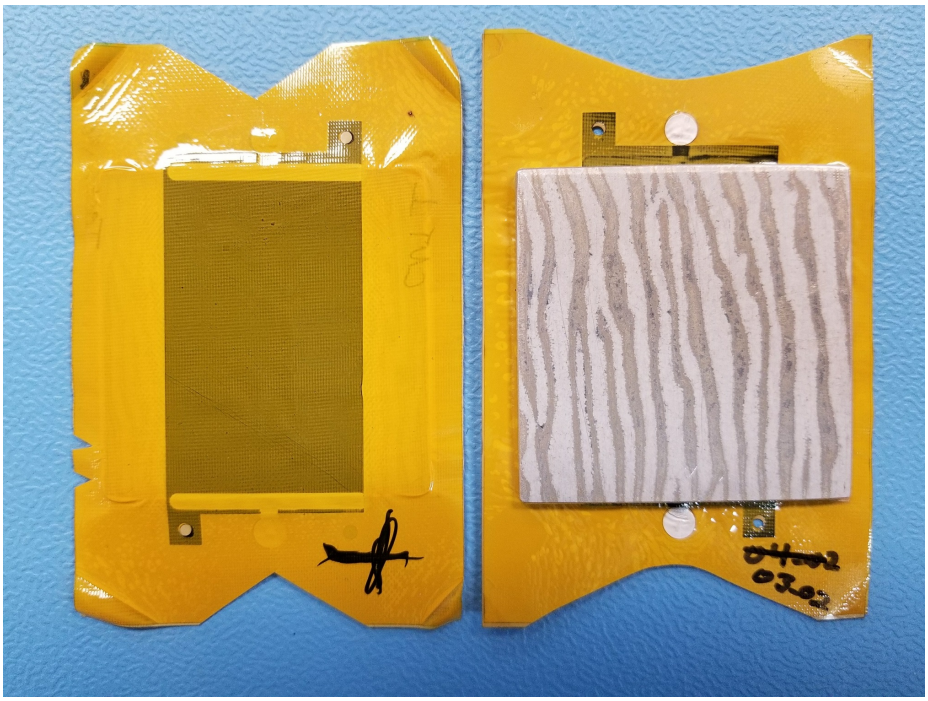

Figure 3.23: Completed RS100 specimen with bonded heat sink plate

3.3.2.2 CNT Heater Fabrication

The CNT heater specimens are fabricated in a similar manner to the RS100 heaters above. Further coupons are cut out using the UV-laser from before. However, while the RS100 has a uniform makeup in all directions and as such no special considerations need to be made during the cutting process, the CNT is different. The CNT has extrusion directionality (prevailing grain direction) associated with the drum feed direction explained in Chapter 2. This means that coupons cut out parallel to the prevailing grain direction may have different characteristics than those cut out perpendicular to the prevailing grain direction. To determine the most efficient means of utilizing this non-uniformity in the design of the thin film heater the coupons mention above are cut out such that some will have the applied current aligned with the prevailing grain direction of the CNT while others are cut such that applied current will be perpendicular to the prevailing grain direction of the CNT. A specimen type,

explained below, is assigned to each of these. Additionally, where the RS100 has only one conductive side, the CNT can pass current from either side of the coupon. As explained in the literature review, passing current across a CNT rather than along it meets with greater resistance. Greater resistance could lead to a difference in heat generation. Knowing this, two additional specimen type variations are assigned. These four specimen configurations are explained further below. (Note: the specimen Type designation was assigned randomly)

Specimen Type 1: CNT cut with the prevailing grain parallel to the direction of intended current flow. Electrical contacts on the same side of the coupon as shown in Figure 3.24.

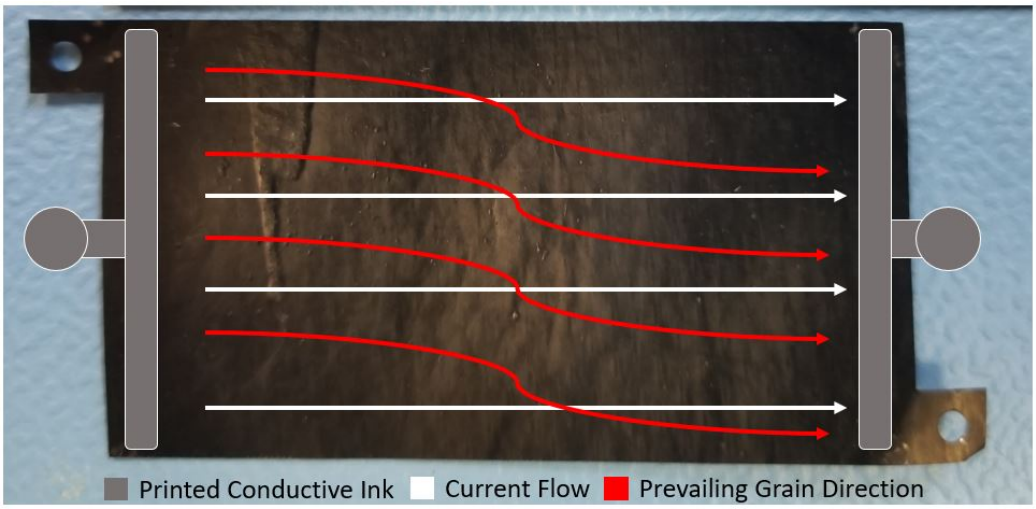

Figure 3.24: CNT specimen with current flow parallel to the net grain alignment and with both electrical terminals on one side of the thin film material

Specimen Type 2: CNT cut with the prevailing grain perpendicular to the direction of intended current flow. Electrical contacts on the same side of the coupon as shown in Figure 3.25.

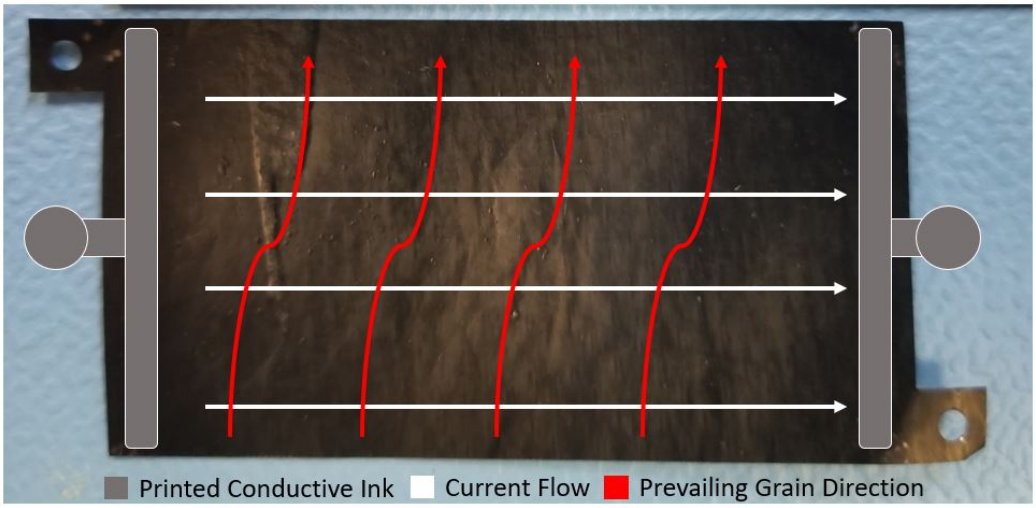

Figure 3.25: CNT specimen with current flow perpendicular to the net grain alignment and with both electrical terminals on one side of the thin film material

Specimen Type 4: CNT cut with the prevailing grain parallel to the direction of intended current flow. Electrical contacts on opposing sides of the coupon as shown in Figure 3.26.

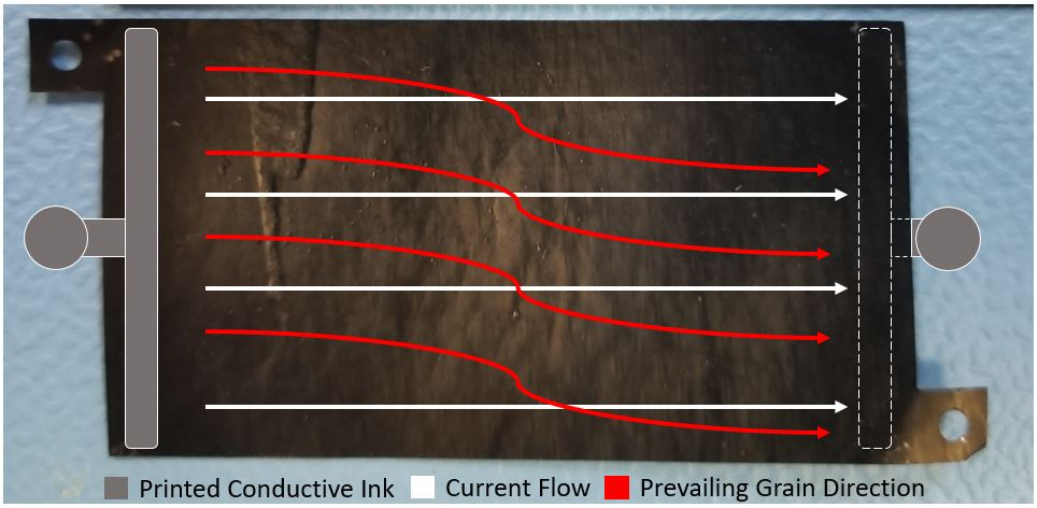

Figure 3.26: CNT specimen with current flow parallel to the net grain alignment and with electrical terminals on either side of the thin film material

Specimen Type 5: CNT cut with the prevailing grain perpendicular to the direc-

tion of intended current flow. Electrical contacts on opposing sides of the coupon as shown in Figure 3.27.

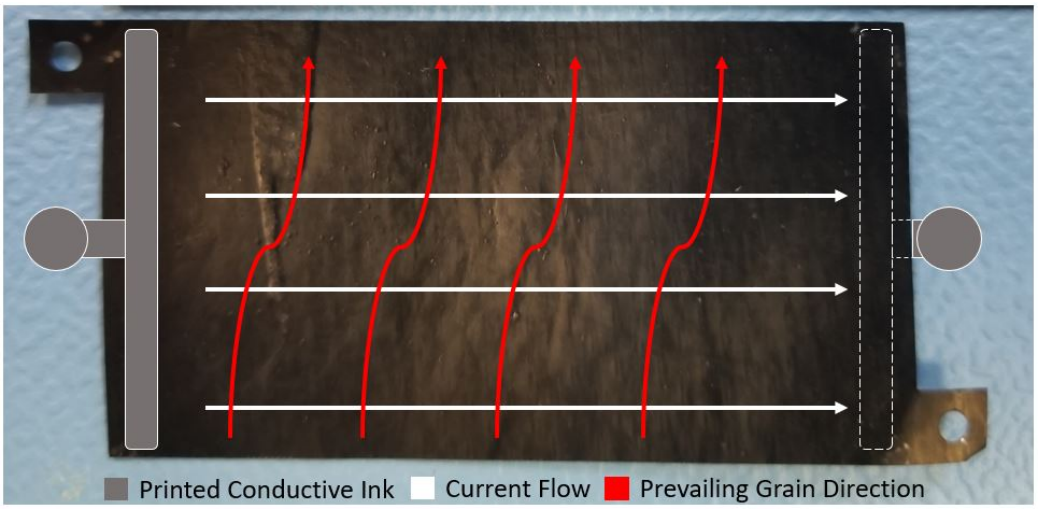

Figure 3.27: CNT specimen with current flow perpendicular to the net grain alignment and with electrical terminals on either side of the thin film material

To facilitate having electrical contacts on both sides of the CNT, the Kapton® substrate design was modified as was the ink pattern as is shown in Figure 3.28.

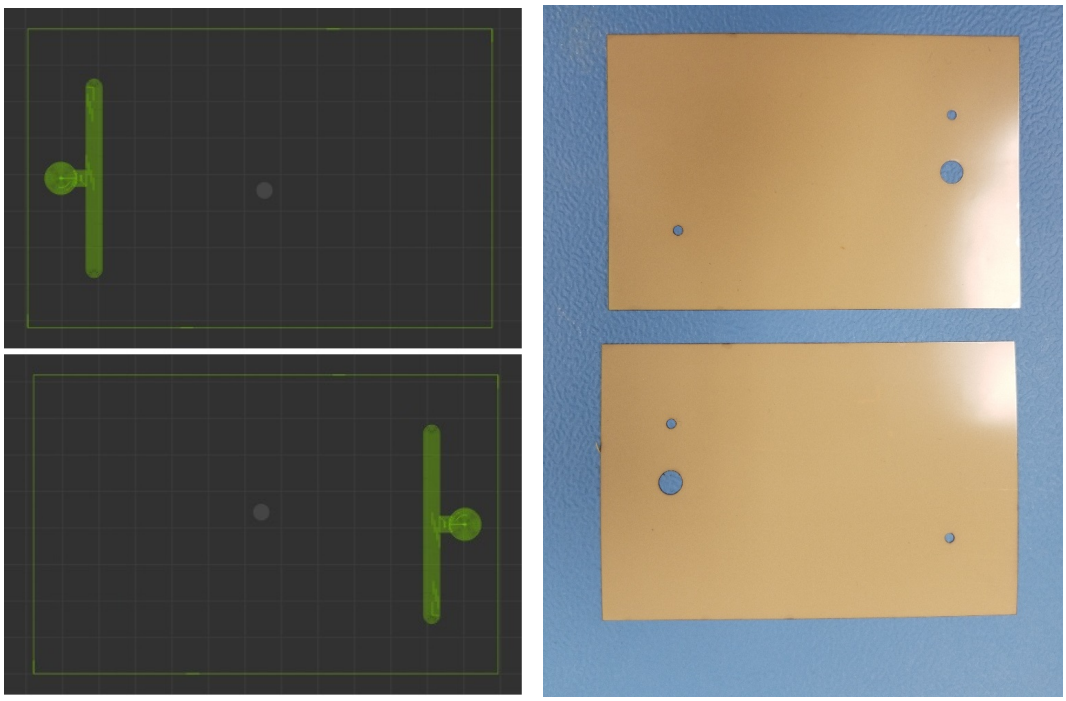

(a) (b)

Figure 3.28: (a) Conductive ink pattern for specimen Types 4 and 5 (b) Kapton® Substrate for specimen Types 4 and 5

Once this was addressed, the remainder of the steps described for preparing the RS100 can be performed on the CNT specimens. The specimens are sent through the press once to complete the bonding process of the laminates and then sent through a second time to affix the heat sink. (note: the two pressing processes cannot be performed concurrently as the heat sink is not the same size as the heater specimen. This would lead to areas of the specimen not being subjected to the same heat and pressure as the rest of the specimen)

3.3.3 Specimen List for Testing

Using the processes listed in the sections above, three of each type of heater was fabricated and prepared for testing. The final quantities to be tested are in Table 3.2.

Table 3.2: Test Specimens

Item	**Qty**
CNT (Type 1) Test specimen	3
CNT (Type 2) Test specimen	3
RS100 (Type 3) Test specimen	3
CNT (Type 4) Test specimen	3
CNT (Type 5) Test specimen	3
Etched Foil (Type 6) Test specimen	3

Using the same test setup as was used to test the current flow characteristics of the thin film materials, these samples must be tested to verify that the fabrication process was successful. To accomplish this each sample will be connected to the power supply at either 16V, for etched foil and RS100 heaters, or 1.5V, for CNT sheet heaters. Passing criterion for this test is that each specimen generates heat across its entire surface. Any specimens that do not pass this test will not be used in the later vacuum chamber testing.

3.4 Section 3: Initial Atmospheric Testing of Thin Film Heaters

This initial testing of the thin film heaters outside the vacuum chamber is necessary as their responses to current loads is unknown. If a specimen were to fail inside the vacuum chamber due to excessive electrical current or heat, it may not be immediately obvious based on the thermistor readings (explained in the next section) or by observations as visibility inside the chamber is severely limited. Thus, the thin film heaters will first be tested at similar power levels to one another up to 2 Watts (The max power level of the etched foil heater is 1.75 Watts). Next, the CNT film heaters, with their lower resistances, will be tested at increasingly higher power levels

to determine if/when failure or damage occurs.

3.4.1 Low Current Atmospheric Testing of the Heaters

The setup for these tests is the same as that for the previous section as is shown in Figure 3.29.

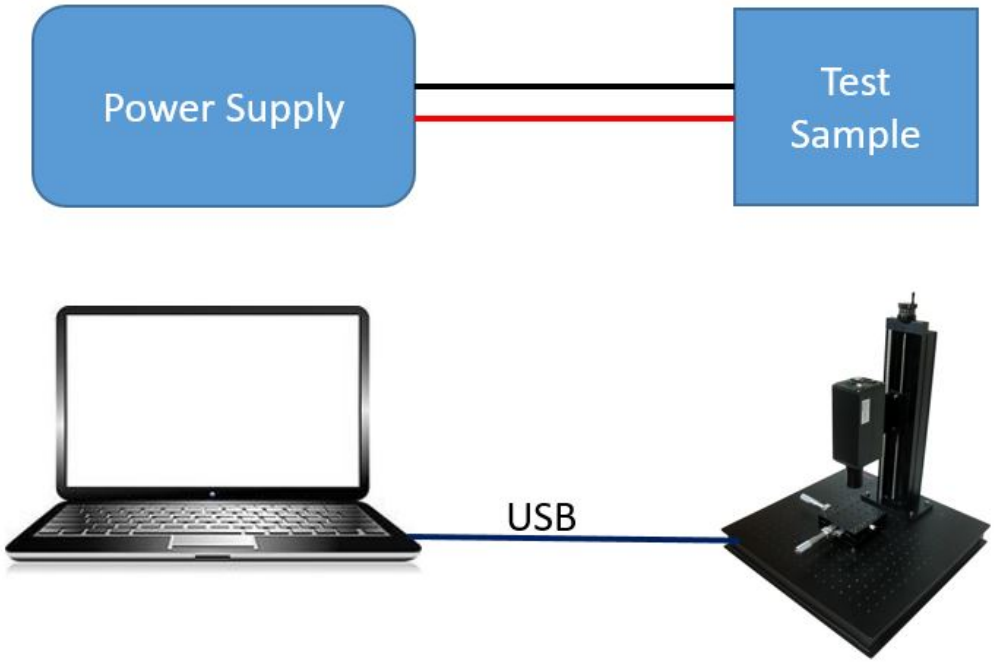

Figure 3.29: Initial atmospheric testing setup diagram

3.4.1.1 Low Current Test Plan

The specimens for these tests are placed with their heat sink facing away from the camera with a sheet of PCB material between it and the base of the camera stand as shown in Figure 3.30. This PCB board eliminates the possibility of the electrical contacts grounding out on the metal base plate.

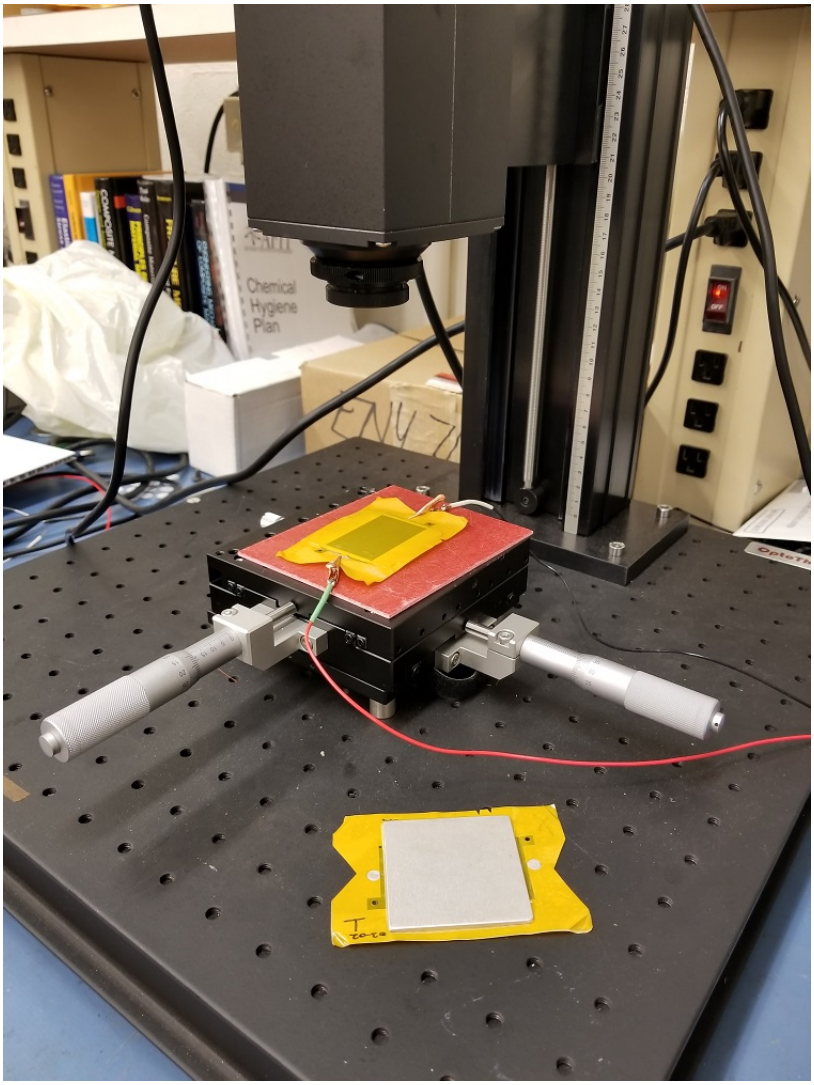

Figure 3.30: Test setup for testing of specimens in atmospheric conditions

For these tests, voltage is arbitrarily selected as the controlled variable and the resulting current is allowed to vary. Multimeter tests show that the RS100 specimens have a higher resistance than the etched foil heaters and as such can use the full 16V available from the power supply without exceeding its 5A maximum rating according to equation 3.2. Therefore, the testing of the RS100 is started at 0V and incrementally increased up to 16V in six equal voltage steps. Current readings from the power supply and thermal images are recorded for each step. The thermal images are collected

once the temperature readings from the IR camera appear to stabilize. Next, the power usages for each of the RS100 steps, calculated using equation 3.1, are used as a guideline for incrementing the voltage settings for the CNT film heater testing. Starting at 0V, the voltage settings on the power supply are adjusted to obtain similar power usages for the CNT film heater as was calculated for the RS100 film heater at each of its incremental steps. Current readings and thermal images are collected for each of these increment as well. The Voltage increments (V), the resulting current (I) in Amps, and the calculated power usages (P) in Watts recorded from these tests are shown below in Chapter 4.

3.4.1.2 High Current Test Plan

Continuing the testing outlined above, the CNT film heaters are next subjected to higher current loads until the maximum power supply voltage, or current, is reached or until damage/failure of the specimen is observed. This time electrical current is the controlled variable as it is unlikely the maximum voltage will be reached before the maximum current is. The current for this test is started at 1.25A and stepped up by 0.25A incrementally until 5.00A is reached. This size of increment was chosen to allow for rapid progression through the various current levels while not allowing for too large of increases. Between each increment the thermal output of the sample is allowed to reach steady state conditions before progressing to the next step level. Selecting one CNT specimen randomly, these higher current increments are experimented with. For this, voltage readings from the power supply and thermal images from the IR camera are recorded at each increment. An example of the thermal readings can be seen in Figure 3.31. Further results can be found in Chapter 4.

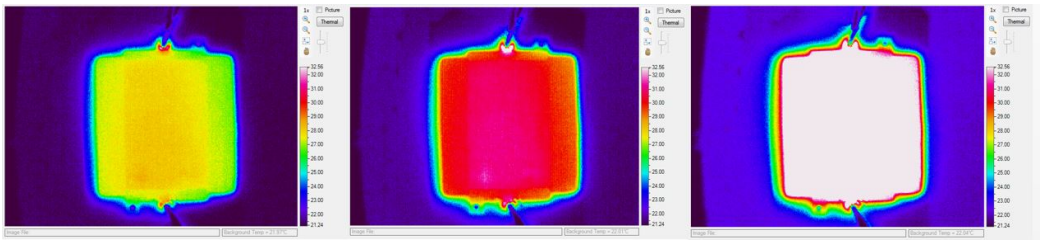

Figure 3.31: Example of CNT testing results with up to 1.6V applied

Knowing the upper limit of either electrical current or heat for the thin film heaters allows for the design of a test plan for use in the vacuum chamber testing.

3.5 Section 4: Comparative Testing of Heaters in Vacuum Environment

The purpose of vacuum chamber testing is to perform comparative tests of the different heater products in an environment similar to that which they could be exposed to. This will allow for meaningful data collection and analysis of each of the heater types to be used for later comparison.

3.5.1 Vacuum Chamber Testing Required Equipment List and Descriptions

For vacuum chamber testing specialized equipment was required as is listed in Table 3.3.

Table 3.3: Vacuum Chamber Testing Supplies and Materials

Ref	**Item**	**Qty**
[1]	Vacuum Chamber	1
[2]	Laptop or PC	1
[3]	Power supply	2
[4]	FLIR camera (SC7000)	1
[5]	FLIR lens (L0106)	1
[6]	Arduino Mega 2560	1
[7]	Custom Arduino Shield	1
	Multimeter (not shown)	1
[8]	Thermistors (100kΩ)	5
[9]	Custom Specimen Mount	1
	Extruded Aluminum Frame components (not shown)	Various
	Electrical components (20 ga. wire, alligator clips, binder clips, etc)	Various
	Kapton® tape	1 roll

See Figure 3.32 for the relative positions of the items above with regard to the test setup

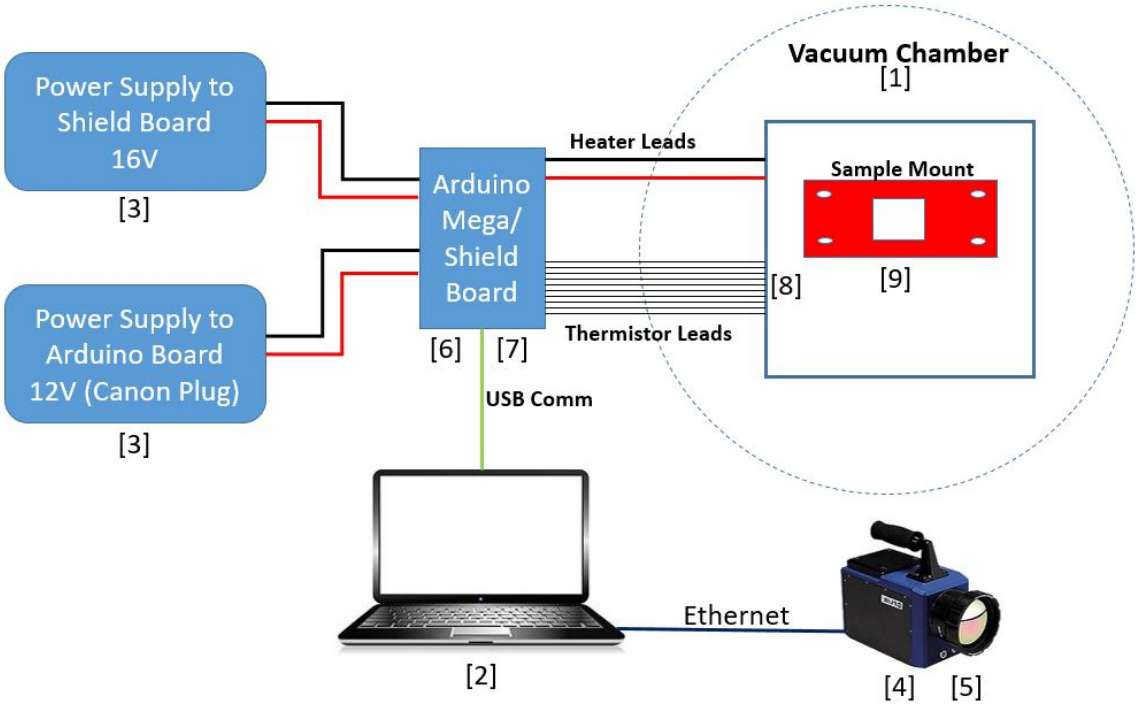

Figure 3.32: Setup diagram for the vacuum chamber testing

3.5.1.1 Vacuum Chamber

The vacuum chamber used for these tests is a horizontal, cylindrical chamber manufactured by Laco Technologies as shown in Figure 3.33. It measures 24 in deep and 23.5 in diameter. The pumping system for the chamber is comprised of a roughing pump and a turbo pump. The roughing pump is a Bluffton Motorworks model: 1201006416. The turbo pump is a compound molecular pump manufactured by Osaka Vaccum, LTD. model: TG800FCAB. Other features of this chamber include several UV view ports and two main pass-through communication/power bundles shown in Figure 3.34. Each wire in both bundles has a number designation. For these tests, power is supplied to the heater through wires 1 and 2 of one of the bundles. The thermistors are connected using wires 1-10 of the second bundle to avoid any possible signal interference from the power leads. The specific lead designations for

the thermistors are shown in Table 3.4.

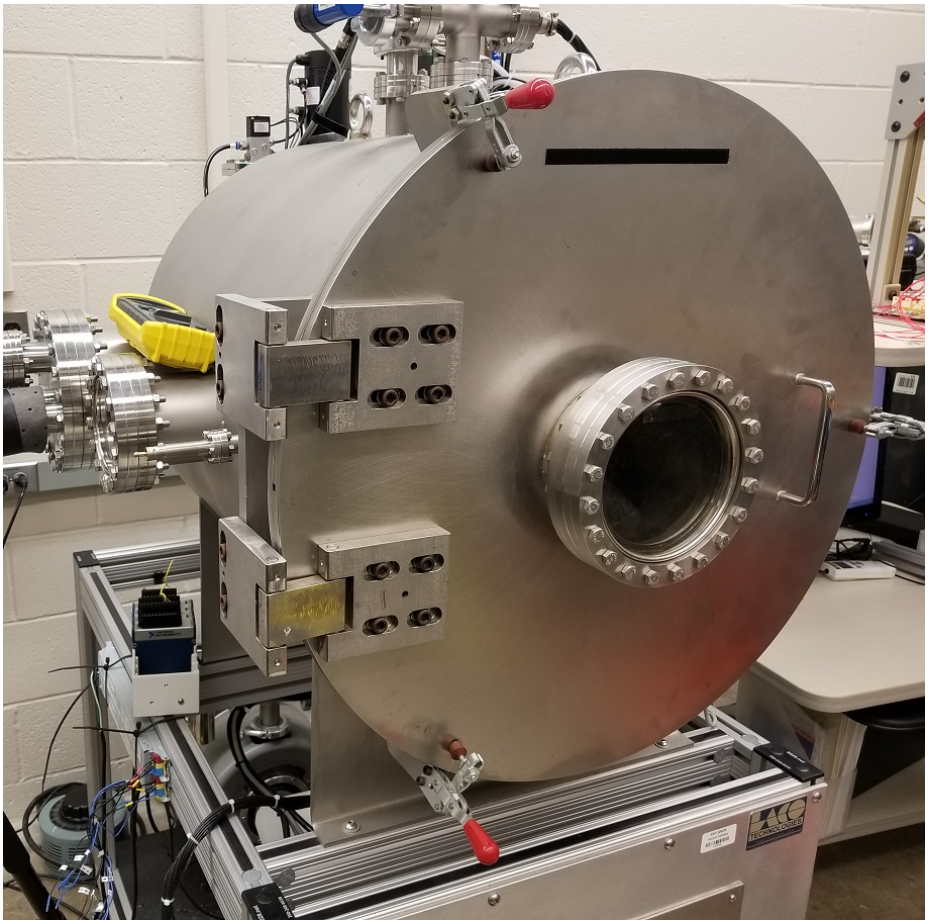

Figure 3.33: Laco Technologies vacuum chamber used for testing

(a) (b)

Figure 3.34: (a) First pass-through communication/power bundle (b) Second pass-through communication/power bundle

3.5.1.2 Thermal Imaging

Thermal images and measurements are collected from all the following experiments using the FLIR SC7000 Infrared (IR) camera, a MWIR lens (L0106), and supplied software. The FLIR SC7000 series of camera was selected for this study as it specifically designed for academic and industrial R&D applications. The camera and supplied software are capable of recording thermal data at a rate of 60 kHz. With a possible wavelength detector range of 7.7-11.4 μm, the camera is well suited for these tests. As thermistors will be used as the primary method of recording thermal data from the specimens, the IR camera will serve as a method of verification and a backup method of recording data. For these tests the camera is placed outside the vacuum chamber with a line of sight to the test specimen through an available view port, made of Germanium glass, on the chamber. The view port available is 0.9 inches in diameter. The camera lens was shielded from ambient light inclusion by using a light absorbing fabric pad wrapped around the lens and view port as is shown in Figure 3.35.

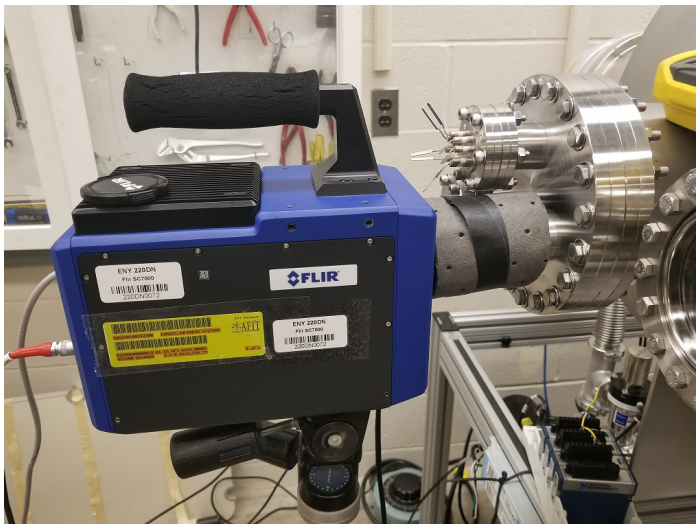

Figure 3.35: FLIR SC7000 IR camera and MWIR L0106 lens used for testing mounted to Germanium viewport window on vacuum chamber

3.5.1.3 Custom Specimen Mount

To facilitate electrical connections to the test specimens, while still maintaining thermal isolation, a custom specimen mount is needed. The one used for these tests is constructed from 0.0735 in (1.85 mm) thick PCB material. A square cutout of dimensions 54 mm tall x 55 mm wide is centrally located in the board for the specimen shown in Figure 3.36. The schematic of the board can be found in Appendix C.

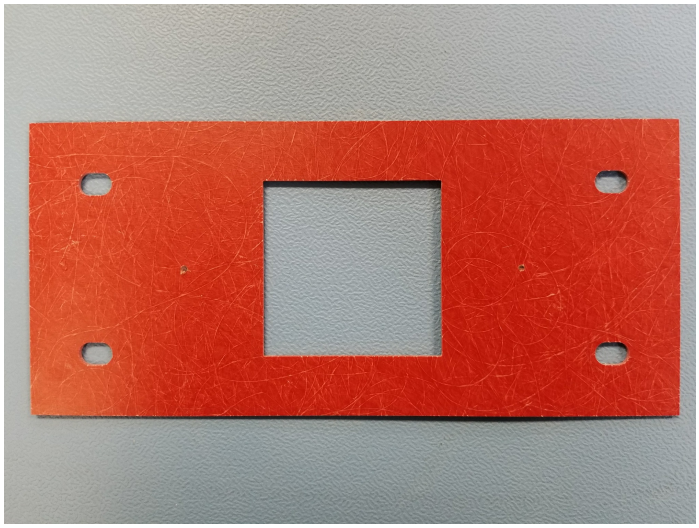

Figure 3.36: Custom PCB specimen mount used for positioning the specimen in the view of the FLIR camera while within the vacuum chamber

As mentioned in the fabrication section, specimen mounting to this board is accomplished using binder clips to secure the excess substrate material to its surface. Mounted alligator clips are then used to connect to the electrical terminals as shown in Figure 3.37. Care is taken to ensure that no part of the heater or the heat sink are in contact with the edges of the mount.

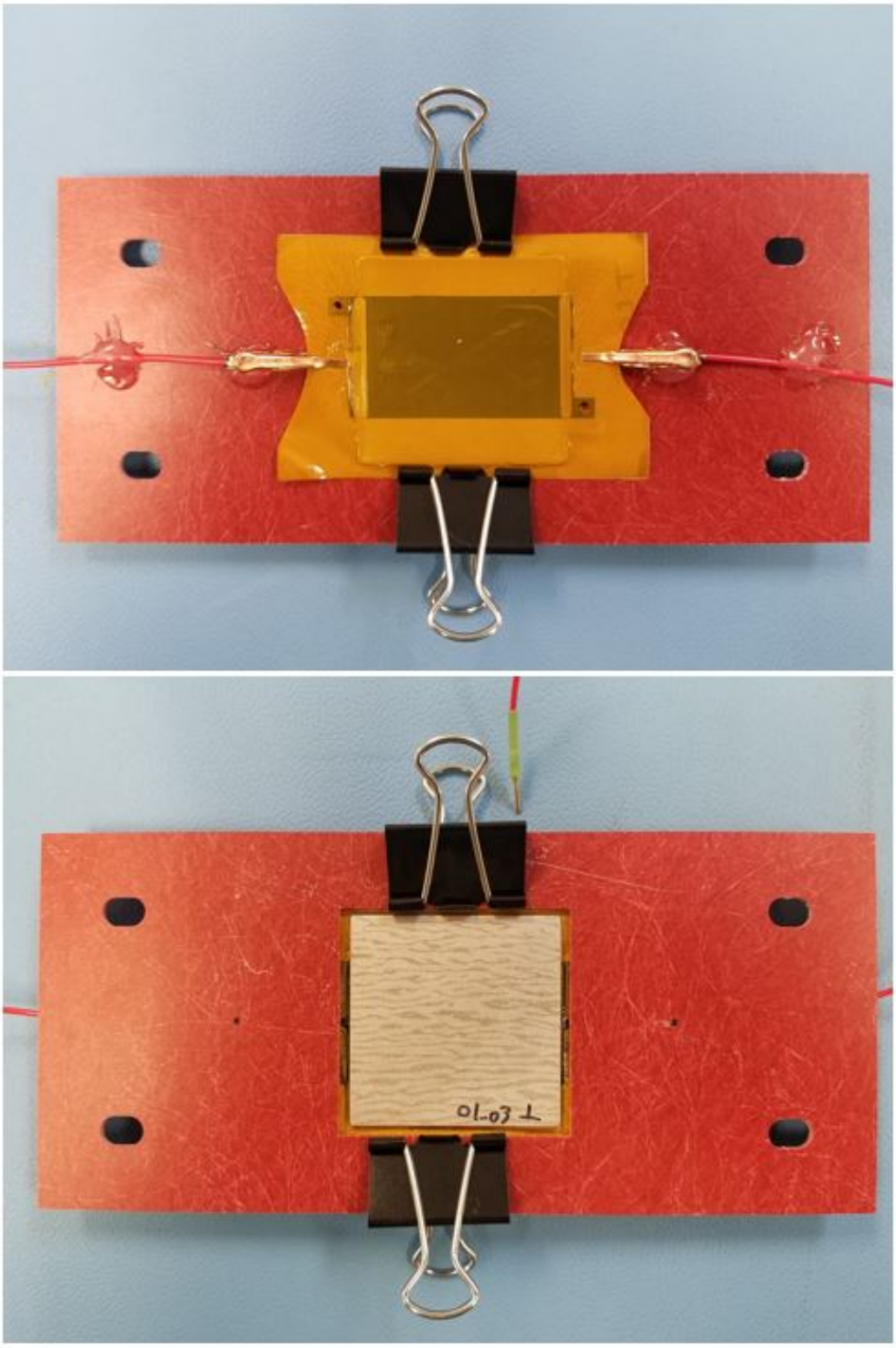

Figure 3.37: Example of the specimen mounted in the custom PCB specimen mount using binder clips and electrically connected via alligator clips

To position the custom mount in the chamber it is fastened to an extruded aluminum frame as shown in Figure 3.38. The frame is constructed such that the specimen mount is at the same level as the view port being used when the frame is in the chamber. The assembly orients the specimen perpendicularly to the view port of the chamber with the heat sink facing away from the camera as shown in Figure 3.39. The specimen is spaced 300 cm from the chamber view port.

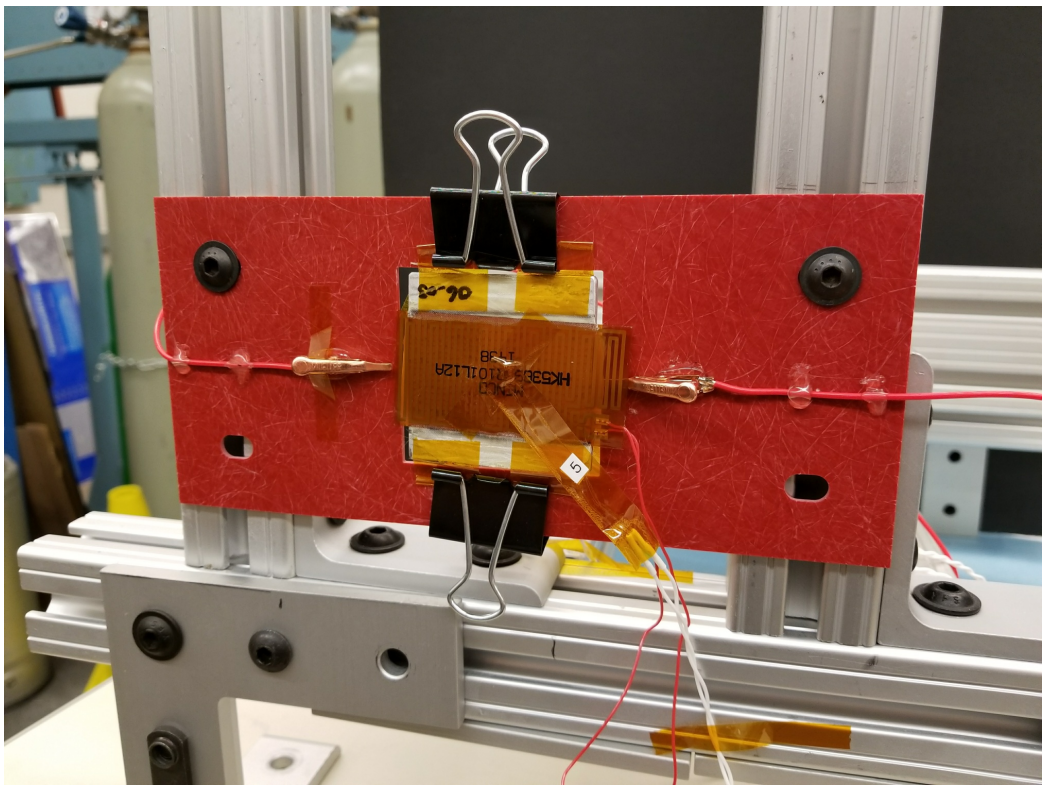

Figure 3.38: Extruded aluminum frame with PCB specimen mount and thermistors attached prior to being placed in the vacuum chamber

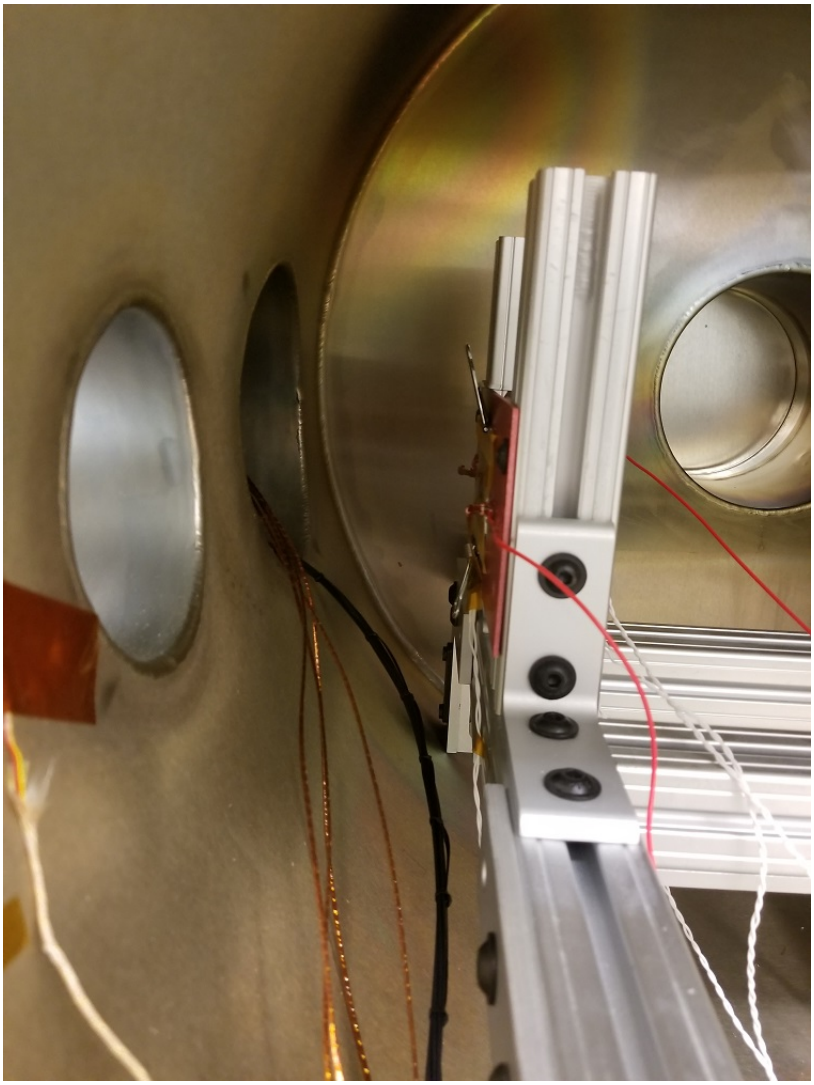

Figure 3.39: PCB specimen mount and extruded aluminum frame positioned in the vacuum chamber

3.5.1.4 Arduino Shield Board Assembly

Standard 8 cell battery packs on-board CubeSats can supply up to 14.7V. As each component on a satellite requires a different voltage, power distribution is usually handled by a power distribution board (PDB). However, for the purposes of these tests, a stand in was developed. The electrical voltage supplied to the heaters in these tests is controlled using an Arduino Mega 2560 and a custom shield board

(PCB schematics can be found in Appendix C) and custom written code (also Found in Appendix C). The components and the assembly can be seen below in Figures 3.40 and 3.41 respectively.

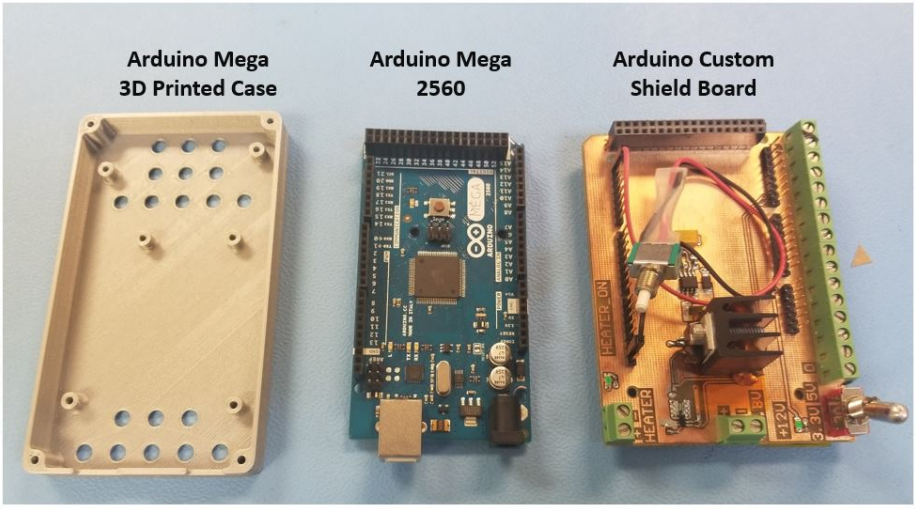

Figure 3.40: Arduino Mega 2560 and custom shield board assembly components

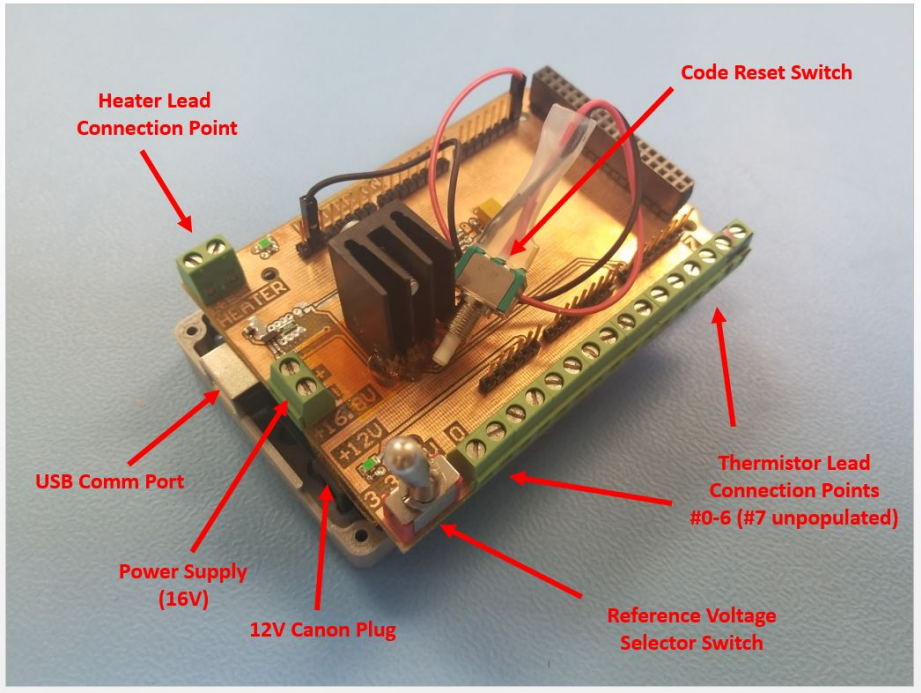

Figure 3.41: Custom shield board features used in testing

The assembly has several key features. The USB Comm port that connects the Arduino board to the laptop allows commands to be sent to the board and readings from the board to be displayed in the serial monitor window of the Arduino software application. Also on the Arduino board is a canon plug receptacle that requires 12V of power to run these tests. On the shield board there is a set of 16V terminals that take in the voltage being sent from the power supply to simulate the satellites battery pack. The Heater Lead Connection point terminals are used to supply voltage to the heater specimen. The Thermistor Lead Connection points are set up to handle inputs from up to seven thermistors (#0-#6) at once (the last port, #7, is unpopulated and therefore is not intended to function). For the thermistors to function they require a reference voltage from the board, for these tests 3.3V is used though a selector switch on the shield allows for the use of a 5V reference voltage if desired. The final feature of the shield board is the Code reset switch which allows any testing to be immediately terminated when the switch is pressed. This resets the code to startup mode and terminates any power being sent to the heater specimen.

While running, the Arduino utilized a Pulse Width Modulation (PWM) device on the shield board to control the amount of voltage being supplied to the test specimen. The code allows for any step size to be used from 0% - 100%. The code starts at the first step increment and progresses up until 100% is reached. Before stepping to the next increment, however, the code is written to allow for the temperature of the specimen to stabilize. Stabilization is deemed to have occurred when measurements from Thermistor #1 (See Figure 3.42 for all thermistor positions) changes by less than, or equal to, 0.25% over the span of 10 seconds.

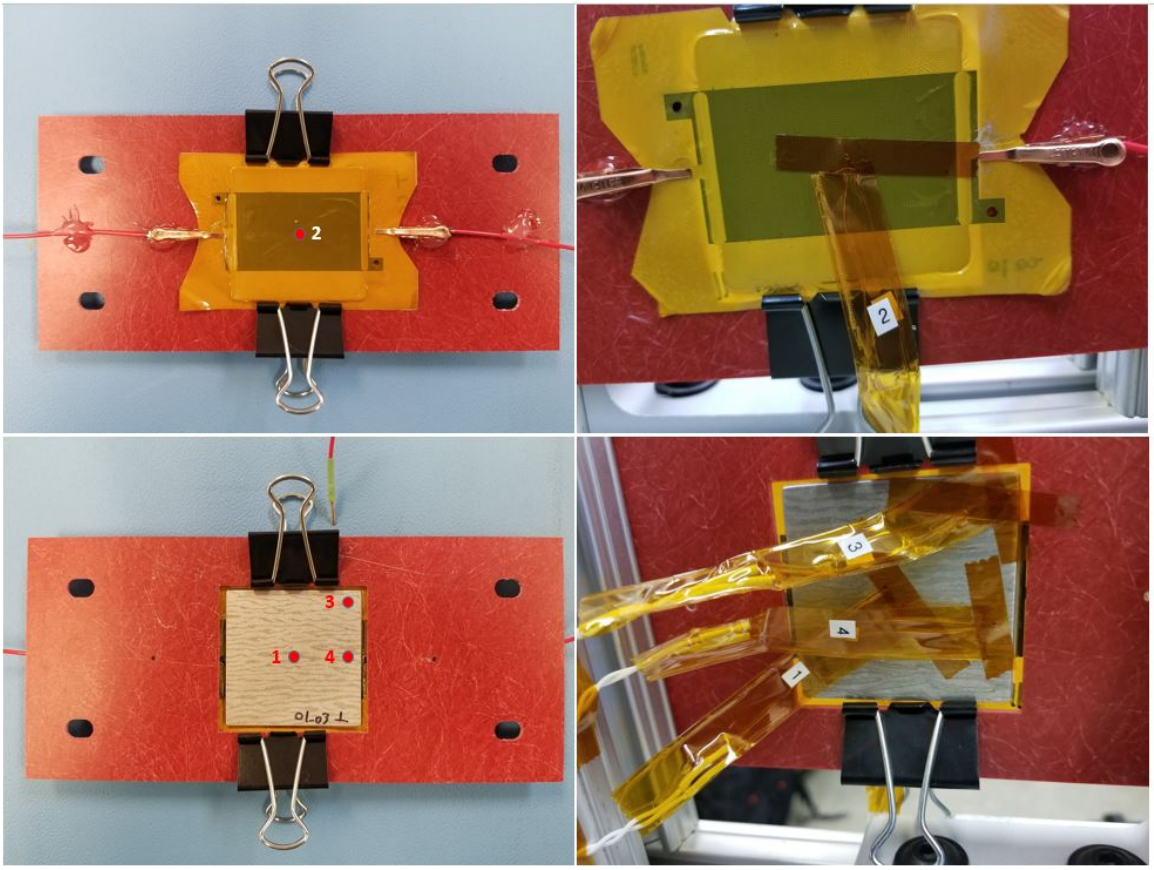

Figure 3.42: Position of thermistors on test specimen for vacuum chamber testing

Once stabilization occurred for the step, the PWM is incremented to the next step and the stabilization process is repeated. Upon reaching stabilization at 100% the voltage being applied is terminated and the specimen is allowed to return to +/- 0.5°C of ambient temperature before the next test begins. Ambient temperature is measured by Thermistor #0 which is placed against the inside of the chamber wall next to an existing thermocouple. Both the thermistor and thermocouple are located approximately 18 in away from the heater on the same side of the vacuum chamber as the view port being used. Thermocouple readings are occasionally compared to the ambient thermistors readings for validation purposes.

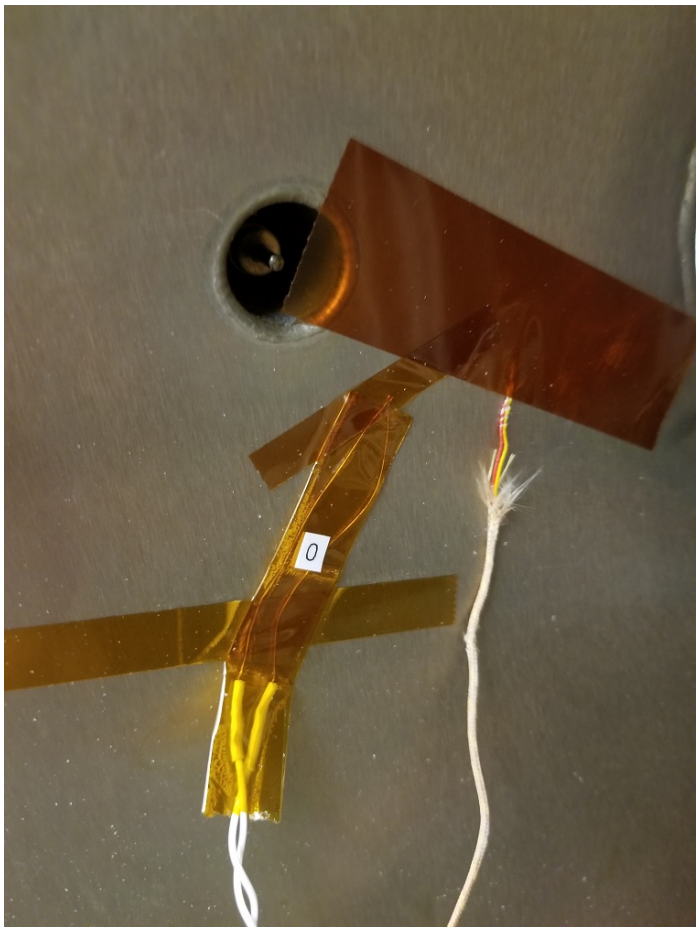

Figure 3.43: Thermistor for reading ambient temperature positioned on wall of vacuum chamber next to thermocouple

3.5.1.5 Data Collection

In addition to Thermistor #0 and #1 mention above, three other thermistors are used during testing (Figure 3.42 & Table 3.4). The data from Thermistor #2, which was placed directly on the heating element, is the primary focus of these tests. Each of the five thermistors (Thermistors #0 - #4) feeds data back to the Ardiuno and is displayed in the Serial Monitor window on the attached laptop. The data from testing is then captured from the Serial Monitor window and recorded for later analysis.

Table 3.4: Thermistor Position and Pass Through Lead Designation

Thermistor #	**Pass-through Leads**	**Location of Thermistor**
0	1,2	On inside wall of vacuum chamber (near thermocouple)
1	3,4	Center of heat sink face (side opposite the heater)
2	5,6	Center of heater face (opposite #1)
3	7,8	Corner of heat sink (side opposite the heater)
4	9,10	Center of outside edge of heat sink (over electrical strip)

3.5.2 Vacuum Chamber Specimen Test Plan

For these tests the vacuum chamber was held at 6 +/-3 $\mu Torr$. The temperature of the chamber could not be controlled so internal temperatures reflected the ambient temperature of the test room. All other details are in the following test plan.

First, the resistance of each of the three types of specimens to be tested was recorded (RS100, CNT, and Etched Foil). (Note: this is not the total resistance of the system but merely a baseline to calculate the appropriate voltage settings). For the RS100 (140 Ω) and the etched foil heater (101 Ω) the full 16V available could be used without exceeding the 5A maximum rating on the power supply according to equation 3.2.

$$V = I * R \tag{3.2}$$

Where V is voltage in Volts, I is current in Amps, and R is resistance in Ohms(Ω). However, for the CNT (1.0-1.5 Ω) the current from the power supply would reach 5A between 5V-7.5V. Therefore, the full 16V available was not usable. Using the etched foil heater as a baseline, and equation 3.3 to determine the top end of the power

being used by the etched foil heater, the necessary voltage setting for the CNT was calculated such that it would use approximately the same amount of power as the etched foil heater. The measured and calculated values are shown in Table 3.5.

Table 3.5: Heater Voltage Settings and Expected Power Usage

Heater	**Resistance (Ω)**	**Voltage (V)**	**Current (A)**	**Power (W)**
Etched Foil	101.0	16.00	0.16	2.53
RS100	140.0	16.00	0.11	1.83
CNT	1.0	1.60	1.60	2.56

$$P = \frac{V^2}{R} \tag{3.3}$$

Where P is power in Watts, V is voltage in Volts, and R is resistance in Ohms(Ω). The power used by the etched foil heater at 16V would be 2.53W. Calculating an average resistance of 1.0 Ω from multiple CNT specimens, the CNT would need to receive 1.60V to consume the same amount of Watts as the etched foil heater does at 16V. The Ardiuno code was written to increment from 0% - 100%, however with the CNT specimens only needing 1/10th the amount of voltage as the RS100 and the etched foil heaters, and the code not capable of incrementing up to only 10% and stopping, the power supply was adjusted to 1.60V for the duration of the CNT testing. Incrementally increasing the PWM from 10% to 100% was defined as one test cycle. Each specimen was subjected to five subsequent test cycles with a return to ambient temperature between each. This data was captured and documented in Chapter 4.

Additional tests are performed to determine the different heaters ramp characteristics (how quickly heat generation increases when 100% of available power is applied

at once). The etched foil and RS100 heaters are tested at 16V while the CNT heaters are tested at 1.60V. Once this testing is complete, the CNT heaters will also be tested at several higher power levels that its low internal resistance make it capable of. The results of these tests, again, can be found in Chapter 4.

3.5.3 Summary

Using this approach, characteristics from all three heaters can be compared. From this the effectiveness of the proposed CNT heater can be determined and compared to the existing products on the market. Additionally, determining the properties of the heaters will allow for future design work where strict control of the internal temperature of batteries, as well as other components, is needed.

IV. Results

4.1 Introduction

This chapter will present the results of the testing described in Chapter 3 of this thesis and address the questions posed at the beginning of this research:

Question 1: How can electrical current be applied to Carbon Nanotube (CNT) sheet and polyimide conductive films such that uniform heating distribution is accomplished?

Question 2: What materials can be used to form flexible heaters using CNT sheets or polyimide conductive films?

Question 3: How does the thermal range of CNT compare to those products that are already on the market?

Question 4: What are the pros/cons of the CNT materials thermal properties over existing heating products?

4.2 Results

4.2.1 Applied Current Characteristics of Thin Film Materials Test Results

This section presents the results of the initial 'point contact' and 'full width contact' testing of the CNT and RS100 specimens. The goal of this testing was to create uniform heating across the entire surface of the thin film materials. By testing the effects of current application on thin film materials using a variety of methods, it is possible to determine the best method of applying current to the heater material.

Following the test plan outlined in 3.2 resulted in the following findings.

As explained in Chapter 3, for these tests, the power supply was set at 16V for the RS100 and at 1.5V for the CNT. The power supply was set at 1.5V for the CNT

material so that both heaters would use approximately 1.85 Watts of power.

As can be seen in Figures 4.1 through 4.3, current passed between the two point contacts on the surface of the CNT specimen leads to a non-uniform heating distribution. Heat is concentrated at the contact points where current passes into, and out of, the material. The current traveling between the two points then spreads out from a line connecting these two points heating different parts of the specimen to various temperatures, leading to little to no heating on the edges. (*Note: The scale on all the following images is given in degrees Celsius)

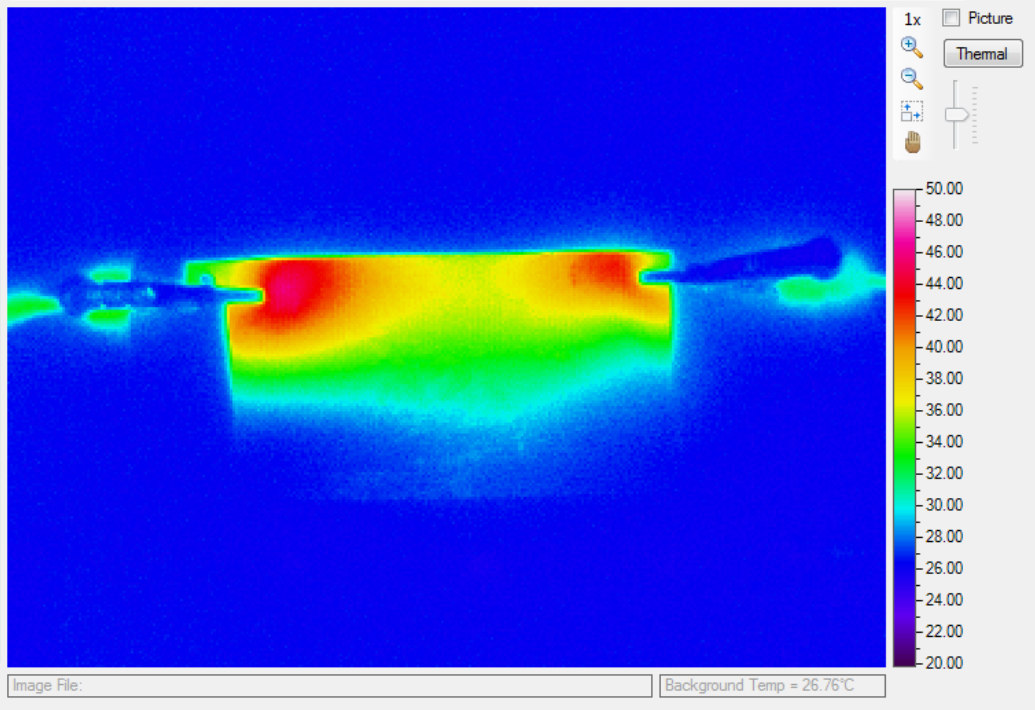

Figure 4.1: Thermal distribution of CNT outside corner points test with 1.6V applied

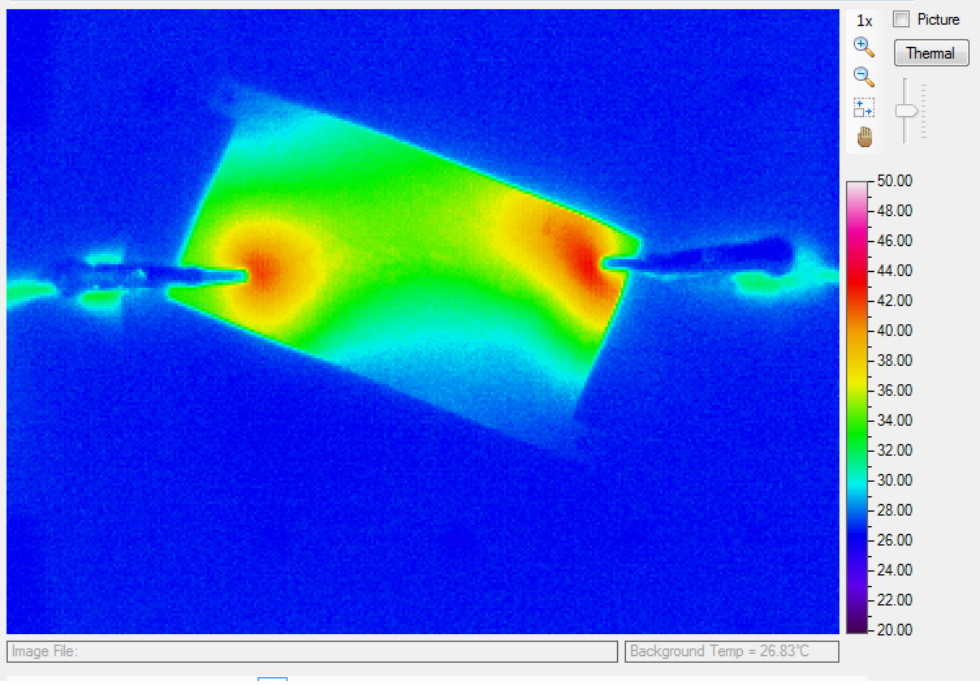

Figure 4.2: Thermal distribution of CNT opposing corner points test with 1.6V applied

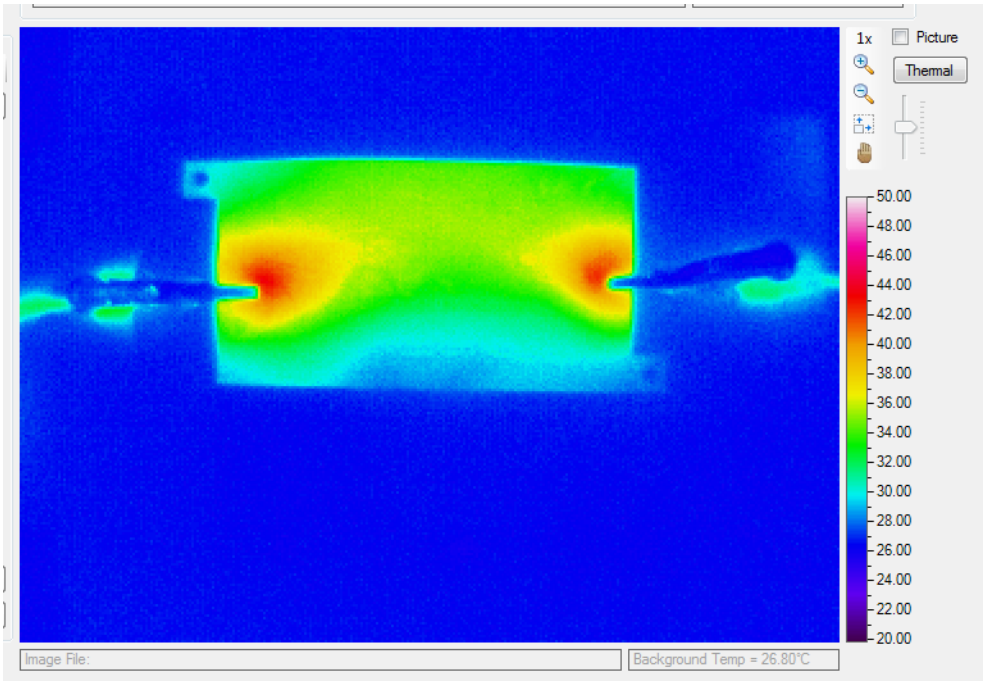

Figure 4.3: Thermal distribution of CNT centered points test with 1.6V applied

Demonstrated in Figures 4.4 through 4.6, the RS100 specimen experienced a similar heat distribution as the CNT specimen, although more heat was generated by the RS100 than the CNT. Heat generation appears greatest at the contact point as was the case with the CNT specimen. Unlike the CNT specimen, a clear line of heating cannot always be seen between the two points of contact of the RS100.

This result was expected as current will follow the path of least resistance. The point contacts do not direct the current to all areas of the thin film materials, therefore this method will not work in creating heaters with uniform heat distribution and may be ill-suited for the required application.

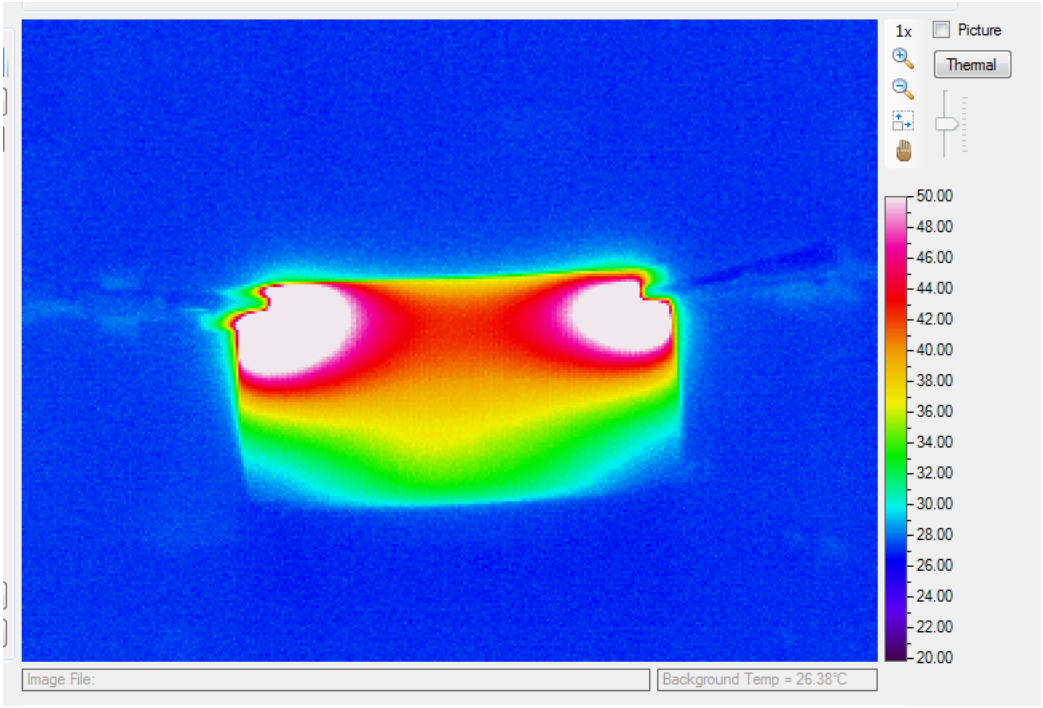

Figure 4.4: Thermal distribution of RS100 outside corner points test with 16V applied

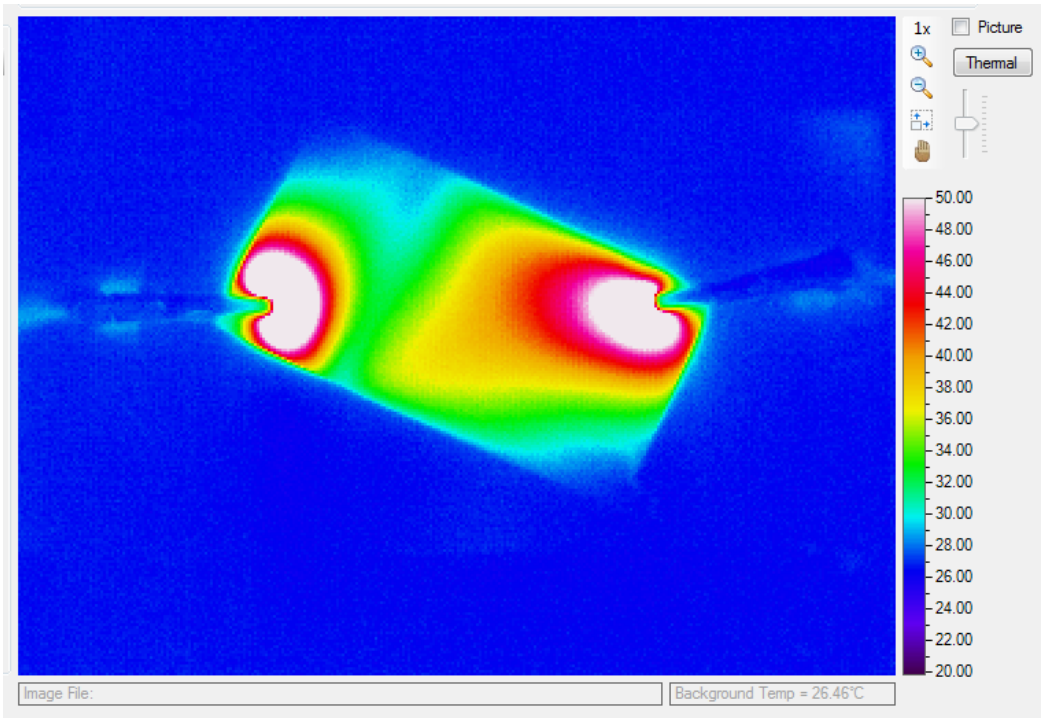

Figure 4.5: Thermal distribution of RS100 opposing corner points test with 16V applied

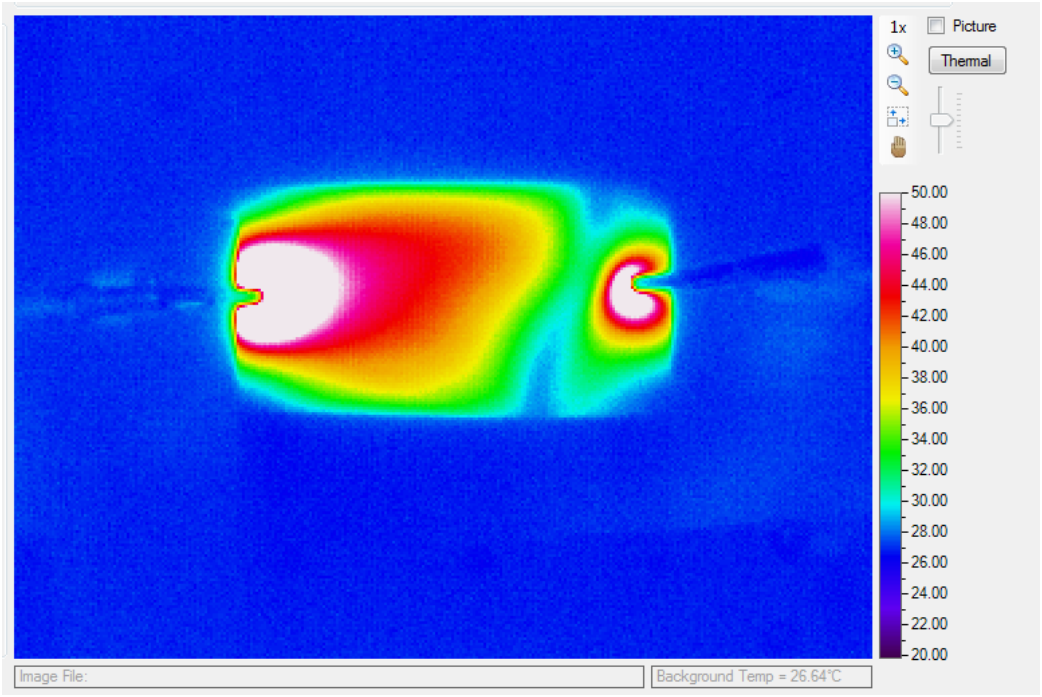

Figure 4.6: Thermal distribution of RS100 centered points test with 16V applied

By replacing the two point contacts with full width contacts gives the thermal distribution shown in Figure 4.7. In contrast to the two point method, specimens with full width contacts form more than one path for the current to follow and a much broader current channel into the material. The core of the specimen shows the highest thermal region, though the majority of the specimen is within 4°C. Thus the resulting heat distribution is more uniform without any hot spots. It was noted that the small red spots in the thermal image coincided with imperfections in the CNT specimens surface and are therefore not hot spots.

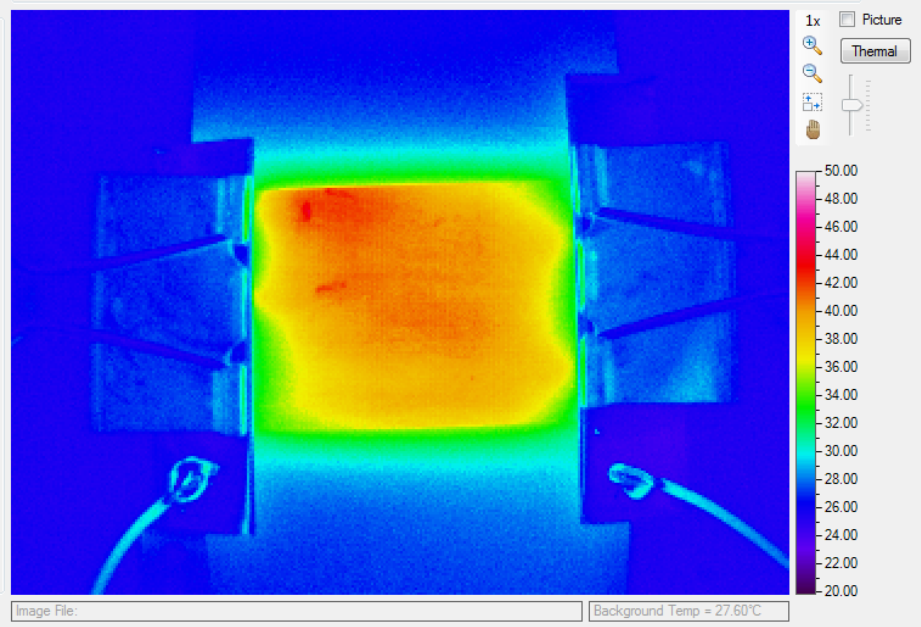

Figure 4.7: Thermal distribution of CNT full width contacts test with 1.6V applied

The RS100 is shown to have a higher thermal range than the CNT at the same power usage. The thermal distribution, like the CNT, is more uniform than it was previously, however it is apparent that the region of greatest heat generation is focused at the midpoint between the two full width contacts. In Figure 4.8 the core of the specimen saturated the camera sensor while the edges of the specimen still remain relatively cool despite the full width contacts.

Though both used the full width contact terminals, the CNT film heater visibly generated more uniform heating than the RS100. The RS100 thin film reached higher temperatures but the focused nature of the heating distribution may cause other problems in future use.

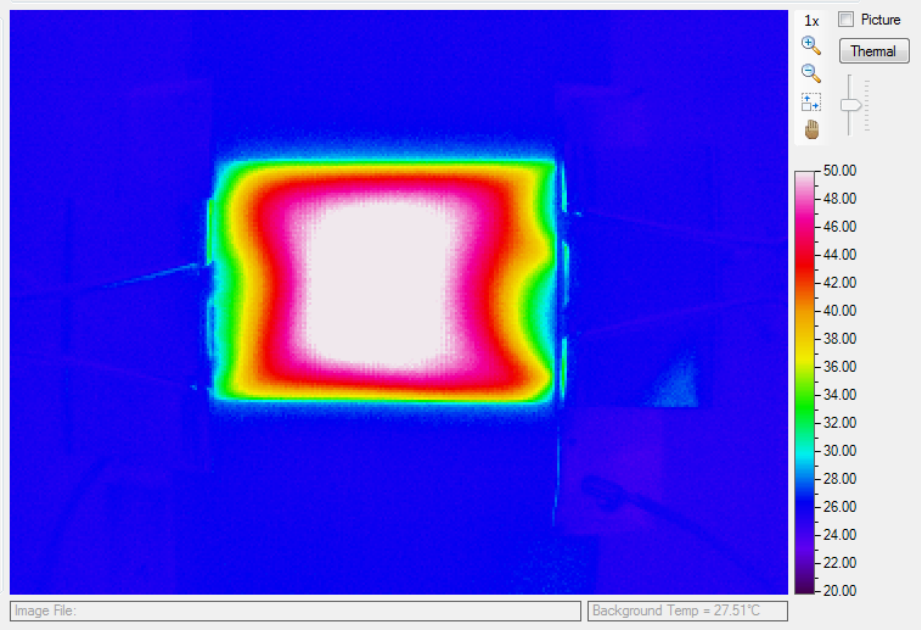

Figure 4.8: Thermal distribution of RS100 full width contacts test with 16V applied

The results from this testing led to the circuit design used in Section 3.3.2 of this report to facilitate the fabrication of the test specimens. The section below explains the results of the fabrication processes.

4.2.2 Fabrication Method of Comparable Heaters Results

This section presents the results of the manufacturing process of the thin film heaters including the best practices and the lessons learned. Of particular interest in this study were the feasibility and benefits of using printed conductive ink circuitry and adhesive Kapton® substrate.

The benefits of using the Voltera V-One circuit printer were the ease of setup and rapid prototyping capability. Using the V-One printer allowed for several changes to be made to the printed circuit design without causing delays in the development schedule. The downside to the process, as mentioned previously, was the inability to get standardized ink deposition. The ink output levels were adjustable on the V-One

but even with the same settings the V-One was not suitable to producing multiple identical printed circuits. Another downside to using the printed ink circuits was the potential for damage caused by the LPKF press during laminate bonding. Deformation of the printed circuit was noticed post press processing. Further deformation occurred when the heat sink was pressed onto the laminate specimen as is shown in Figure 4.9. Though inspection of the specimens showed no visible breaks, several specimens failed the testing criteria, outlined in section 3.4.3., likely due to damage caused to the printed ink circuits.

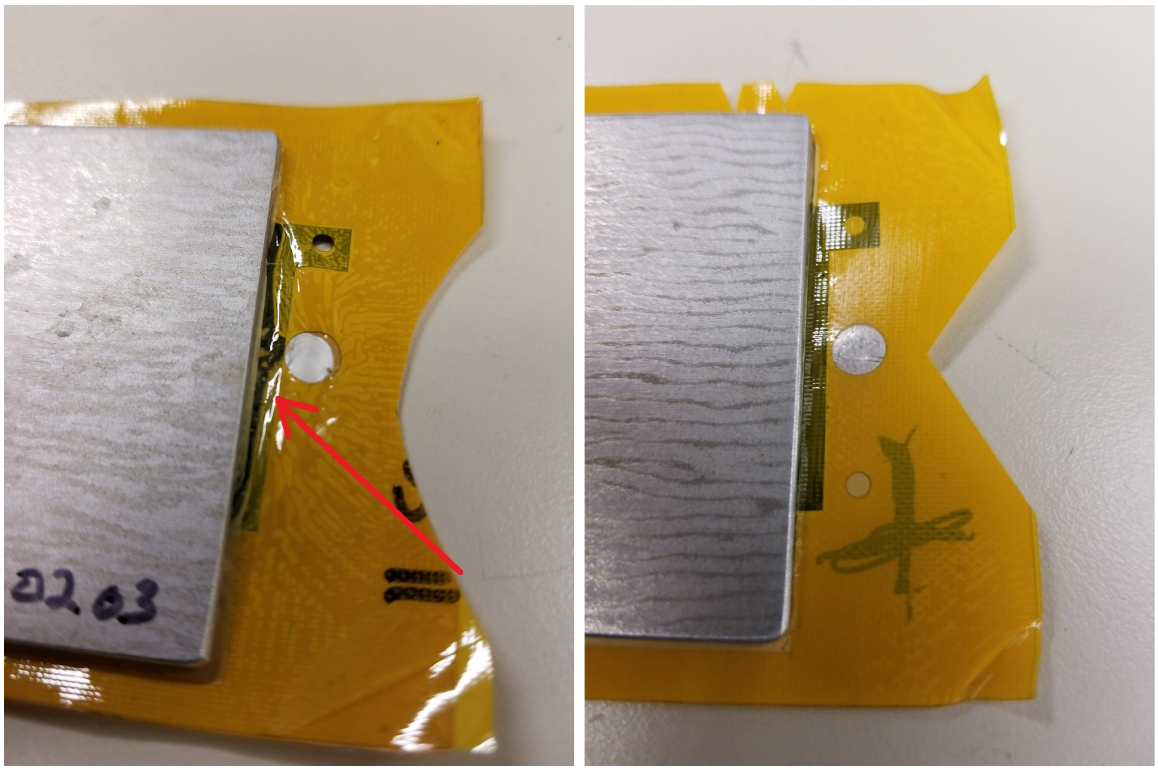

Figure 4.9: (Left) Deformed/damaged specimen post-pressing processing (Red Arrow), (Right) Successful specimen post-press processing

The final issue in specimen preparation was discovered when soldering leads to the terminal pads was attempted. While the conductive ink proved it could be soldered to easily on mosts surfaces, when printed on Kapton® substrate with an adhesive

layer on it the conductive ink failed to facilitate solder flow. Thermal epoxies and liquid solders were also tried but both failed to create a viable connection. Due to the inability to solder to the pads, alligator clips were later used to connect the specimens to the power supply for testing. Testing done by Voltera specialists on test pads provided to them by this study confirmed this phenomenon. It is theorized that a reaction between the adhesive on the Kapton® substrate and the conductive ink is the cause, however future work is required. Aside from the problems described above, specimens that were successfully produced remained flexible and were easily shaped around curved surfaces.

4.2.3 Initial Atmospheric Testing Results of Thin Film Heaters

This initial testing of the thin film heaters outside the vacuum chamber was necessary to determine the thin film's response to current loads prior to vacuum chamber testing. In order to develop the vacuum chamber test plan, the limits on the current range for the RS100 and the CNT were required. As mentioned previously, failure of a specimen while in the vacuum chamber, which may not be immediately apparent, would lead to erroneous data being collected, specimen damage, and schedule slip. As such, both the RS100 and the CNT heaters were first tested at power levels up to approximately 2 Watts. Next, the CNT heater was tested at power levels up to approximately 33 Watts (which coincided with 4.7A for the specimen selected).

4.2.3.1 Low Current Test Results

The following sections outline the results from the low current tests. The voltage supplied to the RS100 heater for this initial testing was incrementally increased from 0V to 16V. The resulting currents, calculated power usages, and maximum observed surface temperatures are recorded in Table 4.1. At the maximum power usage level,

1.824 Watts, visual inspection of the specimen revealed no burning, laminate bubbling, or surface discoloration. The power usage, as calculated from the power supply readings, appeared to remain constant, also suggesting no internal degradation of the specimen either.

Table 4.1: Low Current Power Settings and Results

RS100 Film Heater				**CNT Film Heater**			
Voltage (V)	**Current (I)**	**Power (P)**	**Temp (°C)**	**Voltage (V)**	**Current (I)**	**Power (P)**	**Temp (°C)**
0.00	0.000	0.000	21.8	0.00	0.000	0.000	21.8
2.87	0.020	0.057	22.4	0.20	0.100	0.020	22.0
6.45	0.046	0.297	23.2	0.50	0.330	0.165	22.6
8.84	0.062	0.548	24.8	0.76	0.540	0.410	22.8
11.23	0.078	0.876	26.3	1.16	0.825	0.957	23.9
13.65	0.097	1.324	28.3	1.41	1.042	1.469	24.7
16.00	0.114	1.824	32.0	1.66	1.240	2.058	26.2

**Note: all temperatures are approximations based off of captured thermal images*

Using a similar increment approach for the CNT film heater, the voltage was increased from 0V to 1.66V. This resulted in a maximum power usage of 2.058W. Results of these tests can be found in Table 4.1. At the maximum power level no internal degradation or external deformations were apparent. This was as expected given the low internal resistance of the CNT specimens.

All thermal images captured from these tests can be found in Appendix A.

4.2.3.2 High Current Power Settings

Following on from low current testing, CNT specimens were tested with much higher current loads. For the initial testing of the RS100 specimen testing could only be run at a maximum of 16V (0.114A) or about 1.824W. However, with such a low internal resistance and up to 16V available, the CNT was capable of using more than the 2 Watts it was tested at before. Using specimen Type 1 for this test, and incrementing the current load from 1.25A up to 5A (the maximum available from the power supply) in 0.25A steps, produced the results which can be found in Table A.6.

During testing, at no power level was external deformation or internal degradation apparent. An item of note during this testing was that hot spots, as shown in Figure 4.10 captured from the IR camera, appeared at the electrical contact points. This seems to indicate that the conductive ink had areas of higher resistance when compared to the CNT material. This may be an indication of damage to the ink during the fabrication process or a flaw in the circuit design.

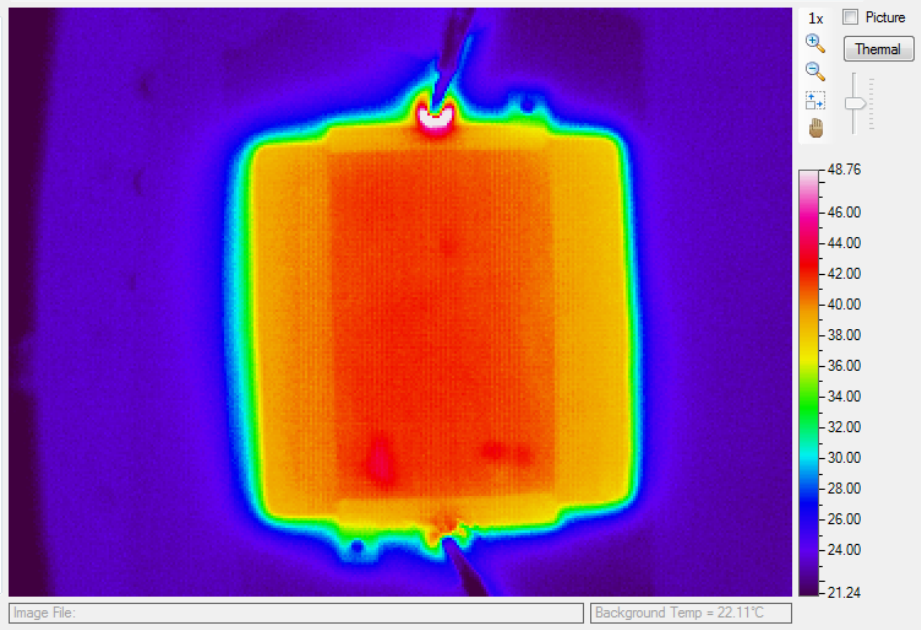

Figure 4.10: Thermal distribution and electrical terminal hot spots (higher resistance points) of a CNT specimen in atmosphere

All thermal images captured from these tests can be found in Appendix A.

4.2.4 Comparative Testing Results of Heaters in Vacuum Environment

This testing involved the use of a vacuum chamber held at 6 +/-3 $\mu Torr$. The chamber used was not equipped to control internal temperature so all testing was done at ambient temperature, between 22°C-27°C. Ambient temperature readings for each test can be found in Tables A.7-A.24.

Each specimen was cycled through testing five times to ensure an adequate data sampling. Figure 4.11 shows an example of the testing results. The remainder of the test results can be found in Appendix B, Figures B.1-B.15.

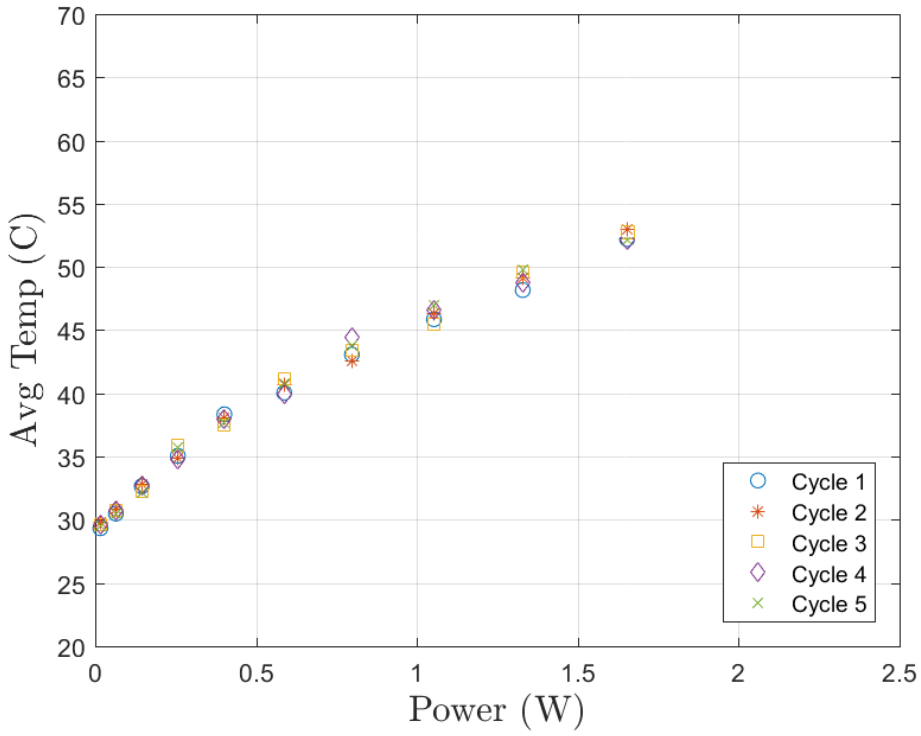

Figure 4.11: Temperature comparison plot of the five test cycles performed on CNT Type 1 Specimen 1

While the data does fluctuate, the trend for each specimens profile remains fairly

consistent. There appears to be no correlation between the number of cycles and the change in temperature profile. If this were not the case, the temperature profile would either progressively increase or progressively decrease through subsequent testing. This indicates that while the material is being thermally cycled that, at these power settings, it is not showing signs of fatigue or degradation. More extensive cycling tests would need to be performed to determine if there are any long term effects.

Next the consistency of the manufacturing process was examined. Three specimens of each type of heater were manufactured and tested. Variations between the different specimens were more apparent than between the cycles of individual specimens mentioned earlier. As can be seen in Figure 4.12, the maximum temperature reached per Watt of power consumed varies between specimens.

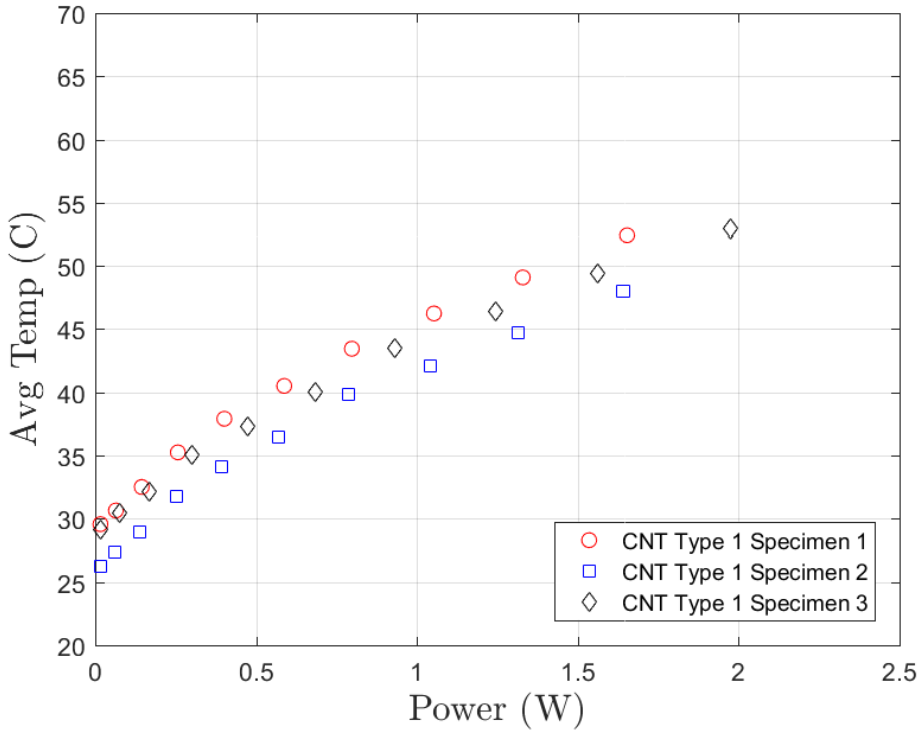

Figure 4.12: Average temperature comparison plot of the three CNT Type 1 specimens tested

The data collected, located in Appendix A Tables A.7-A.24, shows that while the supplied voltage was set at a constant for each test the resulting current, as recorded from the power supply display, varied between test specimens. This may account for the variations in temperatures between samples.

Multimeter testing confirmed that specimen resistance varied between 1.1-1.4 Ω. Using Equation 3.2 and the measured, the total system resistance was determined to vary from 1.46-1.78 Ω between specimens. With nothing in the system being altered between tests, this suggests that the fluctuations in the specimen resistance are being caused by variations in the CNT. Measured specimens of CNT cut from the same sheet as those used in testing showed that the resistance of the CNT alone had a range of 1.11-1.18 Ω with an average of 1.14 Ω for perpendicular grain samples (Specimen Types 2 and 5) and a range of 0.58-0.95 Ω with an average of 0.81 Ω for parallel grain samples (Specimen Types 1 and 4). Variations in the CNT sheet resistance are potentially caused by random orientation of the CNTs alignment or changes in sheet thickness. Another possible source of added resistance is the printed circuits. As mentioned in Chapter 3, the pressing process damaged several specimens. While the specimens tested in the vacuum chamber did pass the screening process in section 3.4.3, their printed circuit resistances could have been altered by the pressing process. Additionally, though each specimens circuit was printed on the same machine and with the same ink, variations in ink quantity and thickness occurred which also could have contributed to variations in resistance. What this means going forward is that the manufacturing process lacks consistency and that the printed ink circuit method may not be the most viable option. Further study into printed circuits on substrates will need to be performed.

Testing also revealed that resistance among specimens was not constant across all temperatures. As can be seen in Figure 4.13, while the etched foil heater and RS100

heater maintained a fairly constant resistance throughout testing, the CNT specimens decreased in resistance as their temperatures increased at a rate of approximately 2%/10°C.

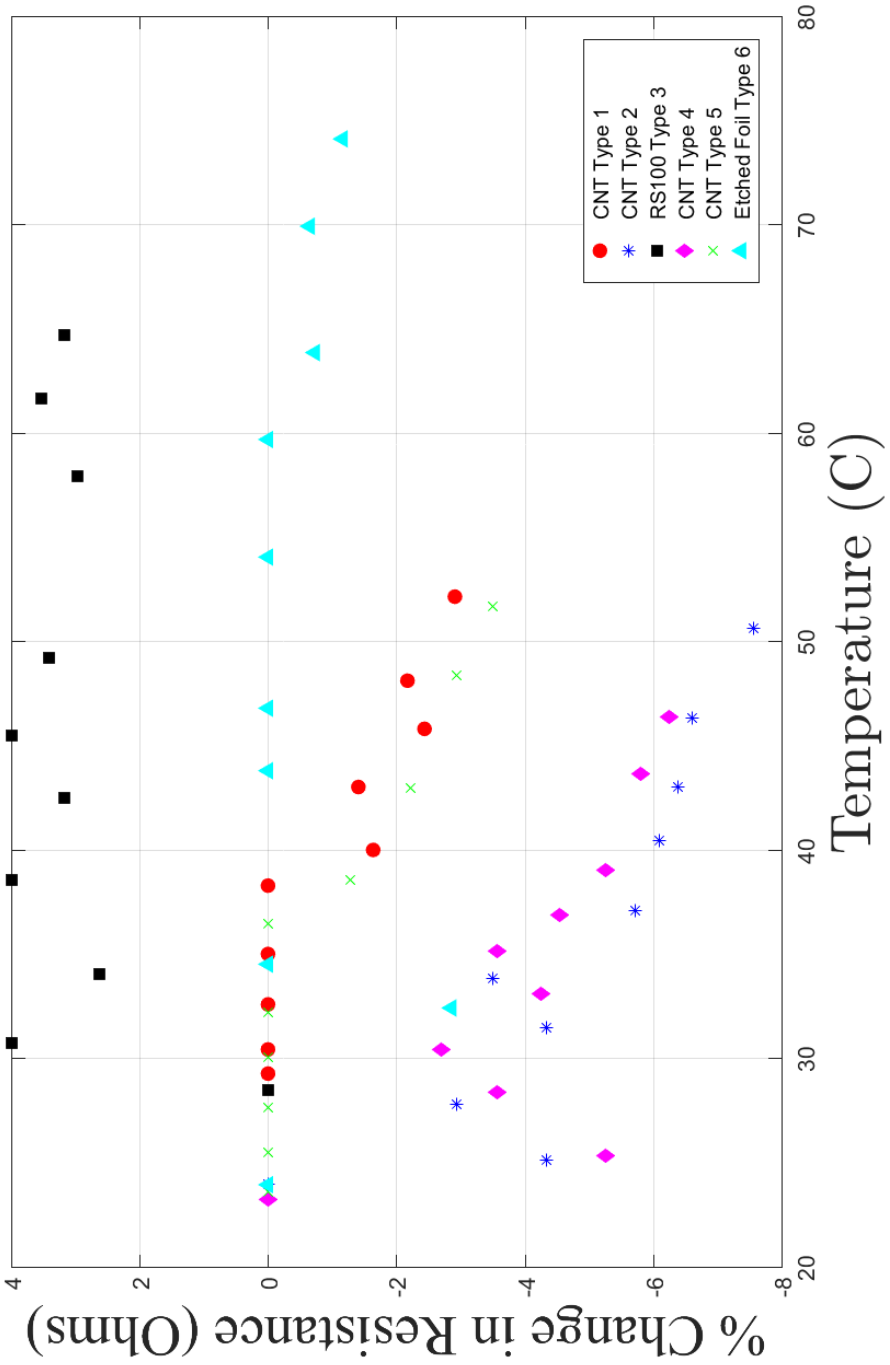

Figure 4.13: Change in resistance of the various specimen types with respect to their temperature

Continuing the analysis of the data shown in Figure 4.12, a 3rd Order Polynomial was found to best fit each of the specimens results. The r-squared values, or correlation coefficients, for these three polynomial fits are 0.9998, 0.9994, and 0.9994 respectively. This indicates that the probability of accurately representing the values between the data points using the polynomial fit line is between 99.94%-99.98%. These trend lines for specimen Type 1 can be seen in Figure 4.14 and the plots for specimen Types 2-6 can be found in Figures B.23-B.27.

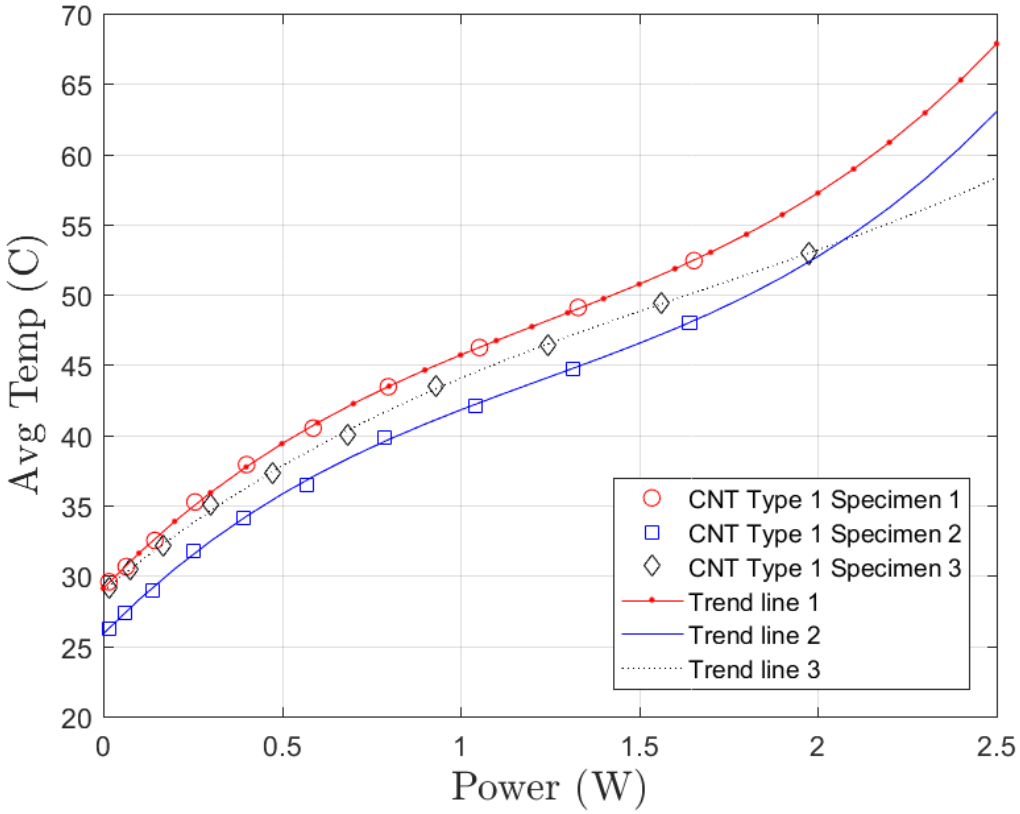

Figure 4.14: This plot shows that a 3rd Order Polynomial curve fitted to the data accurately represents the known data points for Type 1 specimens

The average of these three Type 1 test specimens was taken and can be seen in Figure 4.15 and the plots for specimen Types 2-6 can be found in Figures B.29-B.33. It

is reasonable to represent the data as an average of the three specimen as variations in the CNT material will often result in changes to the temperature profile. An average allows for a baseline in future design work involving CNT thin film heaters.

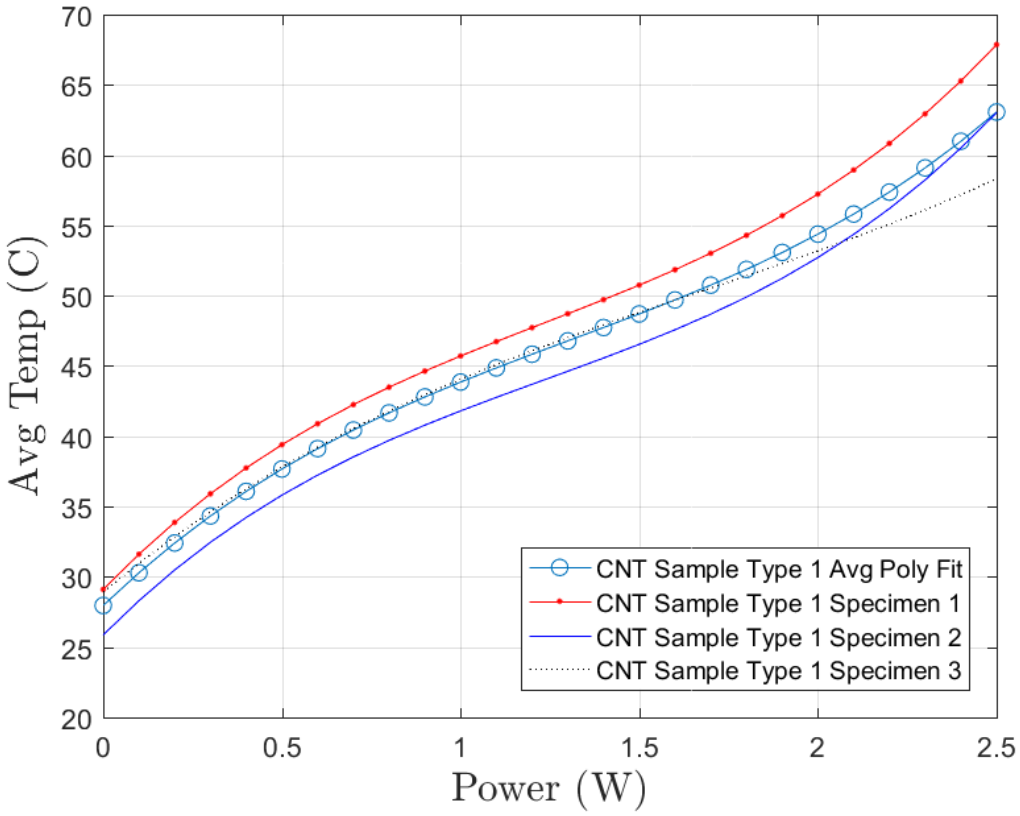

Figure 4.15: The average of the three 3rd Order Polynomial curves plotted with the original fitted curves for CNT Type 1 Specimens 1-3

Finally, the average polynomial fit trend lines for each of the specimen types, including the RS100 and the etched foil specimens, were compared as shown in Figure 4.16. Earlier it was speculated that the different grain orientations would produce different temperature profiles. When averages were calculated and the trend lines compared, the effects of grain orientation appeared negligible for power levels below 2.5 Watts. From Figure 4.15, no clear correlation can be seen between the CNT heater

Type and the temperature profile. Future work in this area will need to be done to determine the thermal effects of further aligning the grain of the CNT specimens and/or increasing the power levels.

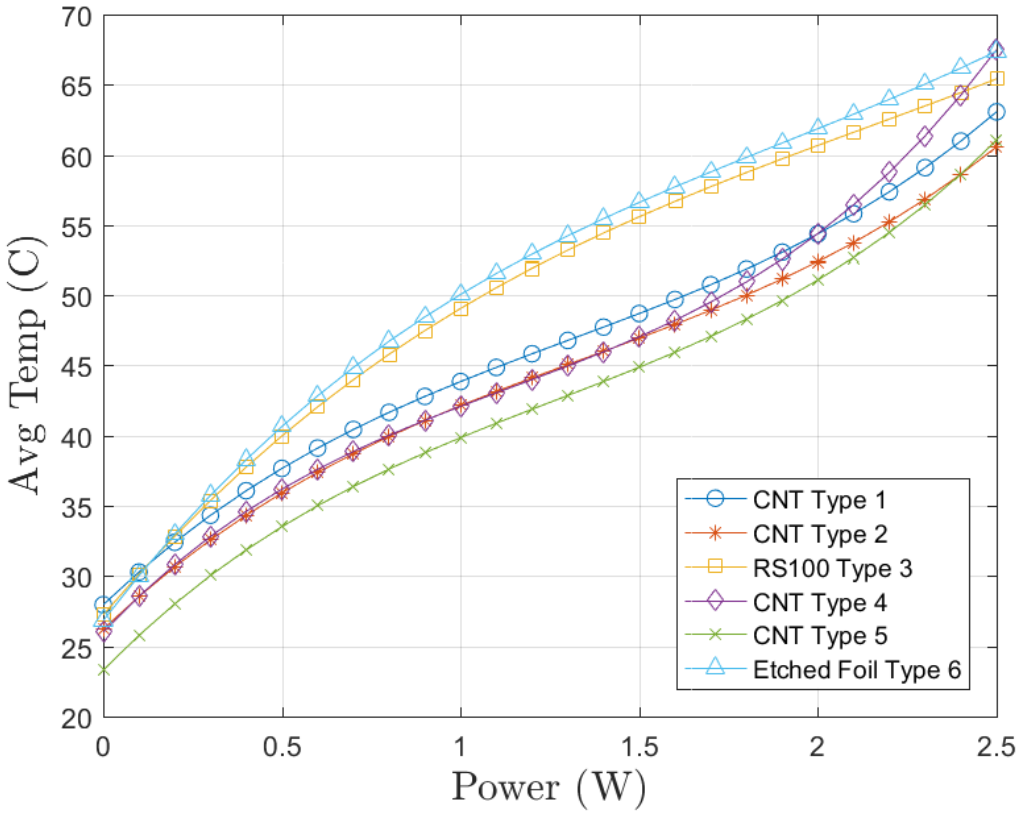

Figure 4.16: Comparison plot of the average trend lines for all specimen types

From the plot above, Figure 4.16, it can be seen that at the lower power levels that the etched foil and RS100 heaters generate more heat per Watt than the CNT heaters. However, it can also be seen that as the power level increases that the CNT heat profile is trending towards an inversion with the etched foil and RS100 heat profiles. Beyond the maximum power consumption of 2.5 Watts for the etched foil and RS100 heaters, CNT heaters continue to increase in thermal output.

In this testing, not only was the thermal output at each power level tested but

also how quickly each type of heater could reach its maximum. This was designated as 'ramp' testing. Each type of specimen was either connected to 16V (RS100 and etched foil) or 1.6V (CNT) from the power supply and the resulting temperature profiles were recorded and plotted in Figure 4.17.

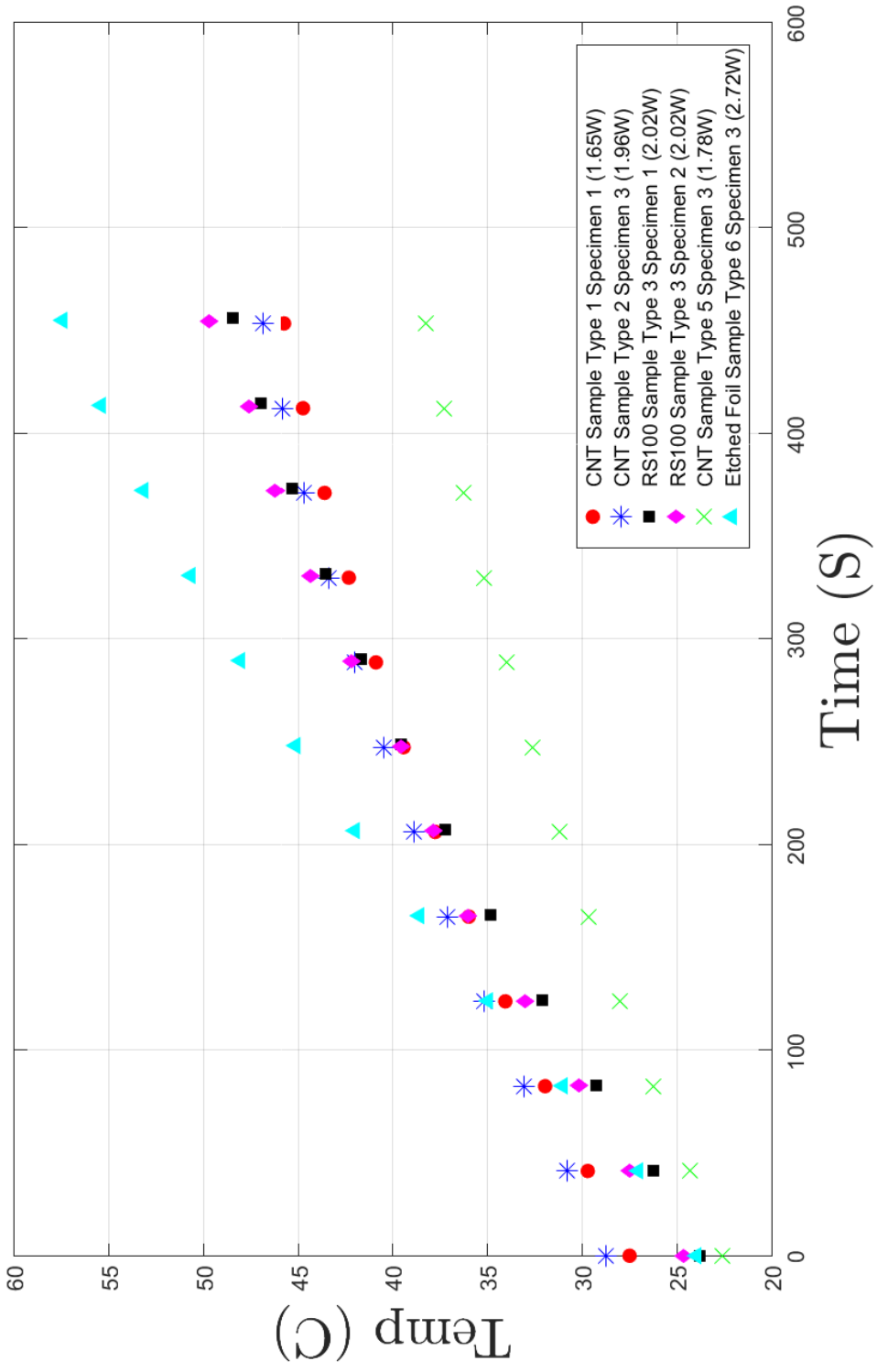

Figure 4.17: Ramp testing data plotted for various specimens across all specimen types

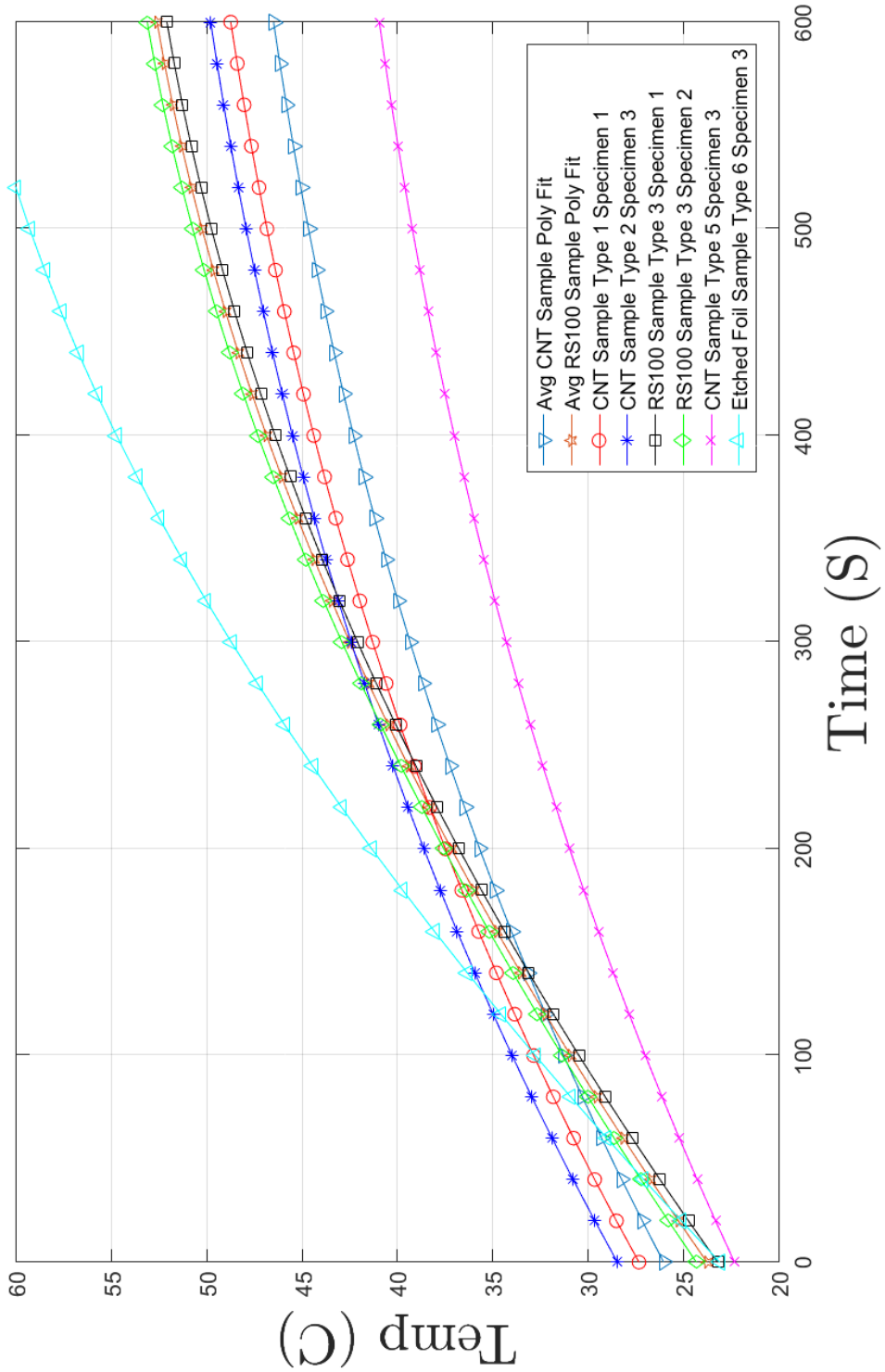

Figure 4.18: 3rd order polynomial fit of all the ramp data and the trend line for the average of each specimen type

3rd Order Polynomial trend lines were found to be an excellent approximation of this data as well with r-squared values ranging from 0.9999-1.0000 (Figure 4.18. The average of the three CNT specimens and the two RS100 specimens tested were included in this figure to show what a baseline for these types of heaters may look like if they were every commercially produced. It can easily be seen that the etched foil heater has a faster ramp response than the RS100 while both were using 16V. At this voltage setting the etched foil was using 2.5 Watts while the RS100 was using 1.83 Watts. The voltage levels for the CNT heaters were calculated and set such that they used 1.83 Watts as well. Their ramp response is shown to be slower than the etched foil heater as well but comparable to the RS100 heaters.

As mentioned before, the CNT heaters do not max out at 1.83 Watts or even 2.5 Watts. Further testing was done to determine the CNT heaters ramp response to higher power levels. The power levels for these test were chosen as 6, 12, 24, and 33 Watts. These power levels corresponded to approximately 2, 3, 4, and 4.7 Amps of current for the specimens used for these tests. The baseline ramp responses of the etched foil and RS100 are included on the graph as well at their respective max power levels. A linear trend line was sufficient to approximate this data and can be seen in Figure 4.19. The calculated ramp rates in $^{\circ}C/sec$ are shown in Table 4.2.

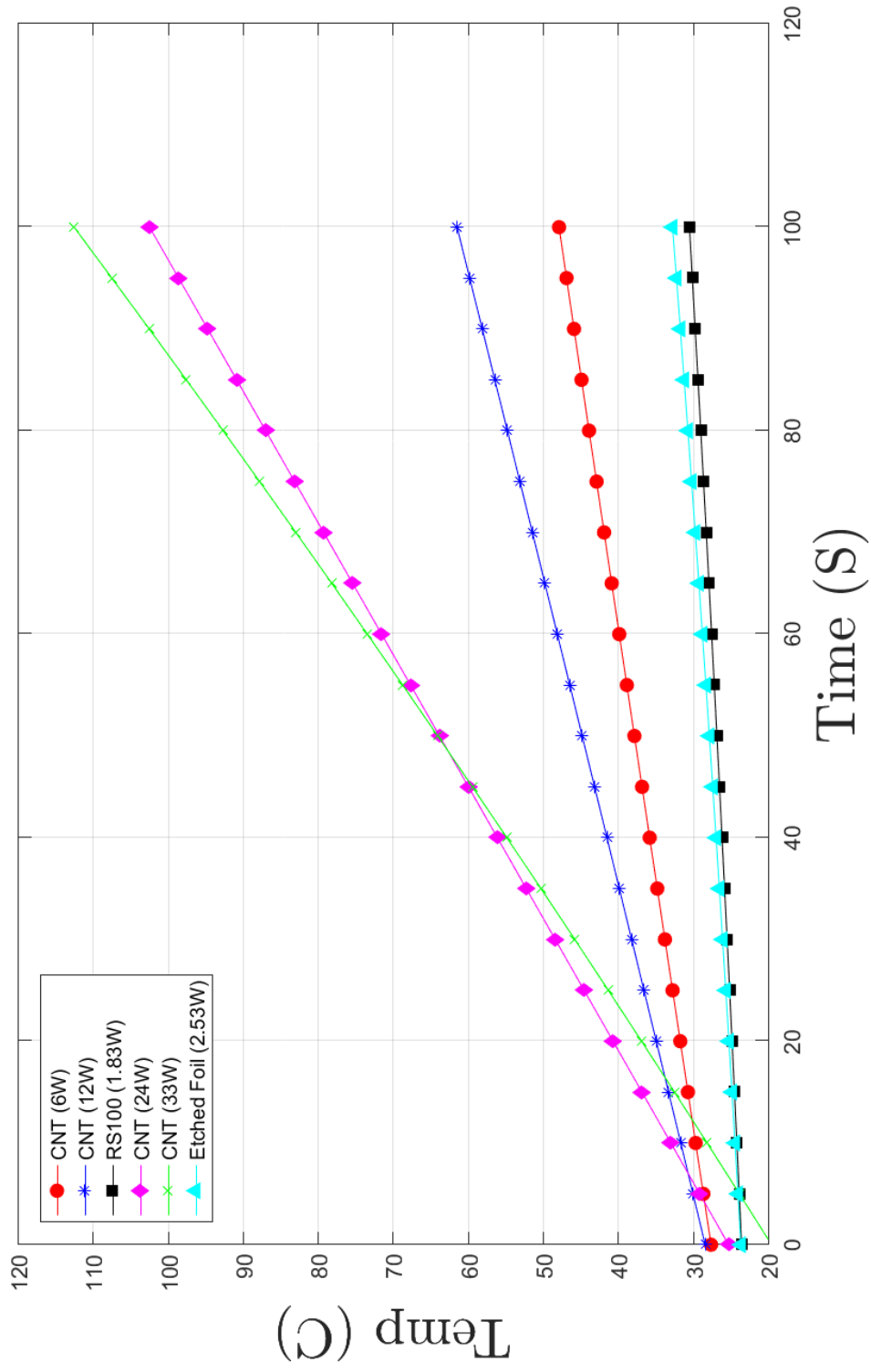

Figure 4.19: Comparison plot of trend lines for the high current ramp responses

Table 4.2: Ramp Response Rates

Heater Type	$^{\circ}C/sec$
CNT (6W)	0.2027
CNT (12W)	0.3308
RS100 (1.83W)	0.0695
CNT (24W)	0.7718
CNT (33W)	0.9297
Etched Foil (2.53W)	0.0911

The benefit in the CNT heaters thermal range and ramp capabilities lies in its ability to supply much higher temperatures to components on-board a spacecraft when they are needed. Additionally, using higher power levels causes the CNT heaters to get up to a desired temperature much faster. Once the desired temperature is reached the power could be reduced and the temperature allowed to stabilize.

4.3 Conclusion

This chapter showed the results of the various tests performed on the CNT thin film heaters as well as the manufacturing processes that were developed to create them. Throughout testing, the RS100 thin film and etched foil heaters were used as a baseline for comparison. Testing showed that the CNT thin film heaters were comparable to the etched foil and RS100 heaters, though, at power levels less than 2.5W they were not able to reach the same temperatures as the etched foil design. It was also shown that, for the limited number of tests performed on each sample, degradation of the CNT specimens was not apparent even at high power levels. Problems did arise in the manufacturing process due to complications with ink application con-

sistency as well as press related damage to the circuits. An unforeseen consequence of the pressing process did arise during vacuum chamber testing. Trapped air in the laminate was allowed to expand, coupled with heat from the sample, which caused delamination of the specimen. One final discovery that occurred during testing was that the grain alignment in the CNT sheets was not sufficient to cause a noticeable difference in temperature profiles between test specimens.

V. Conclusions and Recommendations

The purpose of this study was to analyze the thermal properties, limitations, and physical characteristics of carbon based thin film heaters and to develop means of utilizing them for space vehicle applications. This was accomplished through comparative testing between various configurations of Carbon Nanotube (CNT) sheets, a new polyimide film material by Dupont^{TM}, RS100, and the existing standard of film heaters, etched foil.

5.1 Discussion of Findings

At the beginning of this study, Section 1.7.1, it was asked how could electrical current be applied to CNT sheets and polyimide conductive films such that uniform heating distribution would be accomplished. The theory was that using copper, or similar, conductors spanning the full width of the CNT coupon at each end would produce uniform heating when current was applied. It was also believed that if the conductor was narrower than the CNT sheet or polyimide film, the current would not flow uniformly to all areas. This study found that CNT sheets and polyimide films both require full width terminal current application to successfully heat their entire surfaces. This adds a level of complexity to the design and manufacturing of these thin film heaters.

It was also asked, Section 1.7.2, what materials could be used to form flexible heaters using CNT sheets or polyimide films. Early research showed that substrate materials such as products from Kapton® have been used in the past for space qualified patch heaters. As CNT sheets are very thin and flexible it was believed that they could be applicable to Kapton® substrates without altering their physical or conductive properties. This study found that CNT sheets can be applied successfully to

substrates if that substrate has an adhesive layer or if an adhesive film can be added. It was determined, however, that steps should be taken to minimize the potential for trapped air in the laminate. It was also found that these specimens could easily be formed to a contoured surface. While extensive shape testing was not performed, the specimens maintained most of the flexibility inherent in their parent materials. This allows them to be formed to any shape that the substrate material or the CNT sheet material was already capable of being formed to.

Addressing the question posed in Section 1.7.3, the thermal range of CNT thin film heaters when compared to other products on the market was the next area of study from the beginning of this research. With a lower resistance value, using the same power source as for etched foil heaters, it was estimated that the top of the thermal range would be much higher for CNT heaters. When compared to the etched foil and polyimide film heaters, it was found that the CNT thin film heaters tested in this study were not as efficient, lower temperature per Watt. However, because of its low internal resistance, the thermal range of the CNT heater was proven to be far greater than either of the other two. This is a beneficial feature for applications requiring higher temperatures with limited voltage availability.

The final question to be answered by this research, Section 1.7.4, is what are the pros/cons of the CNT thin film heaters over existing heating products. It was theorized that CNT sheet material would be less susceptible to total failure than etched foil heaters. It was also predicted CNT should be able to heat larger areas using the available on-board power. It was found during the point contact testing that current will continue to flow through the thin film materials so long as there is a complete circuit. While this is also true for the etched foil heaters, thin film materials provide a much broader area for current to flow. If an etched foil design were to sustain damage it is almost certain that its single circuit would be severed and

total failure would occur. Similar damage to part of a film material would not result in failure, though, as was shown, the thermal distribution would be altered. With the inability to service spacecraft, this resiliency of on-board components is crucial to mission success.

5.2 Implications for Practice

Using CNT sheets as thin film heaters was the main focus of this study. This research showed that CNT thin film heaters offer capabilities that current products do not. These thin film heaters can be applied to a multitude of shapes and of varying sizes. With their low internal resistance these heaters can easily be scaled up to cover much larger areas than the etched foil heaters are capable of heating given a standard CubeSats available on-board power. Finally, given that these heaters are far less susceptible to single point failure, they also offer a higher degree of reliability which is crucial for satellite survivability.

5.3 Future Research

This study mainly focused on the possibility of CNT thin film sheets being used as heaters. While it was shown that they could be used, no tests were done to determine how the thickness of the CNT affected the heating properties. Future work should be done that isolates how varying the thickness of the material affects the heating profile and power consumption.

Another area of study for future work is that of CNT grain alignment and how it affects the efficiency of the heater. As shown in Chapter 3, when CNT undergoes strain its grain structure becomes more aligned. Theoretically the more the grains are aligned the more resistance the material should have when measured perpendicular to the grain alignment.

From the methodology section, it was discovered that printed conductive ink circuits created using the V-One printer yielded non-uniform results. Alternate means of circuit creation should be explored such as screen printed circuits or etched foil circuits.

Finally, research into material fatigue should be conducted. LEO satellites orbit approximately 16 times/day for many years. How the CNT heaters performance is affected by this level of cycling, both at low current and high current levels, is information that could be crucial to proper satellite operation and survival.

5.4 Conclusion

Carbon Nanotube sheets being used as thin film heaters show promise when compared next to etched foil heaters. Further research is required, though, before this can be made a reality. Improvements to manufacturing processes and more extensive testing needs to be accomplished to successfully produce a usable product for use in the space industry.

Appendix A. Test Results Data and Thermal Images

A.1 Initial Atmospheric Testing Results of Thin Film Heaters

A.1.1 Atmospheric Testing of the Heaters

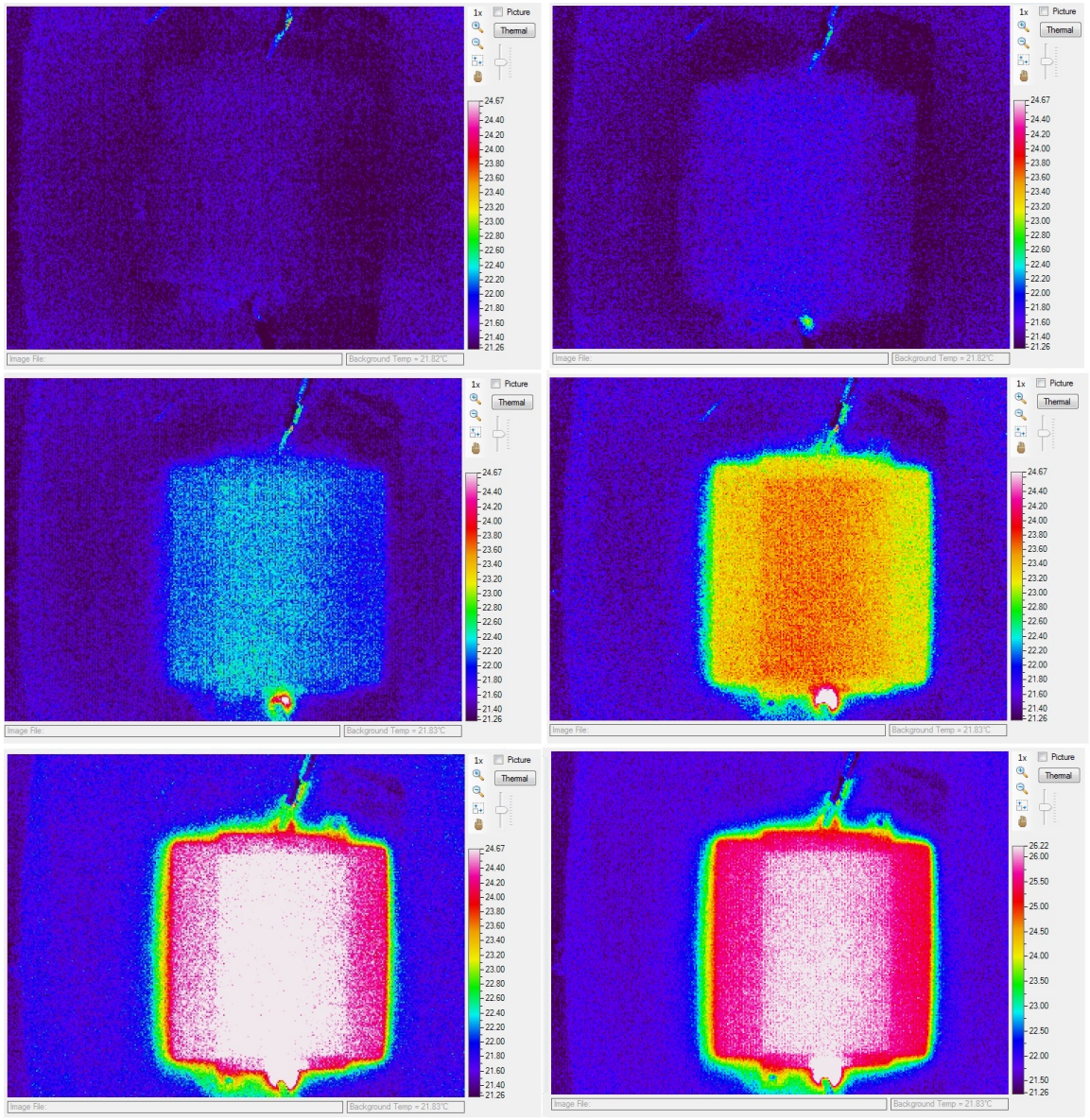

Figure A.1: Initial thermal testing in atmosphere of CNT specimen Type 1 for 0-1.6V applied

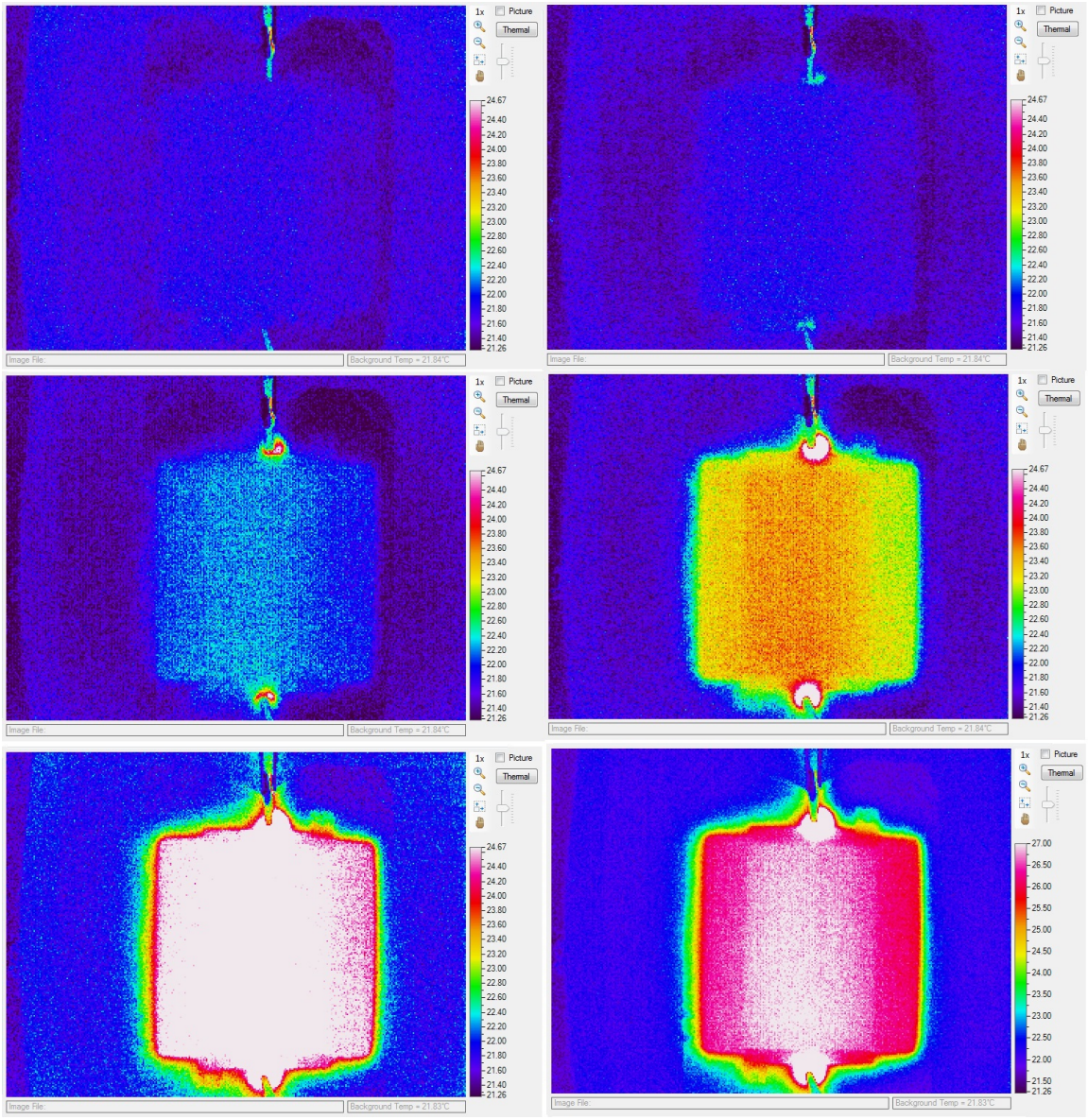

Figure A.2: Initial thermal testing in atmosphere of CNT specimen Type 2 for 0-1.6V applied

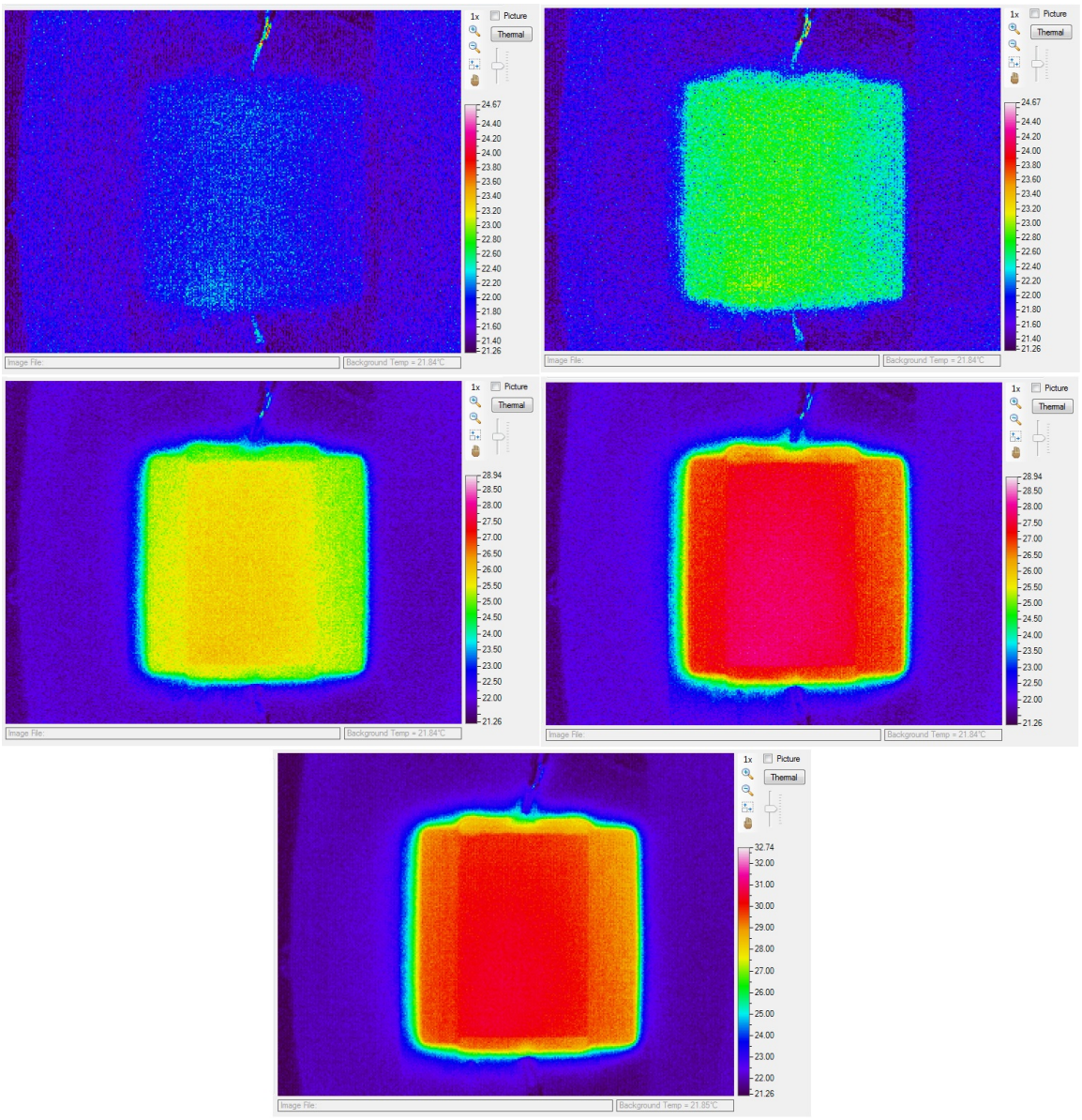

Figure A.3: Initial thermal testing in atmosphere of RS100 specimen Type 3 for 0-16V applied

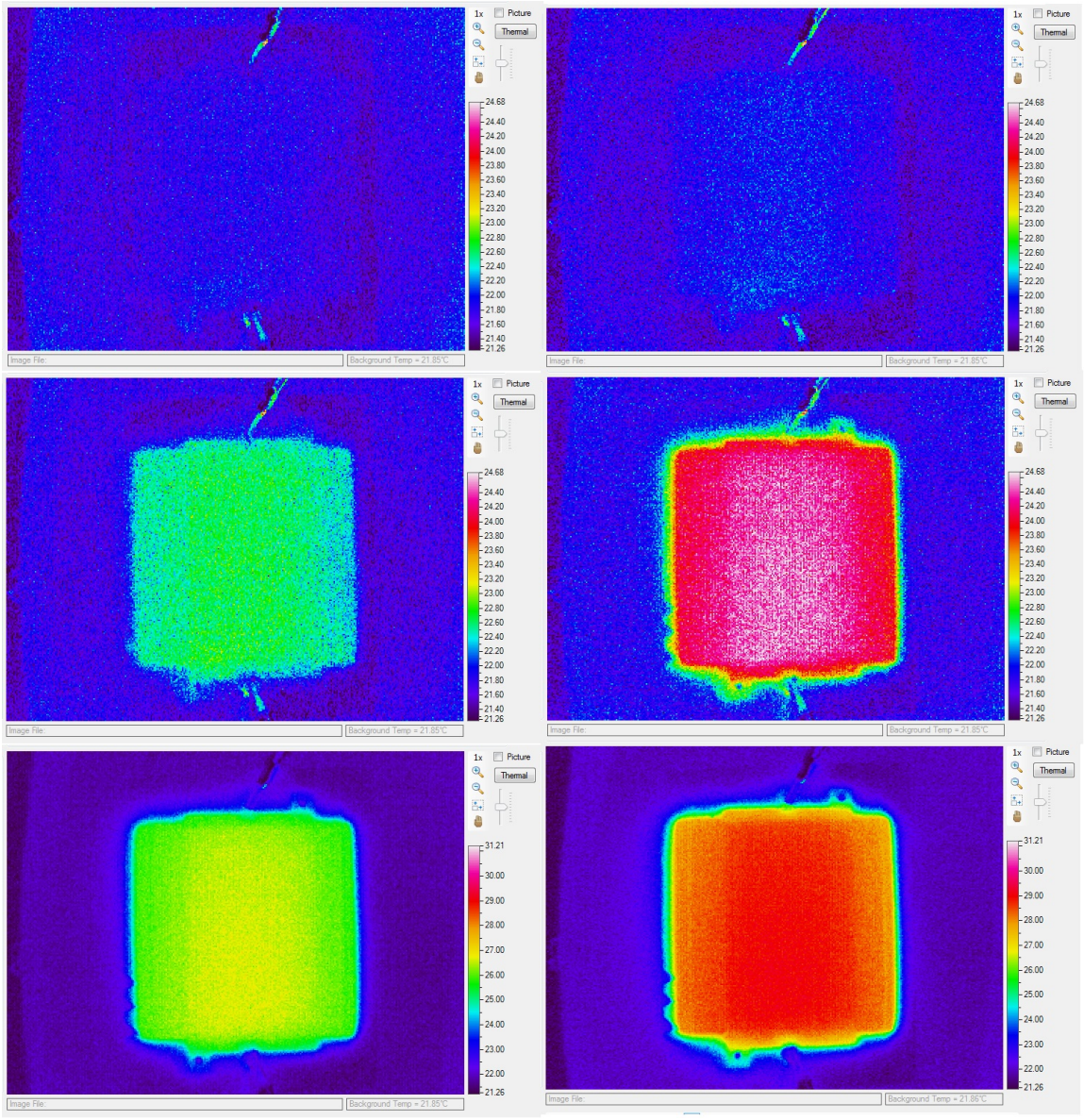

Figure A.4: Initial thermal testing in atmosphere of CNT specimen Type 4 for 0-1.6V applied

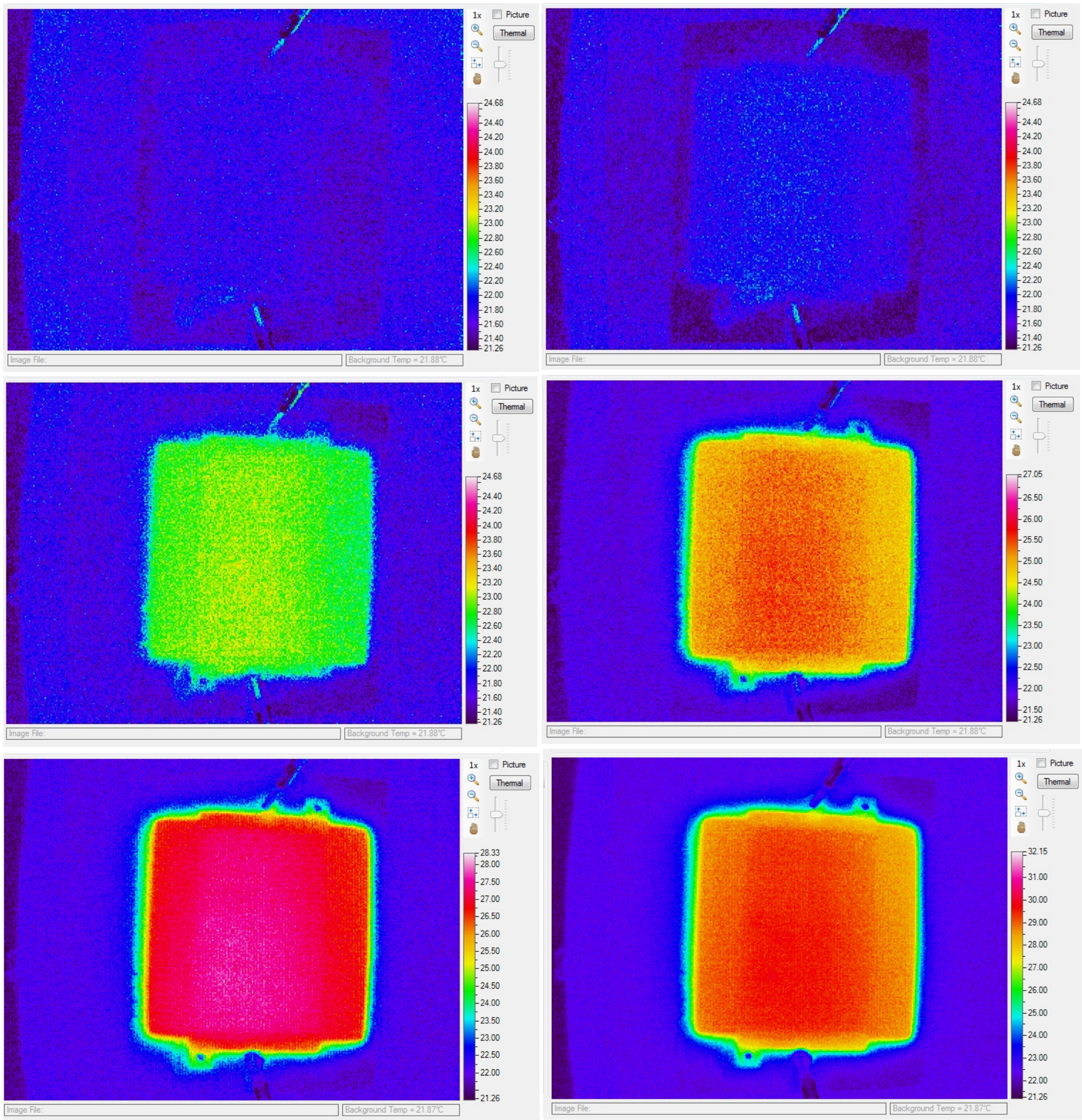

Figure A.5: Initial thermal testing in atmosphere of CNT specimen Type 5 for 0-1.6V applied

Table A.1: CNT Type 1 Low Current Tests

Specimen	**V**	**I**	**P**	**Ambient Temp**	**Max Temp**	**Delta**
01-01	0.00	0.000	0.000	21.82	21.82	0.00
01-01	0.20	0.100	0.020	21.82	22.00	0.18
01-01	0.50	0.330	0.165	21.82	22.60	0.78
01-01	0.76	0.540	0.410	21.82	22.80	0.98
01-01	1.16	0.825	0.957	21.82	23.90	2.08
01-01	1.41	1.042	1.469	21.82	24.67	2.85
01-01	1.66	1.240	2.058	21.82	26.22	4.40

Table A.2: CNT Type 2 Low Current Tests

Specimen	**V**	**I**	**P**	**Ambient Temp**	**Max Temp**	**Delta**
02-01	0.00	0.000	0.000	21.82	21.82	0.00
02-01	0.20	0.103	0.021	21.82	22.00	0.18
02-01	0.50	0.307	0.154	21.82	22.40	0.58
02-01	0.76	0.546	0.415	21.82	22.60	0.78
02-01	1.17	0.874	1.023	21.82	23.90	2.08
02-01	1.40	1.110	1.554	21.82	24.67	2.85
02-01	1.65	1.335	2.203	21.82	27.00	5.18

Table A.3: RS100 Type 3 Low Current Tests

Specimen	**V**	**I**	**P**	**Ambient Temp**	**Max Temp**	**Delta**
03-01	0.00	0.000	0.000	21.82	21.82	0.00
03-01	2.87	0.020	0.057	21.82	22.40	0.58
03-01	6.45	0.046	0.297	21.82	23.20	1.38
03-01	8.84	0.062	0.586	21.82	24.75	2.93
03-01	11.23	0.078	0.876	21.82	26.30	4.48
03-01	13.65	0.097	1.324	21.82	28.25	6.43
03-01	16.00	0.114	1.824	21.82	32.00	10.18

Table A.4: CNT Type 4 Low Current Tests

Specimen	**V**	**I**	**P**	**Ambient Temp**	**Max Temp**	**Delta**
04-01	0.00	0.000	0.000	21.82	21.82	0.00
04-01	0.23	0.103	0.024	21.82	22.00	0.18
04-01	0.50	0.250	0.125	21.82	22.40	0.58
04-01	0.76	0.454	0.345	21.82	23.10	1.28
04-01	1.17	0.732	0.856	21.82	24.68	2.86
04-01	1.41	0.938	1.323	21.82	27.00	5.18
04-01	1.66	1.116	1.853	21.82	29.00	7.18

Table A.5: CNT Type 5 Low Current Tests

Specimen	**V**	**I**	**P**	**Ambient Temp**	**Max Temp**	**Delta**
05-01	0.00	0.000	0.000	21.82	21.82	0.0
05-01	0.20	0.100	0.020	21.82	22.00	0.18
05-01	0.51	0.315	0.161	21.82	22.40	0.58
05-01	0.76	0.604	0.459	21.82	23.50	1.68
05-01	1.16	0.978	1.134	21.82	25.50	3.68
05-01	1.41	1.207	1.702	21.82	28.00	6.18
05-01	1.64	1.385	2.271	21.82	30.00	8.18

A.1.2 High Current Testing

Table A.6: CNT Type 1 High Current Tests

Specimen	**V**	**I**	**P**	**Temp**	**Amb**	**delta**
01-02	1.83	1.250	2.288	28	21.97	6.03
01-02	2.18	1.493	3.255	32	22.01	9.99
01-02	2.55	1.750	4.463	35	22.04	12.96
01-02	2.98	2.004	5.972	38	22.09	15.91
01-02	3.32	2.252	7.477	43	22.14	20.86
01-02	3.65	2.503	9.136	50	22.24	27.76
01-02	3.93	2.750	10.808	55	22.29	32.71
01-02	4.30	3.006	12.926	60	22.33	37.67
01-02	4.58	3.250	14.885	65	22.38	42.62
01-02	4.91	3.504	17.205	70	22.43	47.57
01-02	5.22	3.745	19.549	75	22.49	52.51
01-02	5.56	4.004	22.262	80	22.44	57.56
01-02	5.84	4.253	24.838	85	22.51	62.49
01-02	6.24	4.502	28.092	92	22.57	69.43
01-02	6.53	4.753	31.037	105	22.62	82.38
01-02	6.73	5.001	33.657	115	22.73	92.27

*Note: Temp is an approximation based off of thermal images collected.

A.2 Comparative Testing Results of Heaters in Vacuum Environment

Specimen Type 1: CNT with terminals on the same side. Grain alignment in the direction of current flow.

Table A.7: CNT Specimen Type 1 Specimen 1 Vacuum Chamber Test Results

PWM %	Volts	I (A)	P (Watts)	Ω	Amb 1	Test 1	Delta 1	Amb 2	Test 2	Delta 2
10	0.1605	0.10	0.0161	1.61	28.91	29.32	0.41	28.85	29.82	0.97
20	0.3210	0.20	0.0642	1.61	28.85	30.48	1.63	28.92	30.85	1.93
30	0.4815	0.30	0.1445	1.61	28.80	32.64	3.84	28.83	32.81	3.98
40	0.6420	0.40	0.2568	1.61	28.80	35.06	6.26	28.83	34.90	6.07
50	0.8025	0.50	0.4013	1.61	28.83	38.34	9.51	28.87	38.07	9.20
60	0.9630	0.61	0.5874	1.58	28.83	40.05	11.22	28.81	40.67	11.86
70	1.1235	0.71	0.7977	1.58	28.85	43.07	14.22	28.83	42.60	13.77
80	1.2840	0.82	1.0529	1.57	28.83	45.86	17.03	28.87	46.28	17.41
90	1.4445	0.92	1.3289	1.57	28.94	48.17	19.23	28.87	49.12	20.25
100	1.6050	1.03	1.6532	1.56	28.85	52.20	23.35	28.87	53.00	24.13

Amb 3	Test 3	Delta 3	Amb 4	Test 4	Delta 4	Amb 5	Test 5	Delta 5	Avg	Delta avg
28.89	29.64	0.75	28.81	29.58	0.77	28.67	29.51	0.84	29.57	0.75
28.85	30.72	1.87	28.78	30.72	1.94	28.63	30.46	1.83	30.65	1.84
28.78	32.24	3.46	28.71	32.72	4.01	28.67	32.13	3.46	32.51	3.75
28.81	35.87	7.06	28.71	34.77	6.06	28.67	35.67	7.00	35.25	6.49
28.85	37.51	8.66	28.74	37.94	9.20	28.78	37.70	8.92	37.91	9.10
28.76	41.13	12.37	28.85	39.92	11.07	28.65	40.80	12.15	40.51	11.73
28.91	43.37	14.46	28.76	44.46	15.70	28.65	43.76	15.11	43.45	14.65
28.81	45.45	16.64	28.76	46.64	17.88	28.65	46.99	18.34	46.24	17.46
28.78	49.57	20.79	28.76	48.76	20.00	28.69	49.81	21.12	49.09	20.28
28.80	52.77	23.97	28.72	52.09	23.37	28.71	52.09	23.38	52.43	23.64

Table A.8: CNT Specimen Type 1 Specimen 2 Vacuum Chamber Test Results

PWM %	Volts	I (A)	P (Watts)	Ω	Amb 1	Test 1	Delta 1	Amb 2	Test 2	Delta 2
10	0.1605	0.09	0.0144	1.78	22.77	23.29	0.52	22.91	23.55	0.64
20	0.3210	0.19	0.0610	1.69	22.79	24.08	1.29	22.89	24.31	1.42
30	0.4815	0.28	0.1348	1.72	22.79	25.48	2.69	23.24	25.48	2.24
40	0.6420	0.38	0.2440	1.69	22.74	27.26	4.52	22.84	27.55	4.71
50	0.8025	0.47	0.3772	1.71	22.77	29.87	7.10	22.89	30.10	7.21
60	0.9630	0.57	0.5489	1.69	22.74	32.58	9.84	22.96	32.83	9.87
70	1.1235	0.67	0.7527	1.68	22.79	34.61	11.82	22.86	35.42	12.56
80	1.2840	0.77	0.9887	1.67	22.74	37.20	14.46	22.88	37.94	15.06
90	1.4445	0.87	1.2567	1.66	22.84	40.24	17.40	22.94	40.80	17.86
100	1.6050	0.98	1.5729	1.64	22.79	42.53	19.74	22.89	43.12	20.23

Amb 3	Test 3	Delta 3	Amb 4	Test 4	Delta 4	Amb 5	Test 5	Delta 5	Avg	Delta avg
23.05	23.68	0.63	23.10	23.76	0.66	23.24	23.76	0.52	23.61	0.59
23.10	24.46	1.36	23.08	24.53	1.45	23.08	24.52	1.44	24.38	1.39
22.96	25.73	2.77	23.08	25.79	2.71	23.12	25.66	2.54	25.63	2.59
22.98	27.23	4.25	23.01	27.16	4.15	23.07	27.05	3.98	27.25	4.32
23.00	29.36	6.36	23.08	30.98	7.90	23.05	29.51	6.46	29.96	7.01
23.03	33.02	9.99	23.08	33.27	10.19	23.08	32.09	9.01	32.76	9.78
23.00	34.80	11.80	23.15	34.84	11.69	23.03	34.75	11.72	34.88	11.92
23.01	37.51	14.50	23.07	37.10	14.03	23.03	36.60	13.57	37.27	14.32
23.03	39.96	16.93	23.05	39.96	16.91	23.03	40.15	17.12	40.22	17.24
23.05	43.58	20.53	23.08	42.91	19.83	23.05	42.44	19.39	42.92	19.94

Table A.9: CNT Specimen Type 1 Specimen 3 Vacuum Chamber Test Results

PWM %	Volts	I (A)	P (Watts)	Ω	Amb 1	Test 1	Delta 1	Amb 2	Test 2	Delta 2
10	0.1605	0.09	0.0144	1.78	22.77	23.29	0.52	22.91	23.55	0.64
20	0.3210	0.19	0.0610	1.69	22.79	24.08	1.29	22.89	24.31	1.42
30	0.4815	0.28	0.1348	1.72	22.79	25.48	2.69	23.24	25.48	2.24
40	0.6420	0.38	0.2440	1.69	22.74	27.26	4.52	22.84	27.55	4.71
50	0.8025	0.47	0.3772	1.71	22.77	29.87	7.10	22.89	30.10	7.21
60	0.9630	0.57	0.5489	1.69	22.74	32.58	9.84	22.96	32.83	9.87
70	1.1235	0.67	0.7527	1.68	22.79	34.61	11.82	22.86	35.42	12.56
80	1.2840	0.77	0.9887	1.67	22.74	37.20	14.46	22.88	37.94	15.06
90	1.4445	0.87	1.2567	1.66	22.84	40.24	17.40	22.94	40.80	17.86
100	1.6050	0.98	1.5729	1.64	22.79	42.53	19.74	22.89	43.12	20.23

Amb 3	Test 3	Delta 3	Amb 4	Test 4	Delta 4	Amb 5	Test 5	Delta 5	Avg	Delta avg
23.05	23.68	0.63	23.10	23.76	0.66	23.24	23.76	0.52	23.61	0.59
23.10	24.46	1.36	23.08	24.53	1.45	23.08	24.52	1.44	24.38	1.39
22.96	25.73	2.77	23.08	25.79	2.71	23.12	25.66	2.54	25.63	2.59
22.98	27.23	4.25	23.01	27.16	4.15	23.07	27.05	3.98	27.25	4.32
23.00	29.36	6.36	23.08	30.98	7.90	23.05	29.51	6.46	29.96	7.01
23.03	33.02	9.99	23.08	33.27	10.19	23.08	32.09	9.01	32.76	9.78
23.00	34.80	11.80	23.15	34.84	11.69	23.03	34.75	11.72	34.88	11.92
23.01	37.51	14.50	23.07	37.10	14.03	23.03	36.60	13.57	37.27	14.32
23.03	39.96	16.93	23.05	39.96	16.91	23.03	40.15	17.12	40.22	17.24
23.05	43.58	20.53	23.08	42.91	19.83	23.05	42.44	19.39	42.92	19.94

Table A.10: CNT Specimen Type 2 Specimen 1 Vacuum Chamber Test Results

PWM %	Volts	I (A)	P (Watts)	Ω	Amb 1	Test 1	Delta 1	Amb 2	Test 2	Delta 2
10	0.1605	0.11	0.0177	1.46	23.55	24.01	0.46	23.94	24.89	0.95
20	0.3210	0.23	0.0738	1.40	23.54	25.17	1.63	23.92	25.82	1.90
30	0.4815	0.34	0.1637	1.42	23.57	27.86	4.29	23.92	27.55	3.63
40	0.6420	0.46	0.2953	1.40	23.59	31.51	7.92	23.92	31.28	7.36
50	0.8025	0.57	0.4574	1.41	23.61	33.91	10.30	23.92	33.46	9.54
60	0.9630	0.70	0.6741	1.38	23.66	37.12	13.46	23.97	36.35	12.38
70	1.1235	0.82	0.9213	1.37	23.75	40.48	16.73	24.03	40.20	16.17
80	1.2840	0.94	1.2070	1.37	23.69	43.05	19.36	24.10	43.16	19.06
90	1.4445	1.06	1.5312	1.36	23.66	46.37	22.71	24.03	46.11	22.08
100	1.6050	1.19	1.9100	1.35	23.71	50.66	26.95	24.03	50.82	26.79

Amb 3	Test 3	Delta 3	Amb 4	Test 4	Delta 4	Amb 5	Test 5	Delta 5	Avg	Delta avg
24.31	25.17	0.86	24.62	25.61	0.99	25.33	26.21	0.88	25.18	0.83
24.25	26.66	2.41	24.66	26.73	2.07	25.20	27.12	1.92	26.30	1.99
24.31	28.80	4.49	24.64	29.14	4.50	25.13	29.43	4.30	28.56	4.24
24.24	30.78	6.54	24.60	31.86	7.26	25.20	31.17	5.97	31.32	7.01
24.31	34.80	10.49	24.85	34.22	9.37	25.13	34.16	9.03	34.11	9.75
24.29	37.22	12.93	24.75	36.88	12.13	25.31	36.43	11.12	36.80	12.40
24.38	39.34	14.96	24.75	39.39	14.64	25.34	39.34	14.00	39.75	15.30
24.32	42.42	18.10	24.83	43.35	18.52	25.68	44.27	18.59	43.25	18.73
24.38	48.04	23.66	24.92	47.46	22.54	25.26	47.69	22.43	47.13	22.68
24.43	51.40	26.97	24.89	50.93	26.04	25.31	50.55	25.24	50.87	26.40

Table A.11: CNT Specimen Type 2 Specimen 2 Vacuum Chamber Test Results

PWM %	Volts	I (A)	P (Watts)	Ω	Amb 1	Test 1	Delta 1	Amb 2	Test 2	Delta 2
10	0.1605	0.09	0.0144	1.78	24.60	24.78	0.18	25.22	25.94	0.72
20	0.3210	0.19	0.0610	1.69	24.66	26.09	1.43	25.18	27.03	1.85
30	0.4815	0.29	0.1396	1.66	24.76	27.86	3.10	25.22	28.43	3.21
40	0.6420	0.39	0.2504	1.65	24.69	31.66	6.97	25.24	30.34	5.10
50	0.8025	0.49	0.3932	1.64	24.76	33.18	8.42	25.26	33.77	8.51
60	0.9630	0.59	0.5682	1.63	24.73	35.63	10.90	25.27	36.41	11.14
70	1.1235	0.70	0.7865	1.61	24.82	38.50	13.68	25.26	39.39	14.13
80	1.2840	0.81	1.0400	1.59	24.83	40.87	16.04	25.24	41.48	16.24
90	1.4445	0.91	1.3145	1.59	24.76	43.97	19.21	25.38	44.30	18.92
100	1.6050	1.02	1.6371	1.57	24.87	47.49	22.62	25.34	46.89	21.55

Amb 3	Test 3	Delta 3	Amb 4	Test 4	Delta 4	Amb 5	Test 5	Delta 5	Avg	Delta avg
25.63	26.53	0.90	25.96	26.87	0.91	26.39	27.21	0.82	26.27	0.71
25.63	27.71	2.08	26.00	27.80	1.80	26.34	28.34	2.00	27.39	1.83
25.68	29.14	3.46	26.03	29.64	3.61	26.37	29.71	3.34	28.96	3.34
25.71	31.36	5.65	26.07	32.39	6.32	26.39	33.19	6.80	31.79	6.17
25.66	34.18	8.52	26.05	34.06	8.01	26.35	35.32	8.97	34.10	8.49
25.61	35.95	10.34	26.05	37.49	11.44	26.37	37.08	10.71	36.51	10.91
25.70	39.60	13.90	26.14	40.15	14.01	26.39	41.46	15.07	39.82	14.16
25.66	42.62	16.96	26.21	42.64	16.43	26.40	42.98	16.58	42.12	16.45
25.70	45.41	19.71	26.18	45.22	19.04	26.46	44.79	18.33	44.74	19.04
25.77	48.61	22.84	26.16	49.46	23.30	26.46	47.49	21.03	47.99	22.27

Table A.12: CNT Specimen Type 2 Specimen 3 Vacuum Chamber Test Results

PWM %	Volts	I (A)	P (Watts)	Ω	Amb 1	Test 1	Delta 1	Amb 2	Test 2	Delta 2
10	0.1605	0.11	0.0177	1.46	27.12	27.42	0.30	27.37	28.16	0.79
20	0.3210	0.23	0.0738	1.40	27.03	28.67	1.64	27.37	29.43	2.06
30	0.4815	0.35	0.1685	1.38	27.07	30.72	3.65	27.41	32.45	5.04
40	0.6420	0.47	0.3017	1.37	27.08	33.60	6.52	27.32	34.00	6.68
50	0.8025	0.58	0.4655	1.38	27.10	36.35	9.25	27.37	37.61	10.24
60	0.9630	0.71	0.6837	1.36	27.14	39.28	12.14	27.42	40.28	12.86
70	1.1235	0.83	0.9325	1.35	27.14	42.71	15.57	27.42	41.99	14.57
80	1.2840	0.96	1.2326	1.34	27.17	45.24	18.07	27.48	45.41	17.93
90	1.4445	1.08	1.5601	1.34	27.21	48.45	21.24	27.51	48.12	20.61
100	1.6050	1.22	1.9581	1.32	27.23	50.91	23.68	27.50	51.26	23.76

Amb 3	Test 3	Delta 3	Amb 4	Test 4	Delta 4	Amb 5	Test 5	Delta 5	Avg	Delta avg
27.60	28.43	0.83	27.84	28.87	1.03	27.93	28.80	0.87	28.34	0.76
27.62	29.69	2.07	27.75	29.82	2.07	27.91	29.75	1.84	29.47	1.94
27.59	31.25	3.66	27.71	31.98	4.27	27.89	31.58	3.69	31.60	4.06
27.60	35.02	7.42	27.77	34.73	6.96	27.96	35.20	7.24	34.51	6.96
27.60	37.74	10.14	27.77	37.04	9.27	27.93	37.00	9.07	37.15	9.59
27.59	39.30	11.71	27.84	39.62	11.78	27.95	40.67	12.72	39.83	12.24
27.68	43.48	15.80	27.84	42.53	14.69	27.95	42.62	14.67	42.67	15.06
27.68	45.57	17.89	27.78	46.74	18.96	28.02	45.36	17.34	45.66	18.04
27.68	48.63	20.95	27.82	49.36	21.54	27.95	48.94	20.99	48.70	21.07
27.68	52.04	24.36	27.84	52.51	24.67	27.98	52.34	24.36	51.81	24.17

Table A.13: RS100 Specimen Type 3 Specimen 1 Vacuum Chamber Test Results

PWM %	Volts	I (A)	P (Watts)	Ω	Amb 1	Test 1	Delta 1	Amb 2	Test 2	Delta 2
10	1.6000	0.01	0.0208	123.08	27.39	28.52	1.13	27.57	30.06	2.49
20	3.2000	0.03	0.0800	128.00	27.23	30.76	3.53	28.47	31.98	3.51
30	4.8000	0.04	0.1824	126.32	27.68	34.08	6.40	26.74	36.47	9.73
40	6.4000	0.05	0.3200	128.00	27.84	38.61	10.77	27.24	41.77	14.53
50	8.0000	0.06	0.5040	126.98	27.55	42.55	15.00	27.98	44.41	16.43
60	9.6000	0.08	0.7200	128.00	27.66	45.53	17.87	28.11	47.74	19.63
70	11.2000	0.09	0.9856	127.27	27.28	49.28	22.00	27.95	50.66	22.71
80	12.8000	0.10	1.2928	126.73	27.30	57.97	30.67	27.89	54.58	26.69
90	14.4000	0.11	1.6272	127.43	27.24	61.71	34.47	27.73	64.60	36.87
100	16.0000	0.13	2.0160	126.98	27.30	64.72	37.42	27.10	67.04	39.94

Amb 3	Test 3	Delta 3	Amb 4	Test 4	Delta 4	Amb 5	Test 5	Delta 5	Avg	Delta avg
28.54	30.30	1.76	28.16	30.95	2.79	28.40	30.35	1.95	30.04	2.02
27.23	32.13	4.90	28.34	33.62	5.28	28.91	33.12	4.21	32.32	4.29
27.16	35.22	8.06	28.34	39.03	10.69	28.94	36.39	7.45	36.24	8.47
27.16	40.09	12.93	27.64	41.20	13.56	28.91	39.92	11.01	40.32	12.56
28.20	44.65	16.45	27.73	43.30	15.57	28.29	45.14	16.85	44.01	16.06
27.66	47.84	20.18	27.66	49.36	21.70	28.40	47.46	19.06	47.59	19.69
27.68	53.90	26.22	28.42	52.71	24.29	27.57	51.10	23.53	51.53	23.75
27.32	59.20	31.88	27.41	58.90	31.49	29.00	60.68	31.68	58.27	30.48
27.60	61.57	33.97	27.39	63.03	35.64	28.00	64.64	36.64	63.11	35.52
27.80	66.50	38.70	28.20	66.25	38.05	27.87	69.39	41.52	66.78	39.13

Table A.14: RS100 Specimen Type 3 Specimen 2 Vacuum Chamber Test Results

PWM %	Volts	I (A)	P (Watts)	Ω	Amb 1	Test 1	Delta 1	Amb 2	Test 2	Delta 2
10	1.6000	0.01	0.0192	133.33	23.52	23.78	0.26	23.47	25.77	2.30
20	3.2000	0.02	0.0768	133.33	23.69	25.45	1.76	23.40	30.71	7.31
30	4.8000	0.04	0.1776	129.73	23.36	30.65	7.29	23.03	32.41	9.38
40	6.4000	0.05	0.3136	130.61	23.52	32.87	9.35	23.24	35.57	12.33
50	8.0000	0.06	0.4960	129.03	24.10	36.80	12.70	23.66	38.54	14.88
60	9.6000	0.07	0.7104	129.73	23.01	41.02	18.01	23.29	40.41	17.12
70	11.2000	0.09	0.9744	128.74	23.10	44.46	21.36	24.24	44.60	20.36
80	12.8000	0.10	1.2800	128.00	23.22	48.84	25.62	24.39	50.23	25.84
90	14.4000	0.11	1.6272	127.43	23.73	52.34	28.61	23.15	53.66	30.51
100	16.0000	0.13	2.0160	126.98	23.00	55.79	32.79	23.38	56.16	32.78

Amb 3	Test 3	Delta 3	Amb 4	Test 4	Delta 4	Amb 5	Test 5	Delta 5	Avg	Delta avg
23.69	26.69	3.00	22.82	25.48	2.66	23.94	26.67	2.73	25.68	2.19
23.24	30.19	6.95	24.45	27.32	2.87	23.99	27.62	3.63	28.26	4.50
24.29	33.43	9.14	23.43	28.92	5.49	24.03	31.94	7.91	31.47	7.84
23.33	35.71	12.38	22.77	30.98	8.21	23.99	34.16	10.17	33.86	10.49
24.34	37.33	12.99	22.74	34.53	11.79	24.39	41.93	17.54	37.83	13.98
23.73	40.39	16.66	23.69	39.22	15.53	24.11	44.18	20.07	41.04	17.48
23.76	45.24	21.48	23.45	43.51	20.06	23.69	46.15	22.46	44.79	21.14
24.20	54.01	29.81	22.89	48.43	25.54	24.04	52.20	28.16	50.74	26.99
23.54	55.69	32.15	23.31	51.32	28.01	23.21	56.41	33.20	53.88	30.50
24.82	58.53	33.71	23.71	54.67	30.96	24.08	58.80	34.72	56.79	32.99

Table A.15: RS100 Specimen Type 3 Specimen 3 Vacuum Chamber Test Results

PWM %	Volts	I (A)	P (Watts)	Ω	Amb 1	Test 1	Delta 1	Amb 2	Test 2	Delta 2
10	1.6000	0.01	0.0192	133.33	24.57	23.99	-0.58	24.59	25.82	1.23
20	3.2000	0.03	0.0800	128.00	24.17	28.22	4.05	24.15	28.51	4.36
30	4.8000	0.04	0.1776	129.73	24.52	30.21	5.69	24.46	32.07	7.61
40	6.4000	0.05	0.3136	130.61	23.52	34.80	11.28	24.24	34.63	10.39
50	8.0000	0.06	0.4880	131.15	23.68	37.39	13.71	23.92	38.94	15.02
60	9.6000	0.07	0.7104	129.73	23.96	44.48	20.52	23.94	43.65	19.71
70	11.2000	0.09	0.9632	130.23	24.53	48.22	23.69	24.15	47.92	23.77
80	12.8000	0.10	1.2544	130.61	24.11	50.18	26.07	24.15	50.69	26.54
90	14.4000	0.11	1.6128	128.57	23.94	53.84	29.90	23.73	53.95	30.22
100	16.0000	0.12	1.9840	129.03	24.27	58.70	34.43	24.11	56.63	32.52

Amb 3	Test 3	Delta 3	Amb 4	Test 4	Delta 4	Amb 5	Test 5	Delta 5	Avg	Delta avg
24.11	26.26	2.15	23.97	26.58	2.61	24.67	26.39	1.72	25.81	1.43
24.29	27.95	3.66	24.69	29.03	4.34	24.97	28.18	3.21	28.38	3.92
23.96	29.95	5.99	23.82	31.32	7.50	24.64	29.49	4.85	30.61	6.33
25.33	34.08	8.75	25.13	37.02	11.89	25.27	33.58	8.31	34.82	10.12
23.87	36.98	13.11	25.33	39.79	14.46	24.55	36.13	11.58	37.85	13.58
23.90	39.60	15.70	24.82	45.05	20.23	25.71	40.96	15.25	42.75	18.28
23.90	47.61	23.71	25.11	50.23	25.12	24.50	46.03	21.53	48.00	23.56
24.64	50.74	26.10	24.64	52.12	27.48	24.31	51.95	27.64	51.14	26.77
24.80	54.37	29.57	25.38	55.03	29.65	24.41	54.85	30.44	54.41	29.96
24.32	58.53	34.21	24.24	59.27	35.03	25.45	58.17	32.72	58.26	33.78

Table A.16: CNT Specimen Type 4 Specimen 1 Vacuum Chamber Test Results

PWM %	Volts	I (A)	P (Watts)	Ω	Amb 1	Test 1	Delta 1	Amb 2	Test 2	Delta 2
10	0.1605	0.09	0.0144	1.78	22.98	23.29	0.31	23.14	24.03	0.89
20	0.3210	0.19	0.0610	1.69	23.00	25.38	2.38	23.10	25.50	2.40
30	0.4815	0.28	0.1348	1.72	23.00	28.43	5.43	23.10	28.07	4.97
40	0.6420	0.37	0.2375	1.74	23.03	30.45	7.42	23.24	30.67	7.43
50	0.8025	0.47	0.3772	1.71	23.05	33.14	10.09	23.07	32.70	9.63
60	0.9630	0.56	0.5393	1.72	23.07	35.22	12.15	23.05	35.55	12.50
70	1.1235	0.66	0.7415	1.70	23.03	36.92	13.89	23.08	37.41	14.33
80	1.2840	0.76	0.9758	1.69	23.05	39.09	16.04	23.03	40.41	17.38
90	1.4445	0.86	1.2423	1.68	23.10	43.69	20.59	23.01	41.90	18.89
100	1.6050	0.96	1.5408	1.67	23.10	46.45	23.35	23.03	46.40	23.37

Amb 3	Test 3	Delta 3	Amb 4	Test 4	Delta 4	Amb 5	Test 5	Delta 5	Avg	Delta avg
23.05	23.90	0.85	23.05	23.90	0.85	23.07	23.90	0.83	23.80	0.75
23.05	25.71	2.66	23.03	25.64	2.61	23.05	25.70	2.65	25.59	2.54
23.05	27.71	4.66	23.24	28.05	4.81	23.05	27.08	4.03	27.87	4.78
23.01	29.18	6.17	23.03	29.53	6.50	22.98	30.06	7.08	29.98	6.92
22.96	32.22	9.26	23.05	31.58	8.53	23.05	32.70	9.65	32.47	9.43
23.03	35.44	12.41	23.07	35.10	12.03	22.98	34.92	11.94	35.25	12.21
23.08	37.94	14.86	23.10	38.05	14.95	23.19	37.43	14.24	37.55	14.45
23.08	40.46	17.38	23.05	40.48	17.43	23.01	40.39	17.38	40.17	17.12
23.03	43.37	20.34	23.05	42.01	18.96	23.01	42.33	19.32	42.66	19.62
23.05	45.34	22.29	23.03	45.22	22.19	22.98	45.05	22.07	45.69	22.65

Table A.17: CNT Specimen Type 4 Specimen 2 Vacuum Chamber Test Results

PWM %	Volts	I (A)	P (Watts)	Ω	Amb 1	Test 1	Delta 1	Amb 2	Test 2	Delta 2
10	0.1605	0.09	0.0144	1.78	25.06	25.64	0.58	25.43	27.64	2.21
20	0.3210	0.19	0.0616	1.67	24.75	27.68	2.93	25.04	28.60	3.56
30	0.4815	0.29	0.1406	1.65	24.76	29.89	5.13	24.83	30.28	5.45
40	0.6420	0.40	0.2549	1.62	24.87	31.17	6.30	25.04	33.58	8.54
50	0.8025	0.50	0.4013	1.61	24.60	33.56	8.96	25.29	35.18	9.89
60	0.9630	0.61	0.5845	1.59	24.50	37.24	12.74	25.80	37.26	11.46
70	1.1235	0.72	0.8044	1.57	25.11	40.18	15.07	25.13	39.90	14.77
80	1.2840	0.83	1.0606	1.55	24.75	42.08	17.33	24.41	45.48	21.07
90	1.4445	0.94	1.3506	1.54	25.08	44.88	19.80	24.64	46.94	22.30
100	1.6050	1.05	1.6869	1.53	25.29	49.94	24.65	25.26	49.97	24.71

Amb 3	Test 3	Delta 3	Amb 4	Test 4	Delta 4	Amb 5	Test 5	Delta 5	Avg	Delta avg
24.76	27.26	2.50	25.84	27.17	1.33	24.82	26.66	1.84	26.87	1.69
24.66	28.56	3.90	24.96	28.45	3.49	23.99	27.53	3.54	28.16	3.48
24.89	31.53	6.64	25.33	30.78	5.45	24.14	29.54	5.40	30.40	5.61
24.83	33.56	8.73	24.57	32.17	7.60	25.38	32.17	6.79	32.53	7.59
24.50	36.11	11.61	24.96	35.95	10.99	24.75	33.58	8.83	34.88	10.06
24.60	38.57	13.97	24.71	37.92	13.21	25.71	35.99	10.28	37.40	12.33
24.94	39.92	14.98	24.15	40.96	16.81	24.94	41.79	16.85	40.55	15.70
25.04	42.13	17.09	25.47	43.67	18.20	25.41	44.09	18.68	43.49	18.47
25.06	44.58	19.52	24.73	45.53	20.80	25.20	47.92	22.72	45.97	21.03
25.11	51.45	26.34	25.24	48.37	23.13	24.64	50.07	25.43	49.96	24.85

Table A.18: CNT Specimen Type 4 Specimen 3 Vacuum Chamber Test Results

PWM %	Volts	I (A)	P (Watts)	Ω	Amb 1	Test 1	Delta 1	Amb 2	Test 2	Delta 2
10	0.1605	0.09	0.0146	1.76	25.18	26.18	1.00	26.10	27.59	1.49
20	0.3210	0.19	0.0623	1.65	25.03	28.09	3.06	25.68	29.60	3.92
30	0.4815	0.29	0.1416	1.64	24.90	30.69	5.79	25.98	30.93	4.95
40	0.6420	0.40	0.2568	1.61	25.36	33.58	8.22	25.80	34.45	8.65
50	0.8025	0.50	0.4045	1.59	25.64	35.32	9.68	25.24	35.85	10.61
60	0.9630	0.61	0.5894	1.57	25.34	37.12	11.78	24.75	38.19	13.44
70	1.1235	0.72	0.8089	1.56	25.38	39.81	14.43	25.79	43.44	17.65
80	1.2840	0.93	1.1954	1.38	25.48	42.80	17.32	25.48	46.57	21.09
90	1.4445	0.94	1.3593	1.54	25.36	45.36	20.00	24.94	48.71	23.77
100	1.6050	1.06	1.6949	1.52	25.26	49.86	24.60	25.48	50.91	25.43

Amb 3	Test 3	Delta 3	Amb 4	Test 4	Delta 4	Amb 5	Test 5	Delta 5	Avg	Delta avg
25.48	27.37	1.89	26.12	27.86	1.74	25.89	27.41	1.52	27.28	1.53
24.36	29.45	5.09	25.93	30.34	4.41	25.56	29.97	4.41	29.49	4.18
26.30	31.06	4.76	24.69	31.32	6.63	24.97	32.02	7.05	31.20	5.84
25.24	32.76	7.52	25.34	34.69	9.35	25.73	33.62	7.89	33.82	8.33
25.70	35.06	9.36	25.73	36.11	10.38	25.84	35.69	9.85	35.61	9.98
25.17	37.22	12.05	26.19	37.82	11.63	26.18	38.52	12.34	37.77	12.25
24.97	41.79	16.82	25.91	41.75	15.84	26.35	43.55	17.20	42.07	16.39
25.73	43.85	18.12	26.16	44.53	18.37	26.16	45.98	19.82	44.75	18.94
25.03	46.96	21.93	26.07	47.04	20.97	26.37	47.77	21.40	47.17	21.61
25.11	49.65	24.54	25.70	51.15	25.45	25.96	49.67	23.71	50.25	24.75

Table A.19: CNT Specimen Type 5 Specimen 1 Vacuum Chamber Test Results

PWM %	Volts	I (A)	P (Watts)	Ω	Amb 1	Test 1	Delta 1	Amb 2	Test 2	Delta 2
10	0.1605	0.11	0.0177	1.46	23.08	23.64	0.56	23.24	24.18	0.94
20	0.3210	0.22	0.0706	1.46	23.08	25.56	2.48	23.15	26.02	2.87
30	0.4815	0.33	0.1589	1.46	23.07	27.68	4.61	23.19	27.82	4.63
40	0.6420	0.44	0.2825	1.46	23.01	30.13	7.12	23.21	31.34	8.13
50	0.8025	0.55	0.4414	1.46	23.14	32.28	9.14	23.17	33.56	10.39
60	0.9630	0.66	0.6356	1.46	23.15	36.51	13.36	23.24	37.74	14.50
70	1.1235	0.78	0.8763	1.44	23.05	38.63	15.58	23.19	40.46	17.27
80	1.2840	0.90	1.1556	1.43	23.05	43.00	19.95	23.21	44.27	21.06
90	1.4445	1.02	1.4734	1.42	23.15	48.40	25.25	23.26	46.96	23.70
100	1.6050	1.14	1.8297	1.41	23.15	51.73	28.58	23.17	51.70	28.53

Amb 3	Test 3	Delta 3	Amb 4	Test 4	Delta 4	Amb 5	Test 5	Delta 5	Avg	Delta avg
23.17	24.13	0.96	23.19	24.08	0.89	23.28	24.24	0.96	24.05	0.86
23.17	25.47	2.30	23.15	25.40	2.25	23.24	26.19	2.95	25.73	2.57
23.17	28.74	5.57	23.14	26.98	3.84	23.26	28.16	4.90	27.88	4.71
23.14	30.93	7.79	23.08	31.62	8.54	23.28	31.08	7.80	31.02	7.88
23.14	34.02	10.88	23.14	34.37	11.23	23.19	33.75	10.56	33.60	10.44
23.14	36.39	13.25	23.07	36.45	13.38	23.21	38.21	15.00	37.06	13.90
23.08	41.35	18.27	23.17	41.46	18.29	23.26	41.66	18.40	40.71	17.56
23.12	44.16	21.04	23.08	44.13	21.05	23.29	44.53	21.24	44.02	20.87
23.12	48.84	25.72	23.14	46.64	23.50	23.29	47.04	23.75	47.58	24.38
23.14	52.91	29.77	23.14	53.60	30.46	23.24	50.69	27.45	52.13	28.96

Table A.20: CNT Specimen Type 5 Specimen 2 Vacuum Chamber Test Results

PWM %	Volts	I (A)	P (Watts)	Ω	Amb 1	Test 1	Delta 1	Amb 2	Test 2	Delta 2
10	0.1605	0.09	0.0144	1.78	23.22	23.55	0.33	23.08	23.75	0.67
20	0.3210	0.18	0.0578	1.78	23.21	24.60	1.39	23.08	24.66	1.58
30	0.4815	0.28	0.1348	1.72	23.17	26.05	2.88	23.05	27.08	4.03
40	0.6420	0.37	0.2375	1.74	23.15	29.82	6.67	23.01	28.85	5.84
50	0.8025	0.46	0.3692	1.74	23.15	32.02	8.87	23.00	31.32	8.32
60	0.9630	0.56	0.5393	1.72	23.28	34.73	11.45	22.96	33.95	10.99
70	1.1235	0.66	0.7415	1.70	23.21	36.76	13.55	23.05	37.33	14.28
80	1.2840	0.75	0.9630	1.71	23.24	39.41	16.17	23.03	38.84	15.81
90	1.4445	0.85	1.2278	1.70	23.21	43.03	19.82	22.98	42.08	19.10
100	1.6050	0.95	1.5248	1.69	23.24	45.31	22.07	22.98	45.60	22.62

Amb 3	Test 3	Delta 3	Amb 4	Test 4	Delta 4	Amb 5	Test 5	Delta 5	Avg	Delta avg
22.93	23.59	0.66	22.84	23.52	0.68	22.77	23.38	0.61	23.56	0.59
22.88	24.48	1.60	22.75	24.36	1.61	22.72	24.52	1.80	24.52	1.60
23.03	26.51	3.48	22.77	26.82	4.05	22.74	26.25	3.51	26.54	3.59
22.86	28.91	6.05	22.75	28.45	5.70	22.72	28.98	6.26	29.00	6.10
22.84	30.32	7.48	22.70	31.36	8.66	22.70	32.02	9.32	31.41	8.53
22.84	34.33	11.49	22.75	33.75	11.00	22.68	33.54	10.86	34.06	11.16
22.88	36.72	13.84	22.75	36.37	13.62	22.67	35.30	12.63	36.50	13.58
22.82	39.51	16.69	22.79	39.07	16.28	22.70	38.59	15.89	39.08	16.17
22.84	41.35	18.51	22.75	41.73	18.98	22.74	41.90	19.16	42.02	19.11
22.84	44.18	21.34	22.77	44.16	21.39	22.72	44.88	22.16	44.83	21.92

Table A.21: CNT Specimen Type 5 Specimen 3 Vacuum Chamber Test Results

PWM %	Volts	I (A)	P (Watts)	Ω	Amb 1	Test 1	Delta 1	Amb 2	Test 2	Delta 2
10	0.1605	0.10	0.0161	1.61	22.55	22.60	0.05	22.84	23.48	0.64
20	0.3210	0.21	0.0674	1.53	22.53	23.85	1.32	22.75	24.32	1.57
30	0.4815	0.32	0.1541	1.50	22.58	26.55	3.97	22.77	26.51	3.74
40	0.6420	0.43	0.2761	1.49	22.56	28.51	5.95	22.77	28.96	6.19
50	0.8025	0.54	0.4334	1.49	22.56	30.72	8.16	22.75	30.97	8.22
60	0.9630	0.65	0.6260	1.48	22.65	33.18	10.53	22.75	34.00	11.25
70	1.1235	0.76	0.8539	1.48	22.67	36.90	14.23	22.82	36.62	13.80
80	1.2840	0.88	1.1299	1.46	22.65	39.11	16.46	22.82	39.09	16.27
90	1.4445	0.99	1.4301	1.46	22.68	40.80	18.12	22.77	42.26	19.49
100	1.6050	1.11	1.7816	1.45	22.70	45.00	22.30	22.77	44.88	22.11

Amb 3	Test 3	Delta 3	Amb 4	Test 4	Delta 4	Amb 5	Test 5	Delta 5	Avg	Delta avg
22.88	23.55	0.67	22.86	23.59	0.73	22.86	23.54	0.68	23.35	0.55
22.86	24.38	1.52	22.86	24.48	1.62	22.82	24.76	1.94	24.36	1.59
22.89	25.94	3.05	22.84	25.80	2.96	22.84	26.71	3.87	26.30	3.52
22.82	29.53	6.71	22.84	29.62	6.78	22.84	28.89	6.05	29.10	6.34
22.79	31.19	8.40	22.84	30.87	8.03	22.86	30.74	7.88	30.90	8.14
22.82	33.64	10.82	22.84	34.14	11.30	22.82	32.87	10.05	33.57	10.79
22.81	37.22	14.41	22.89	36.76	13.87	22.86	35.51	12.65	36.60	13.79
22.82	40.09	17.27	22.81	38.88	16.07	22.82	38.15	15.33	39.06	16.28
22.88	41.48	18.60	22.93	41.22	18.29	22.84	41.97	19.13	41.55	18.73
22.82	44.41	21.59	22.82	43.65	20.83	22.82	43.99	21.17	44.39	21.60

Table A.22: CNT Specimen Type 6 Specimen 1 Vacuum Chamber Test Results

PWM %	Volts	I (A)	P (Watts)	Ω	Amb 1	Test 1	Delta 1	Amb 2	Test 2	Delta 2
10	1.6000	0.02	0.0272	94.12	22.74	23.99	1.25	22.77	28.02	5.25
20	3.2000	0.04	0.1120	91.43	23.40	32.47	9.07	23.54	31.75	8.21
30	4.8000	0.05	0.2448	94.12	22.46	34.57	12.11	23.42	34.71	11.29
40	6.4000	0.07	0.4352	94.12	22.68	43.85	21.17	23.52	38.67	15.15
50	8.0000	0.09	0.6800	94.12	23.83	46.85	23.02	23.69	44.41	20.72
60	9.6000	0.10	0.9792	94.12	22.74	54.10	31.36	23.45	50.80	27.35
70	11.2000	0.12	1.3328	94.12	23.40	59.74	36.34	24.27	55.57	31.30
80	12.8000	0.14	1.7536	93.43	23.08	63.91	40.83	23.22	61.93	38.71
90	14.4000	0.15	2.2176	93.51	23.83	69.97	46.14	23.42	65.08	41.66
100	16.0000	0.17	2.7520	93.02	23.15	74.16	51.01	23.90	72.64	48.74

Amb 3	Test 3	Delta 3	Amb 4	Test 4	Delta 4	Amb 5	Test 5	Delta 5	Avg	Delta avg
23.85	26.05	2.20	24.39	26.58	2.19	24.39	27.12	2.73	26.35	2.72
23.99	30.11	6.12	24.27	28.71	4.44	23.55	29.25	5.70	30.46	6.71
23.78	34.49	10.71	24.31	34.35	10.04	23.75	35.38	11.63	34.70	11.16
25.01	39.17	14.16	23.71	39.75	16.04	24.38	41.11	16.73	40.51	16.65
24.32	47.99	23.67	23.78	44.32	20.54	24.48	48.04	23.56	46.32	22.30
23.82	50.39	26.57	23.96	53.66	29.70	23.99	52.46	28.47	52.28	28.69
24.38	58.23	33.85	24.39	57.74	33.35	23.64	58.76	35.12	58.01	33.99
24.13	66.79	42.66	24.32	61.57	37.25	24.29	63.83	39.54	63.61	39.80
24.06	69.75	45.69	23.75	67.08	43.33	23.97	67.85	43.88	67.95	44.14
24.01	72.99	48.98	24.22	79.24	55.02	23.69	78.58	54.89	75.52	51.73

Table A.23: CNT Specimen Type 6 Specimen 2 Vacuum Chamber Test Results

PWM %	Volts	I (A)	P (Watts)	Ω	Amb 1	Test 1	Delta 1	Amb 2	Test 2	Delta 2
10	1.6	0.017	0.0272	94.11765	23.96	25.8	1.84	23.96	27.17	3.21
20	3.2	0.034	0.1088	94.11765	23.92	29.07	5.15	23.19	29.93	6.74
30	4.8	0.051	0.2448	94.11765	24.27	31.51	7.24	23.15	31.85	8.7
40	6.4	0.068	0.4352	94.11765	24.99	36.03	11.04	23.78	40.63	16.85
50	8	0.085	0.68	94.11765	24.48	39.81	15.33	23.61	46.92	23.31
60	9.6	0.102	0.9792	94.11765	23.43	44.84	21.41	24.5	49.83	25.33
70	11.2	0.118	1.3216	94.91525	23.82	48.86	25.04	23.94	52.66	28.72
80	12.8	0.136	1.7408	94.11765	24.39	52.91	28.52	23.85	57.33	33.48
90	14.4	0.152	2.1888	94.73684	23.4	56.88	33.48	23.26	62.29	39.03
100	16	0.17	2.72	94.11765	24.25	61.85	37.6	23.35	67.25	43.9

Amb 3	Test 3	Delta 3	Amb 4	Test 4	Delta 4	Amb 5	Test 5	Delta 5	Avg	Delta avg
22.63	26.96	4.33	22.96	26.09	3.13	24.15	25.86	1.71	26.376	2.844
23.64	30.06	6.42	22.81	28.54	5.73	23.12	28.2	5.08	29.16	5.824
23.31	32.68	9.37	23.29	31.23	7.94	23.62	30.41	6.79	31.536	8.008
23.48	36.37	12.89	23.52	33.85	10.33	23.99	36.68	12.69	36.712	12.76
22.75	40.33	17.58	23.19	38.59	15.4	23.55	43.44	19.89	41.818	18.302
24.06	44.72	20.66	23.68	42.28	18.6	23.17	47.44	24.27	45.822	22.054
23.48	50.29	26.81	23.59	47.97	24.38	23.28	50.58	27.3	50.072	26.45
23.1	58.2	35.1	23.68	55.88	32.2	23.4	54.01	30.61	55.666	31.982
23.61	62.07	38.46	23.92	59.67	35.75	23.26	57.81	34.55	59.744	36.254
23.31	67.33	44.02	22.93	64.8	41.87	23.48	61.67	38.19	64.58	41.116

Table A.24: CNT Specimen Type 6 Specimen 3 Vacuum Chamber Test Results

PWM %	Volts	I (A)	P (Watts)	Ω	Amb 1	Test 1	Delta 1	Amb 2	Test 2	Delta 2
10	1.6000	0.02	0.0272	94.12	25.54	27.37	1.83	26.10	29.32	3.22
20	3.2000	0.03	0.1088	94.12	26.00	32.41	6.41	25.61	31.19	5.58
30	4.8000	0.05	0.2448	94.12	26.53	34.71	8.18	26.94	36.23	9.29
40	6.4000	0.07	0.4352	94.12	26.57	38.71	12.14	26.50	39.94	13.44
50	8.0000	0.09	0.6800	94.12	26.76	42.76	16.00	27.14	42.53	15.39
60	9.6000	0.10	0.9792	94.12	26.78	48.63	21.85	26.67	49.44	22.77
70	11.2000	0.12	1.3328	94.12	26.44	55.03	28.59	26.37	55.60	29.23
80	12.8000	0.14	1.7408	94.12	26.71	59.54	32.83	26.78	58.60	31.82
90	14.4000	0.15	2.2032	94.12	25.59	65.24	39.65	26.64	62.81	36.17
100	16.0000	0.17	2.7200	94.12	26.28	75.32	49.04	26.23	68.89	42.66

Amb 3	Test 3	Delta 3	Amb 4	Test 4	Delta 4	Amb 5	Test 5	Delta 5	Avg	Delta avg
26.66	30.10	3.44	26.09	29.62	3.53	26.10	30.32	4.22	29.35	3.25
26.83	31.43	4.60	25.94	33.75	7.81	25.27	34.47	9.20	32.65	6.72
26.03	33.37	7.34	26.18	39.64	13.46	25.64	36.51	10.87	36.09	9.83
26.18	37.74	11.56	27.19	43.83	16.64	25.80	45.07	19.27	41.06	14.61
26.14	45.14	19.00	26.42	46.52	20.10	25.31	47.87	22.56	44.96	18.61
26.32	48.99	22.67	26.23	54.55	28.32	25.43	51.32	25.89	50.59	24.30
26.39	53.63	27.24	26.00	58.40	32.40	25.94	54.91	28.97	55.51	29.29
26.48	57.58	31.10	25.93	61.89	35.96	25.64	58.56	32.92	59.23	32.93
25.66	61.75	36.09	26.37	65.72	39.35	25.64	64.72	39.08	64.05	38.07
26.66	67.46	40.80	26.32	74.68	48.36	25.93	70.30	44.37	71.33	45.05

Appendix B. Data Plots

B.1 Cycle Test Plots

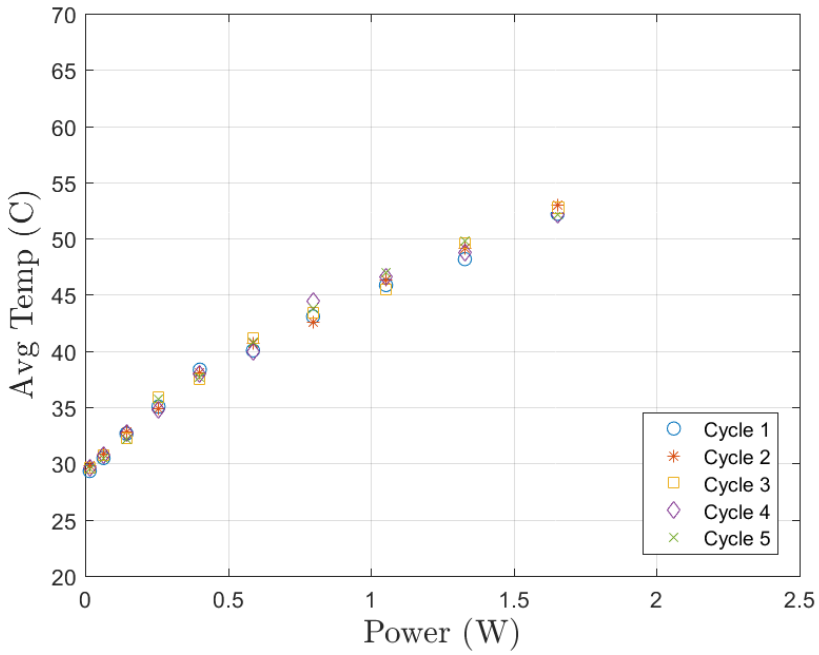

Figure B.1: Temperature comparison plot of the five test cycles performed on CNT Type 1 Specimen 1

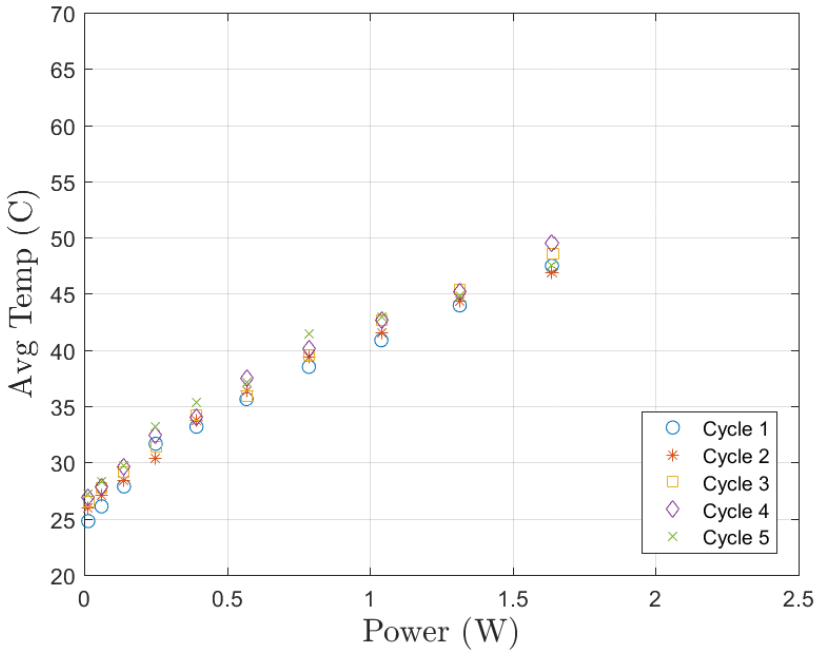

Figure B.2: Temperature comparison plot of the five test cycles performed on CNT Type 1 Specimen 2

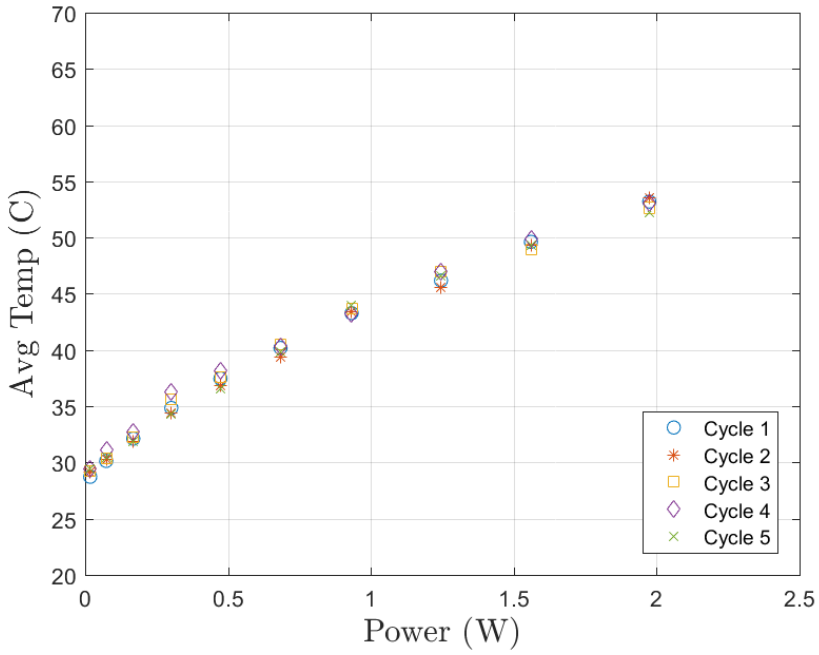

Figure B.3: Temperature comparison plot of the five test cycles performed on CNT Type 1 Specimen 3

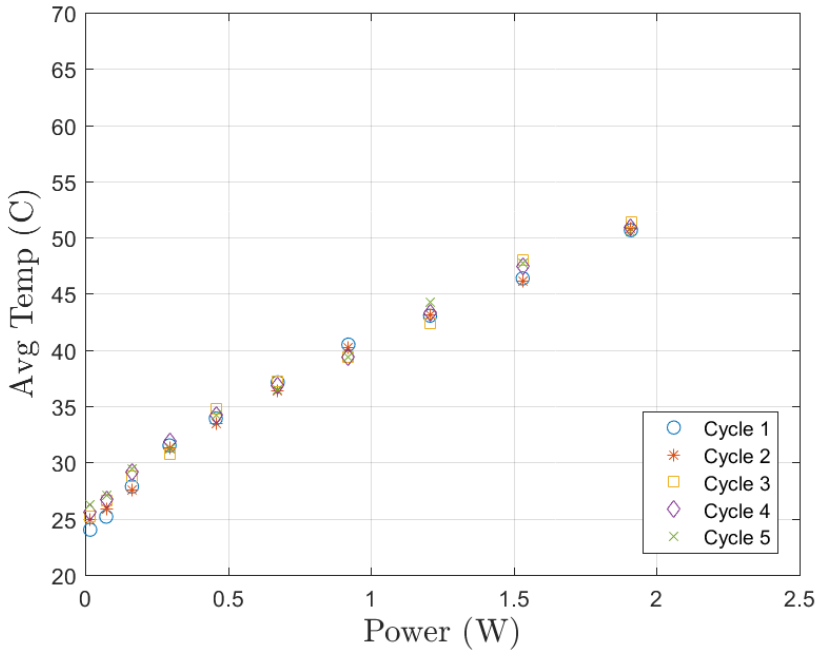

Figure B.4: Temperature comparison plot of the five test cycles performed on CNT Type 2 Specimen 1

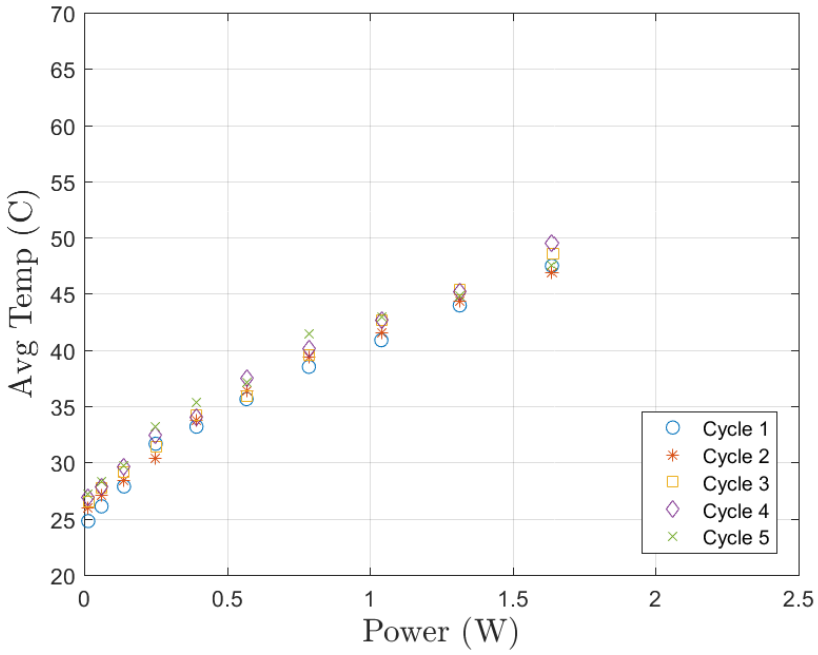

Figure B.5: Temperature comparison plot of the five test cycles performed on CNT Type 2 Specimen 2

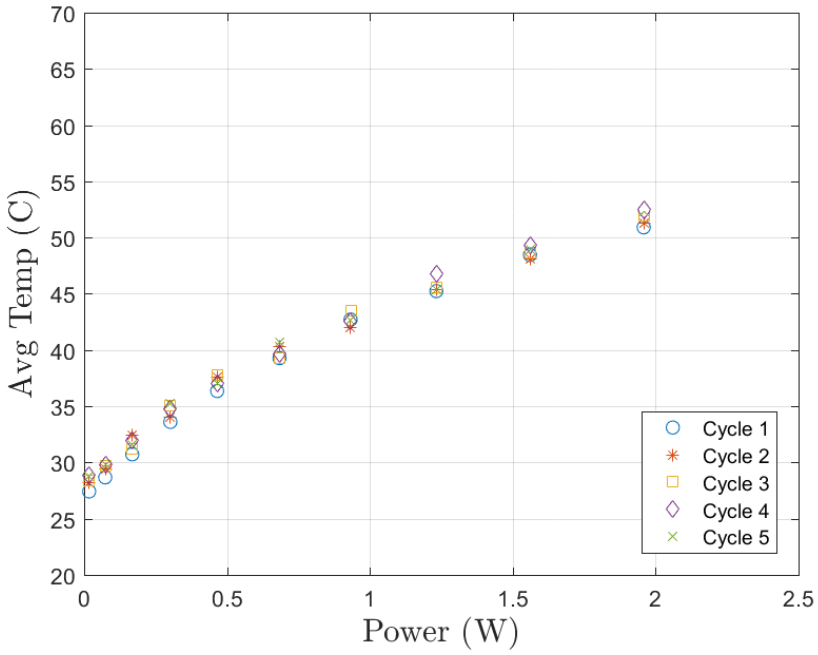

Figure B.6: Temperature comparison plot of the five test cycles performed on CNT Type 2 Specimen 3

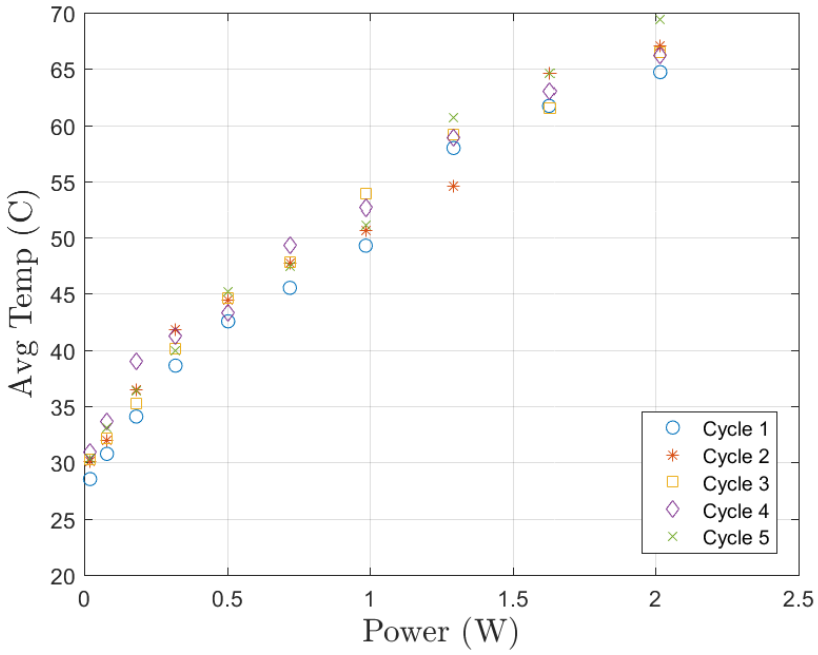

Figure B.7: Temperature comparison plot of the five test cycles performed on RS100 Type 3 Specimen 1

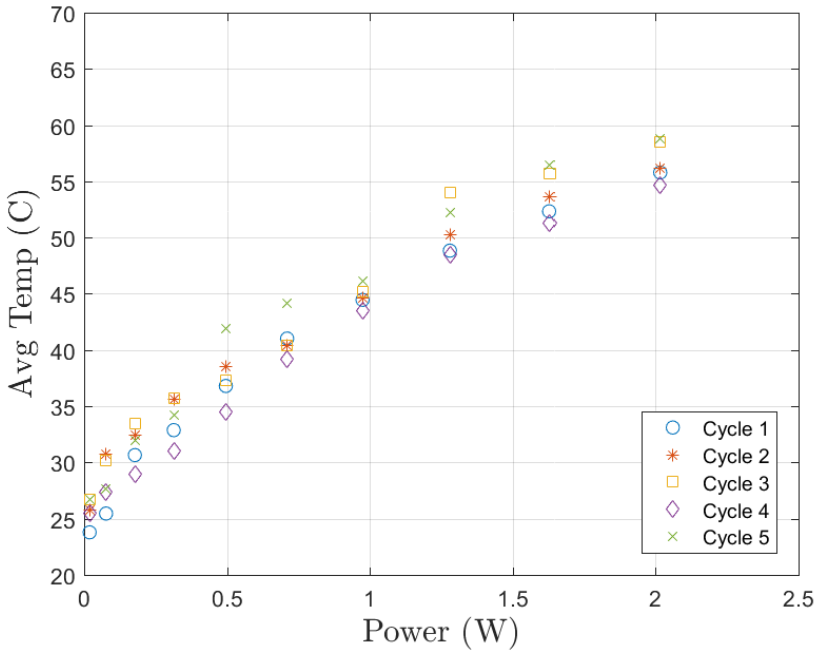

Figure B.8: Temperature comparison plot of the five test cycles performed on RS100 Type 3 Specimen 2

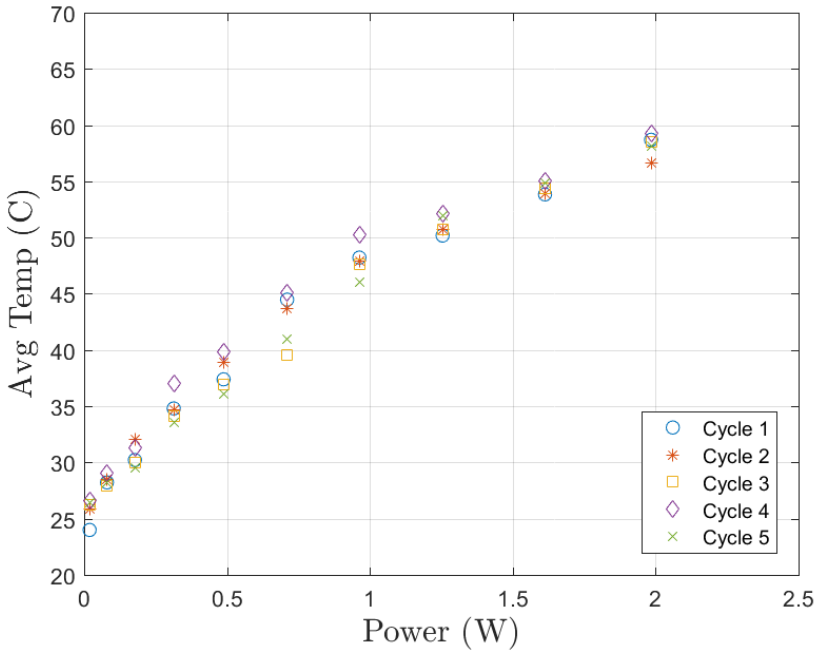

Figure B.9: Temperature comparison plot of the five test cycles performed on RS100 Type 3 Specimen 3

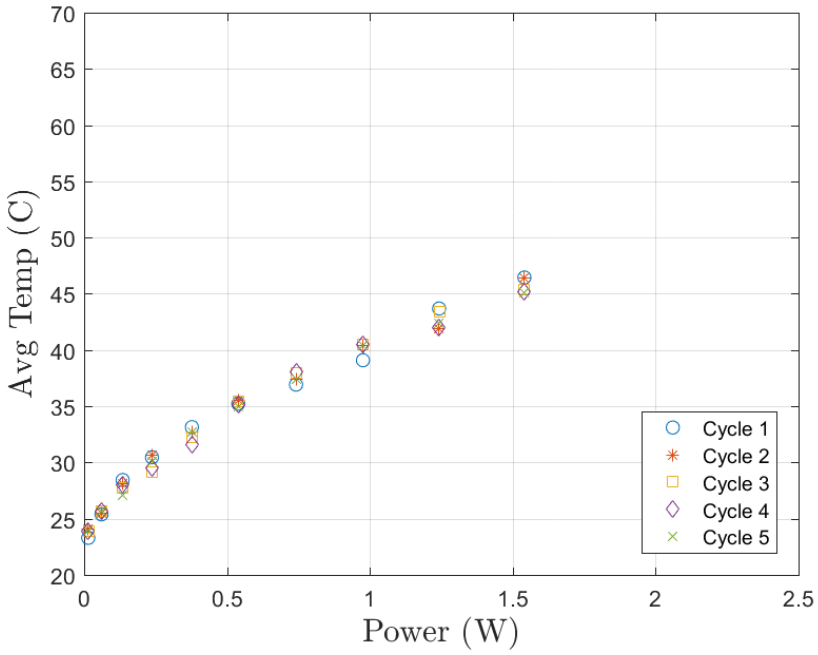

Figure B.10: Temperature comparison plot of the five test cycles performed on CNT Type 4 Specimen 1

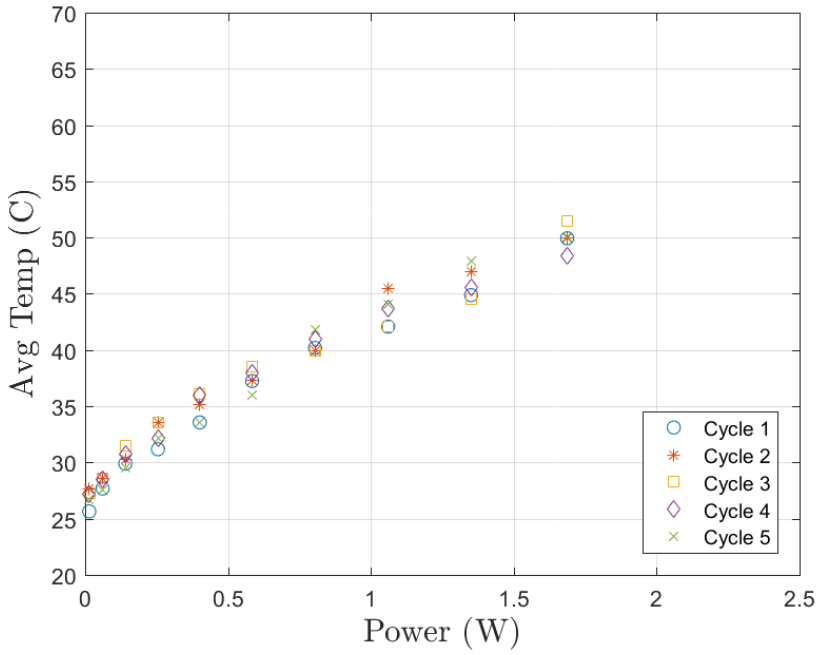

Figure B.11: Temperature comparison plot of the five test cycles performed on CNT Type 4 Specimen 2

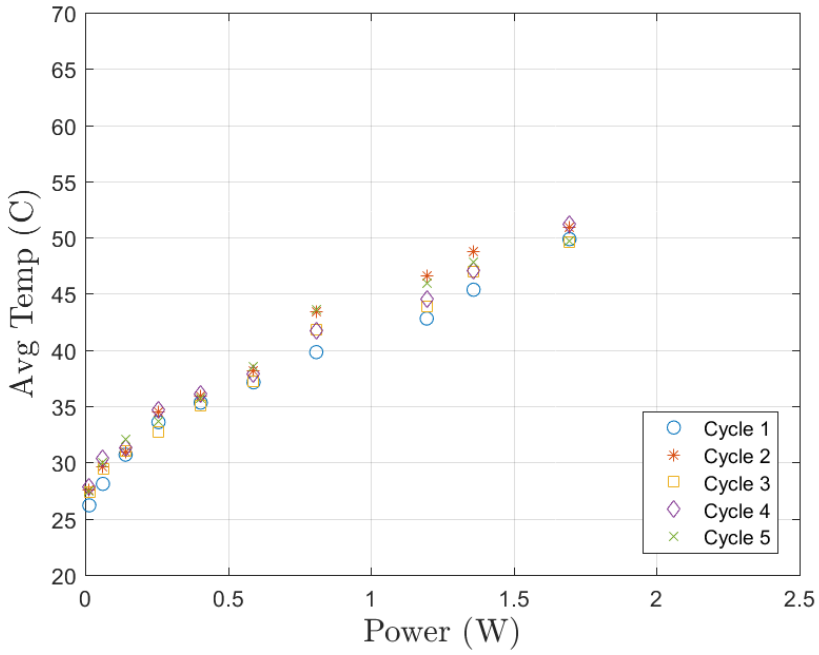

Figure B.12: Temperature comparison plot of the five test cycles performed on CNT Type 4 Specimen 3

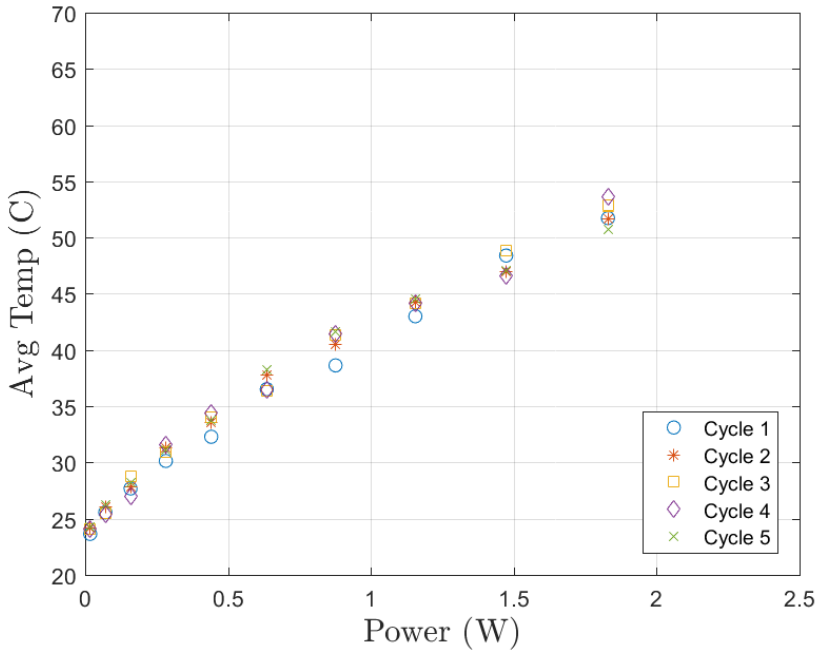

Figure B.13: Temperature comparison plot of the five test cycles performed on CNT Type 5 Specimen 1

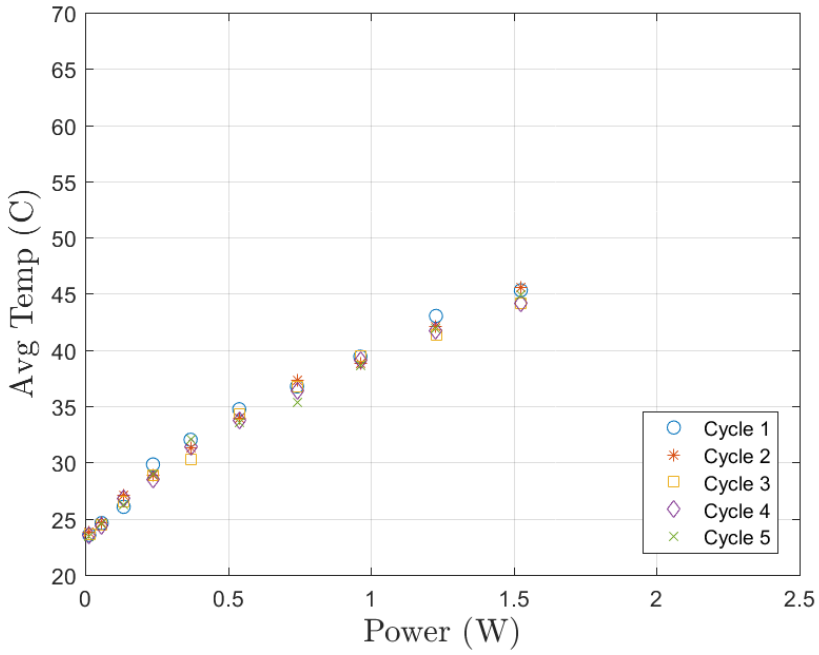

Figure B.14: Temperature comparison plot of the five test cycles performed on CNT Type 5 Specimen 2

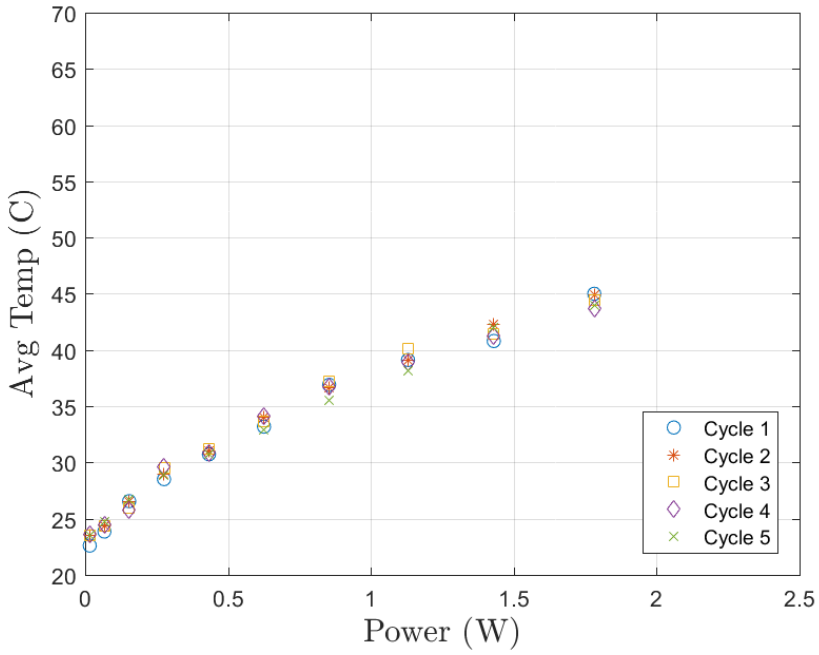

Figure B.15: Temperature comparison plot of the five test cycles performed on CNT Type 5 Specimen 3

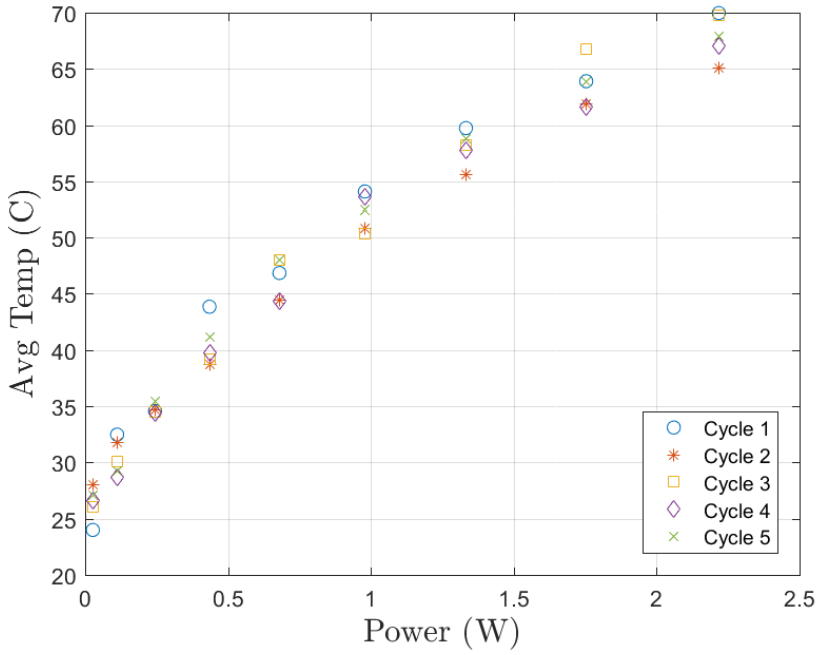

Figure B.16: Temperature comparison plot of the five test cycles performed on Etched Foil Type 6 Specimen 1

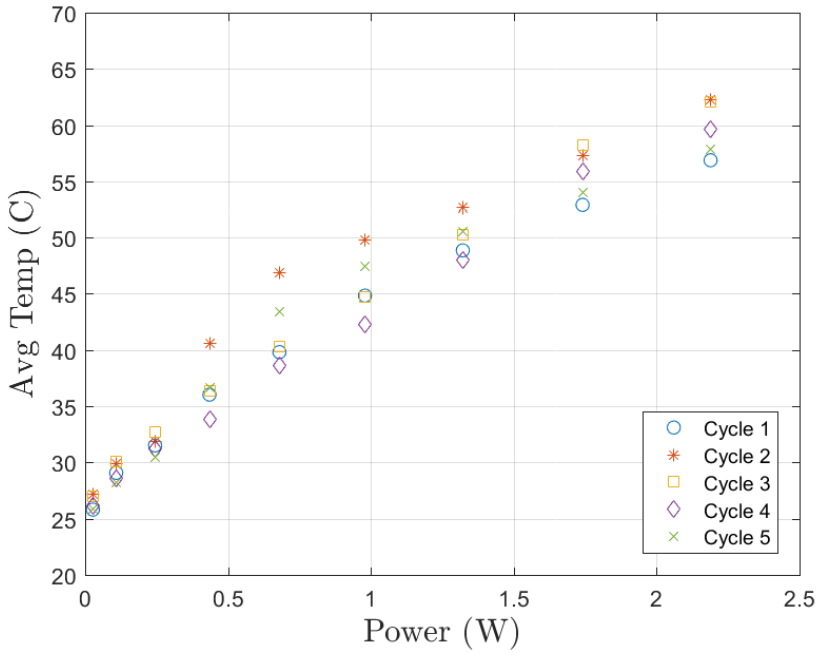

Figure B.17: Temperature comparison plot of the five test cycles performed on Etched Foil Type 6 Specimen 2

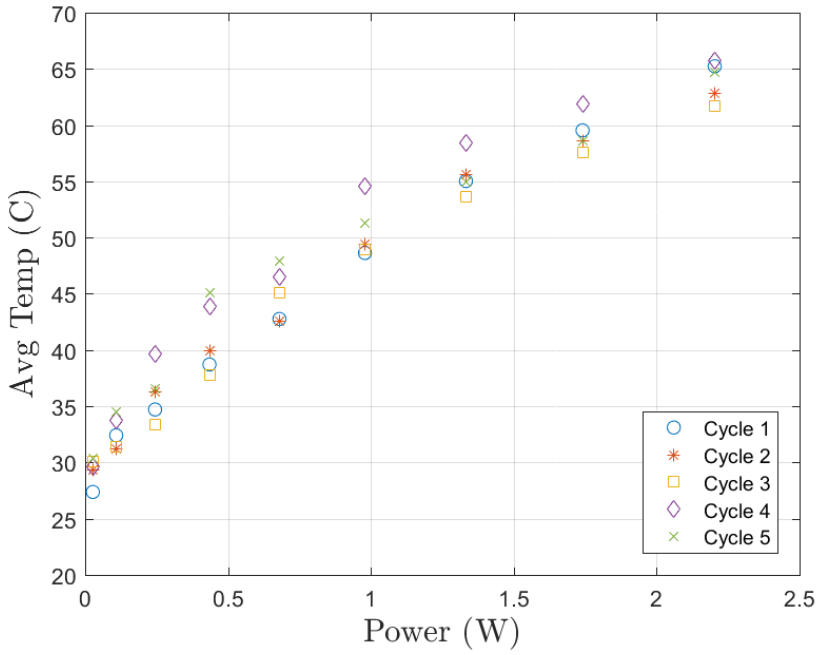

Figure B.18: Temperature comparison plot of the five test cycles performed on Etched Foil Type 6 Specimen 3

B.2 Specimen Comparison Plots

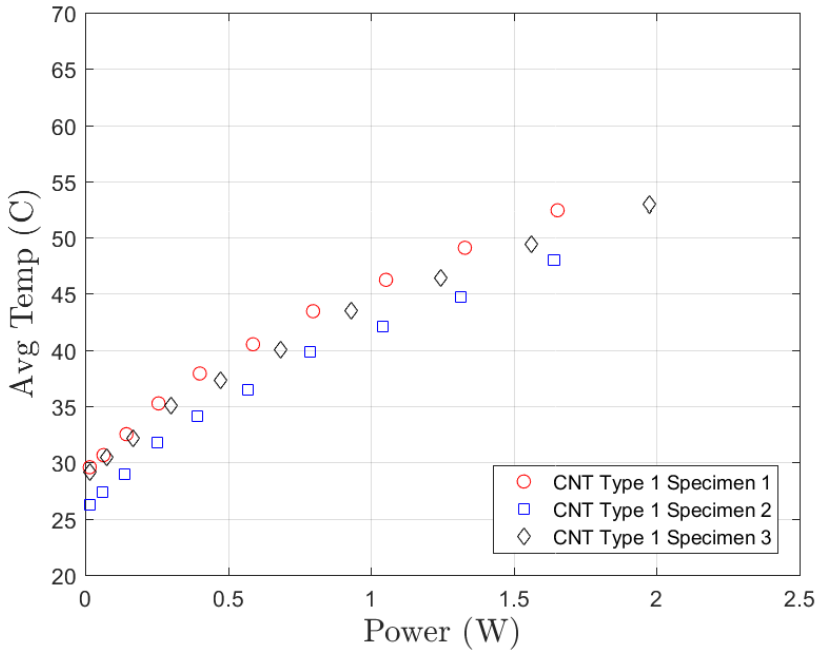

Figure B.19: Average temperature comparison plot of the three CNT Type 1 specimens tested

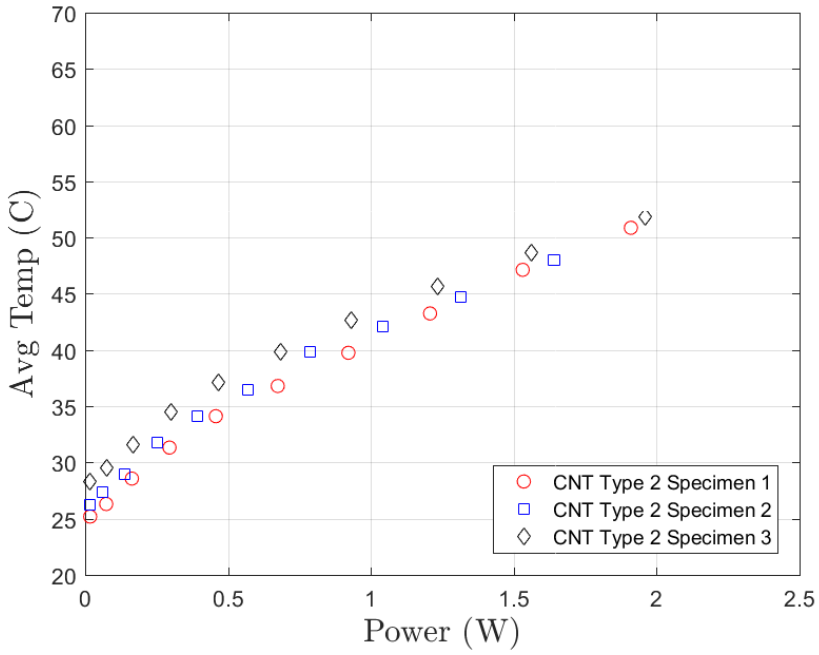

Figure B.20: Average temperature comparison plot of the three CNT Type 2 specimens tested

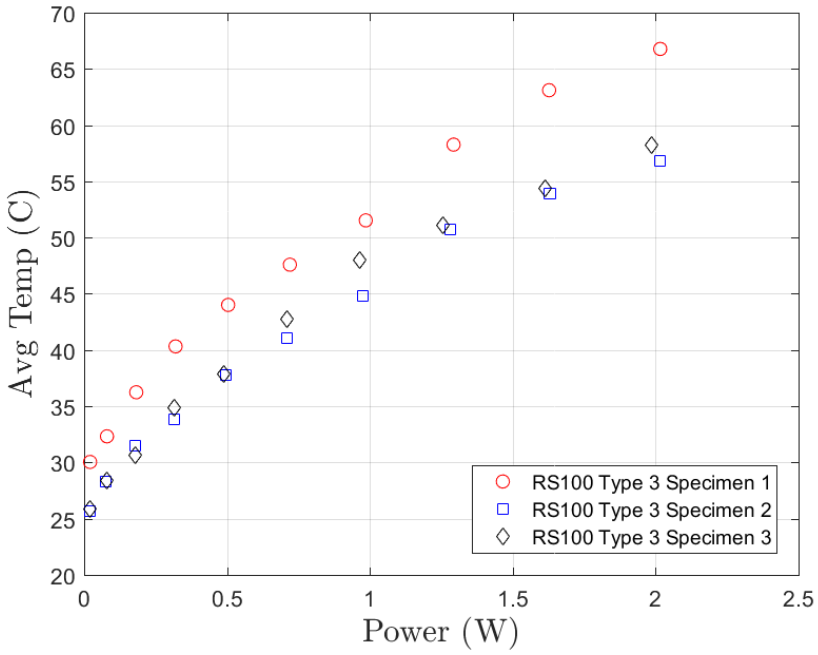

Figure B.21: Average temperature comparison plot of the three RS100 Type 3 specimens tested

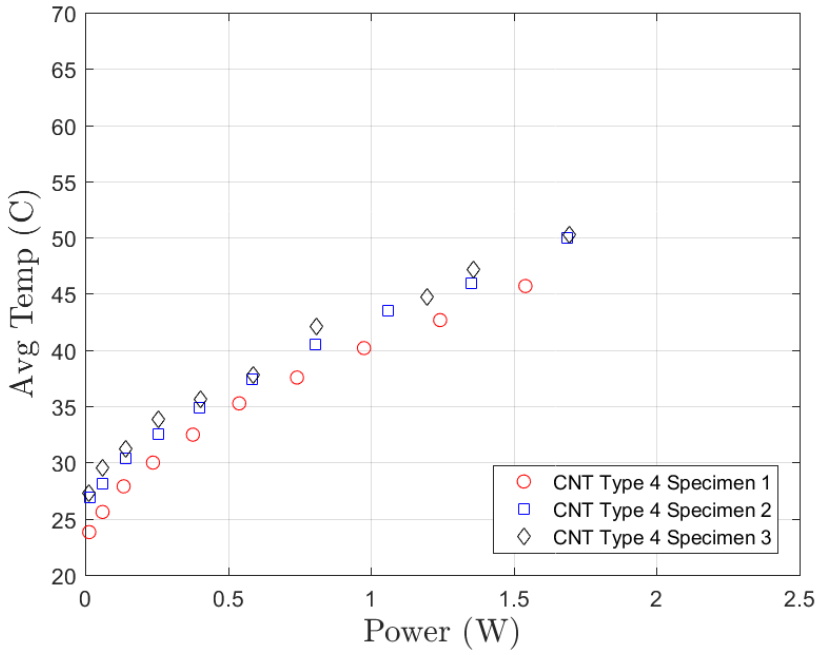

Figure B.22: Average temperature comparison plot of the three CNT Type 4 specimens tested

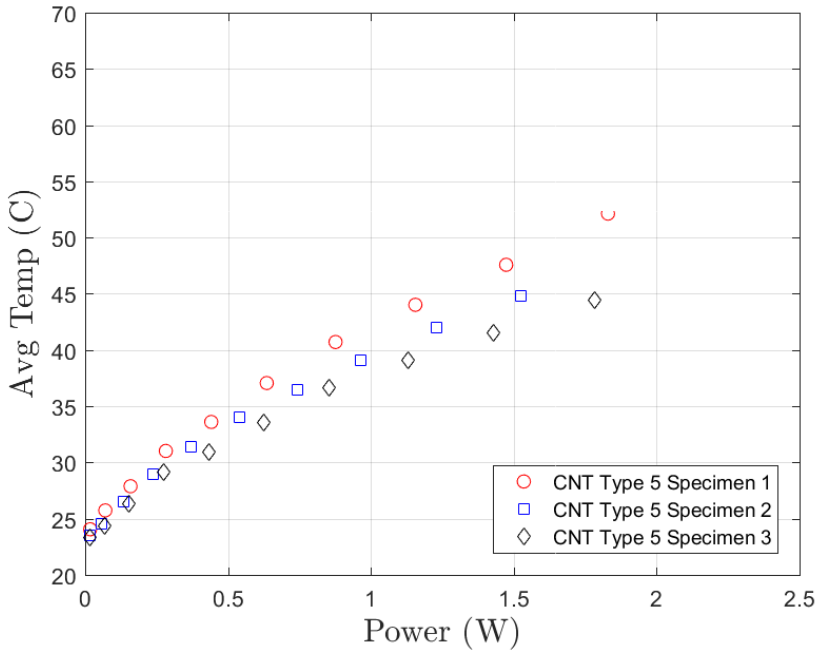

Figure B.23: Average temperature comparison plot of the three CNT Type 5 specimens tested

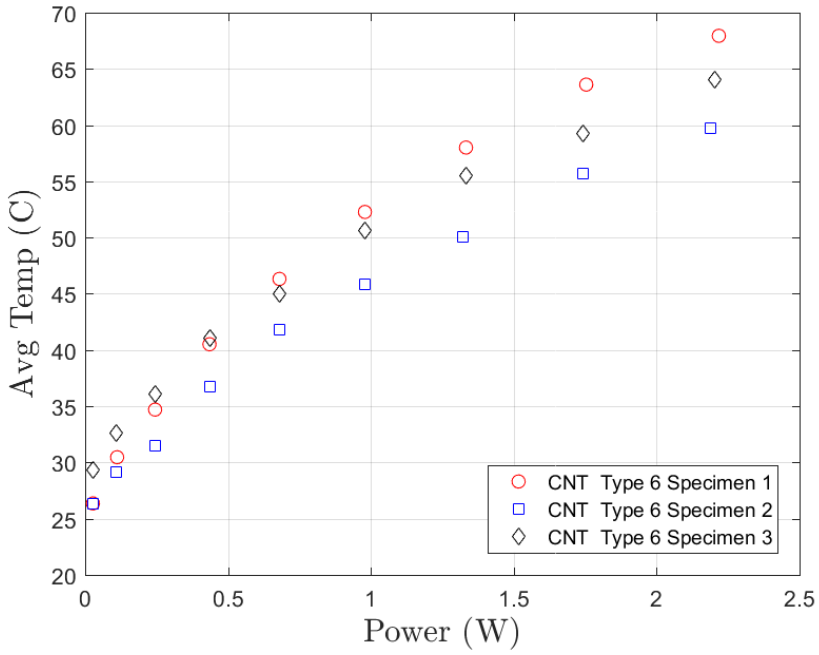

Figure B.24: Average temperature comparison plot of the three Etched Foil Type 6 specimens tested

B.3 Polyfit Line Plots

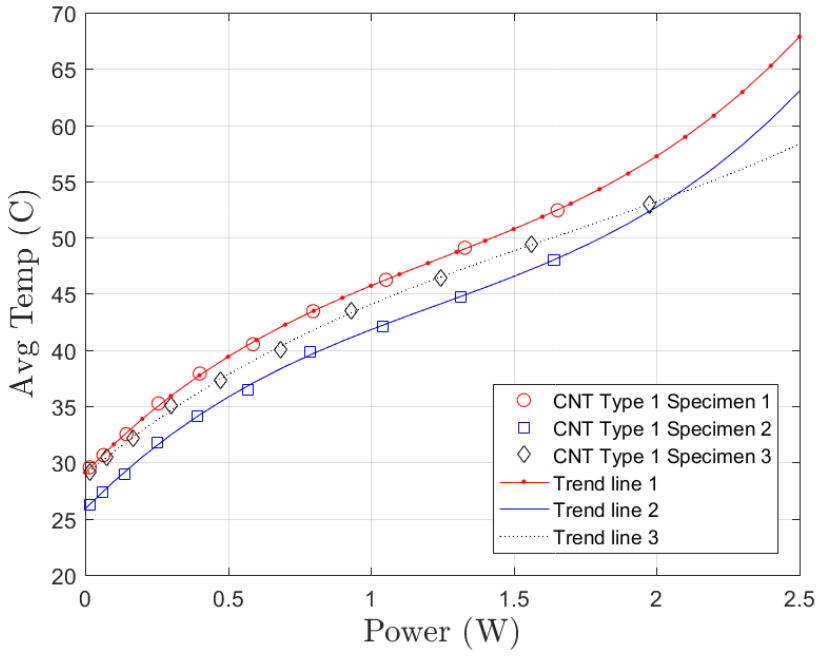

Figure B.25: This plot shows that a 3rd Order Polynomial curve fitted to the data accurately represents the known data points for Type 1 specimens

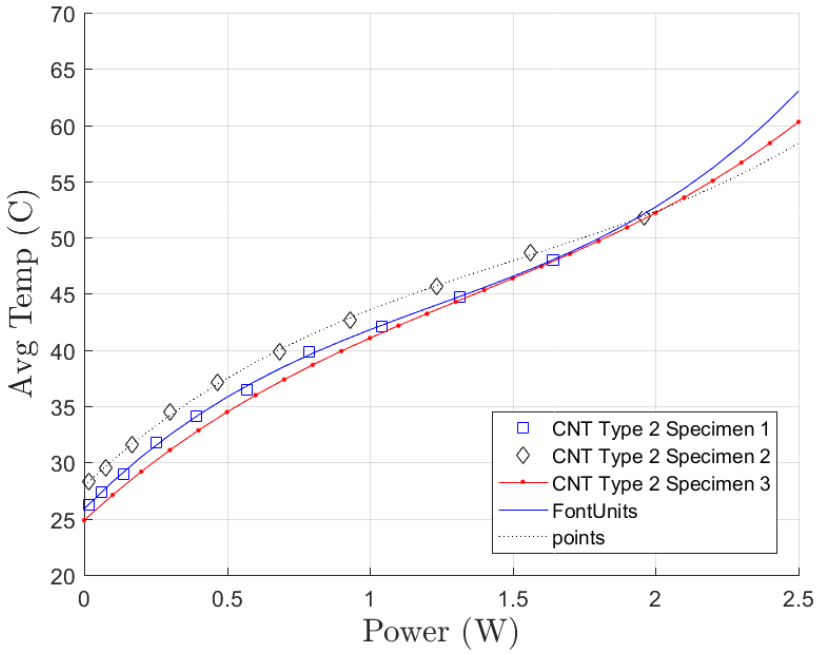

Figure B.26: This plot shows that a 3rd Order Polynomial curve fitted to the data accurately represents the known data points for Type 2 specimens

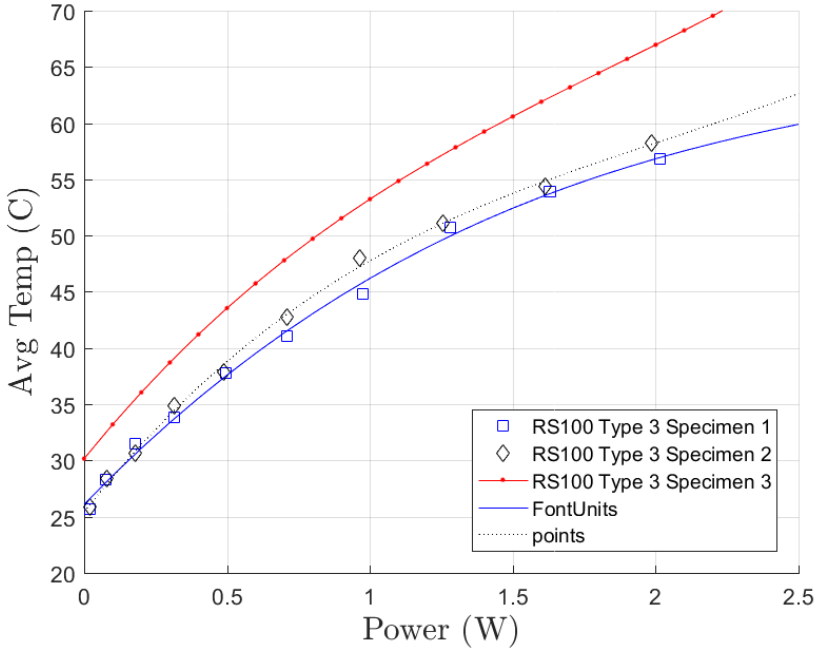

Figure B.27: This plot shows that a 3rd Order Polynomial curve fitted to the data accurately represents the known data points for Type 3 specimens

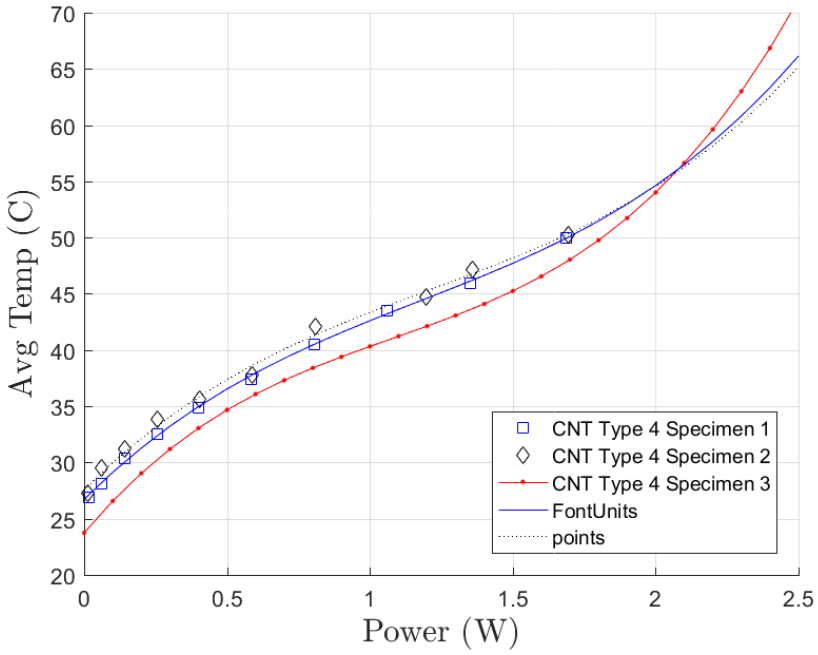

Figure B.28: This plot shows that a 3rd Order Polynomial curve fitted to the data accurately represents the known data points for Type 4 specimens

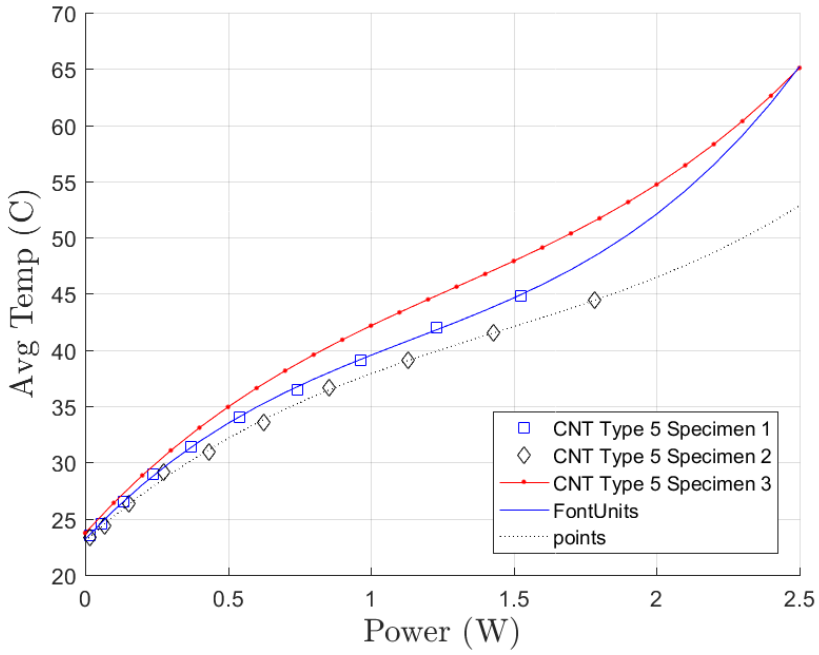

Figure B.29: This plot shows that a 3rd Order Polynomial curve fitted to the data accurately represents the known data points for Type 5 specimens

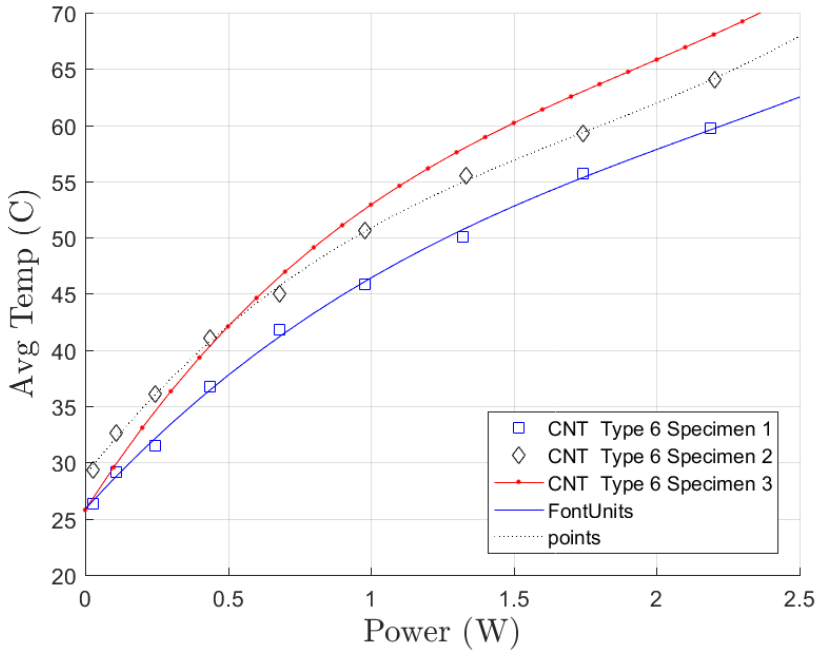

Figure B.30: This plot shows that a 3rd Order Polynomial curve fitted to the data accurately represents the known data points for Type 6 specimens

B.4 Avg Polyfit Line Plots

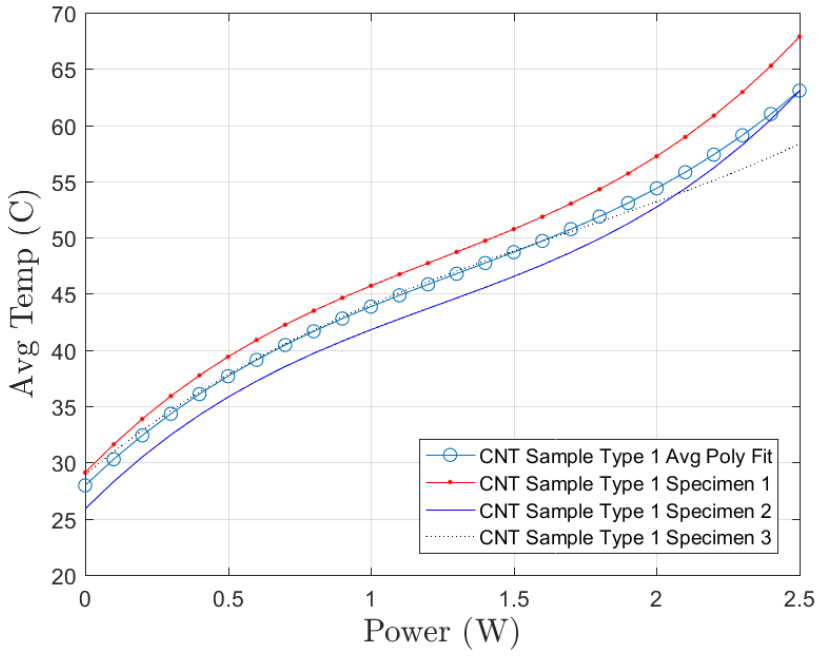

Figure B.31: The average of the three 3rd Order Polynomial curves plotted with the original fitted curves for CNT Type 1 Specimens 1-3

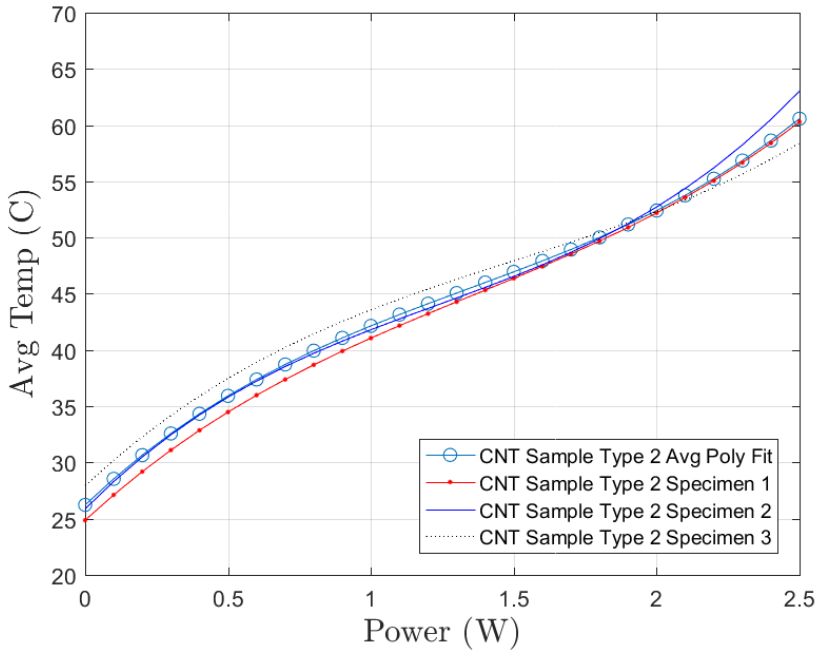

Figure B.32: The average of the three 3rd Order Polynomial curves plotted with the original fitted curves for CNT Type 2 Specimens 1-3

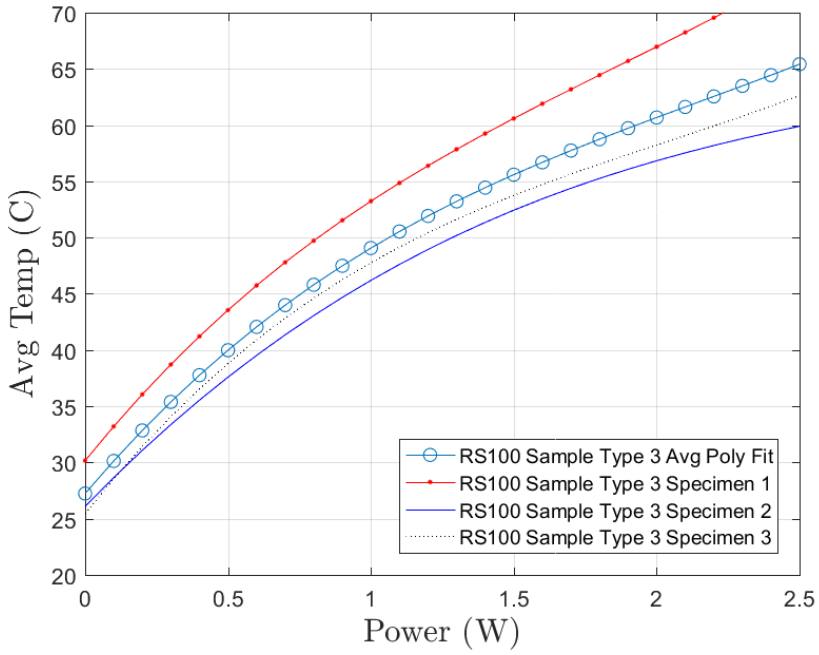

Figure B.33: The average of the three 3rd Order Polynomial curves plotted with the original fitted curves for RS100 Type 3 Specimens 1-3

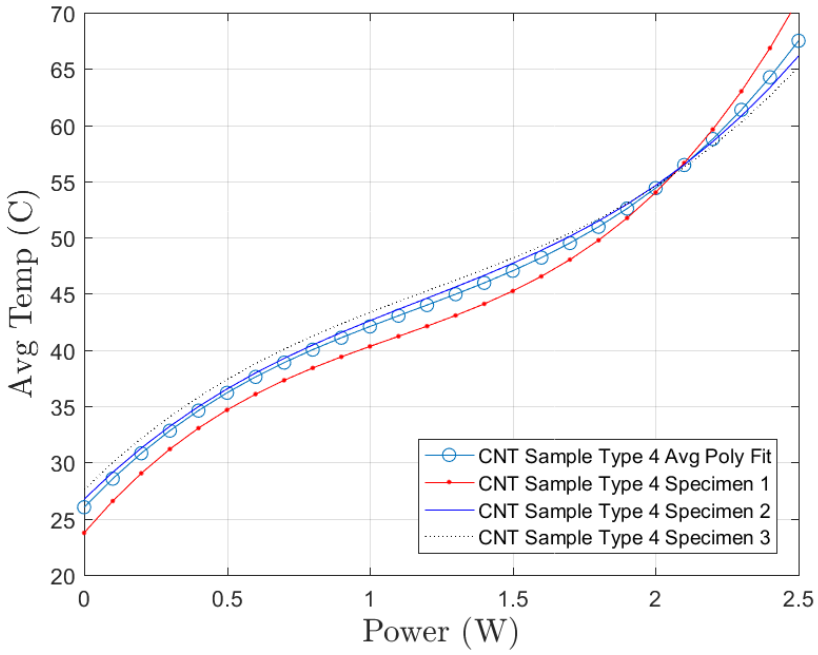

Figure B.34: The average of the three 3rd Order Polynomial curves plotted with the original fitted curves for CNT Type 4 Specimens 1-3

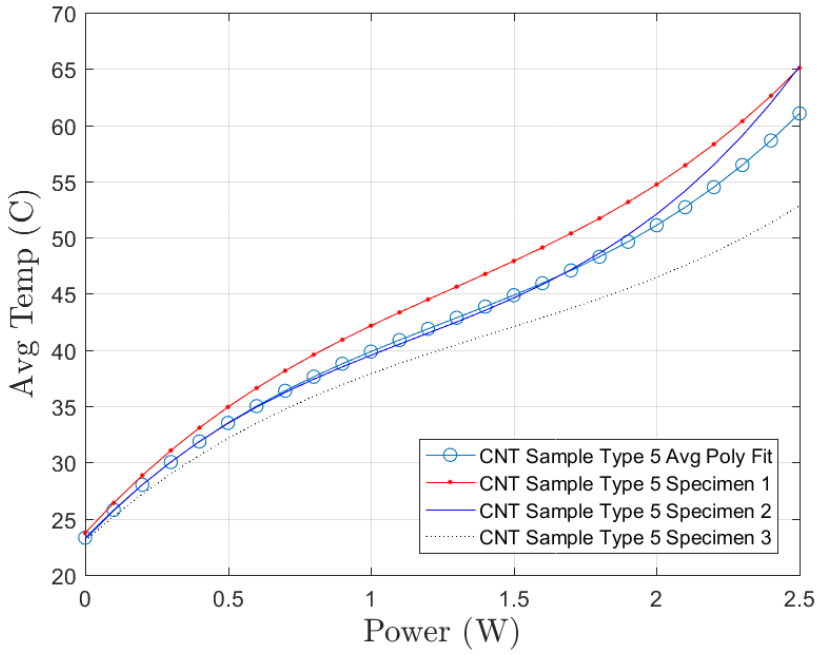

Figure B.35: The average of the three 3rd Order Polynomial curves plotted with the original fitted curves for CNT Type 5 Specimens 1-3

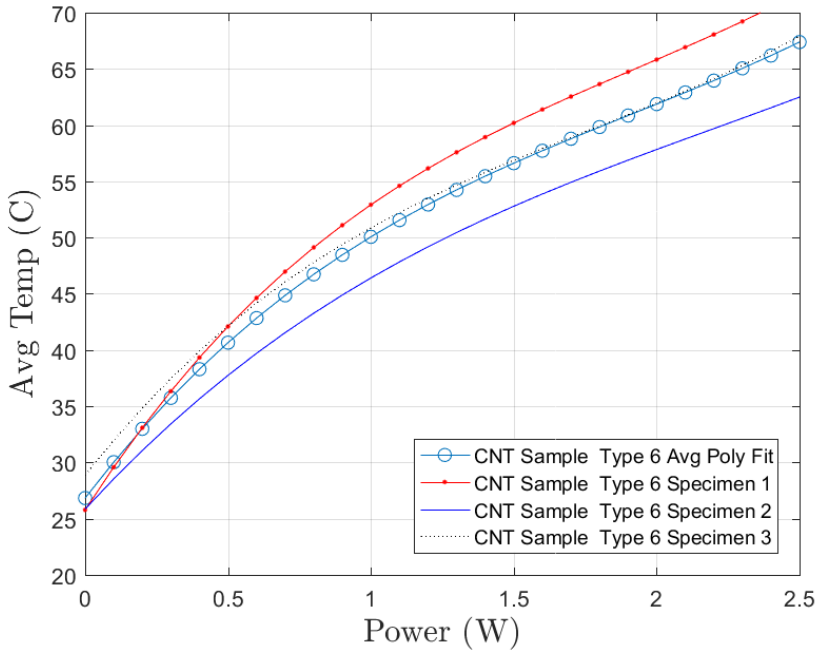

Figure B.36: The average of the three 3rd Order Polynomial curves plotted with the original fitted curves for Etched Foil Type 6 Specimens 1-3

B.5 Comparative Heater Ramp Plots

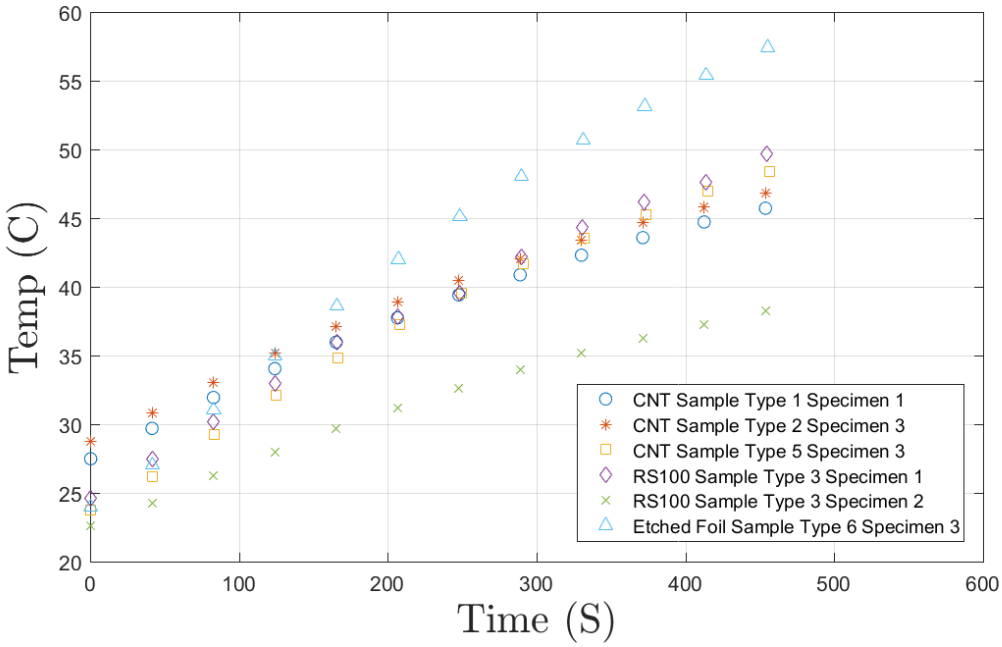

Figure B.37: Ramp testing data plotted for various specimens across all specimen types

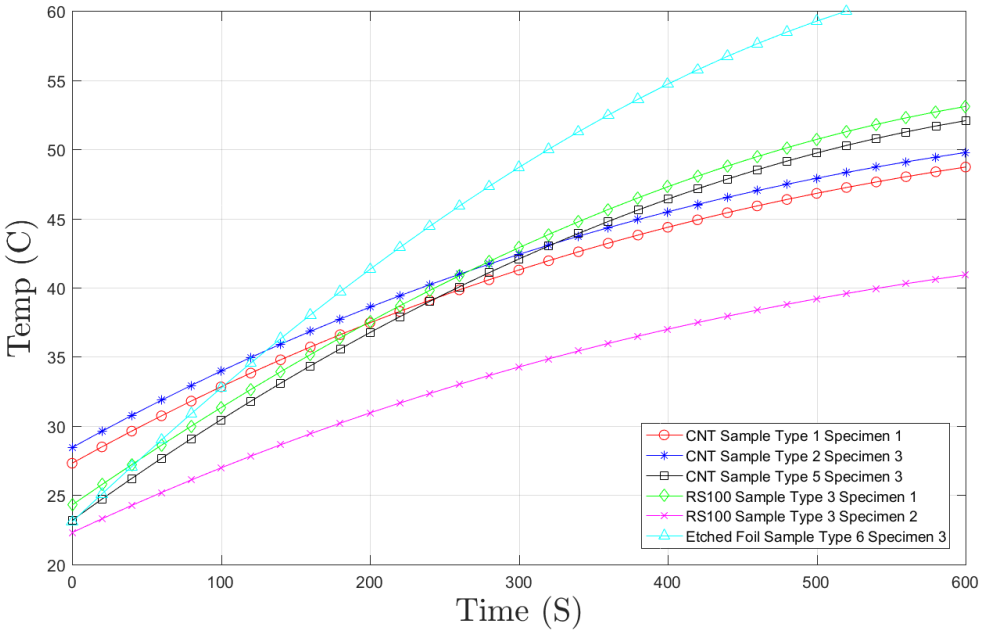

Figure B.38: 3rd order polynomial fit of all the ramp data for the specimens

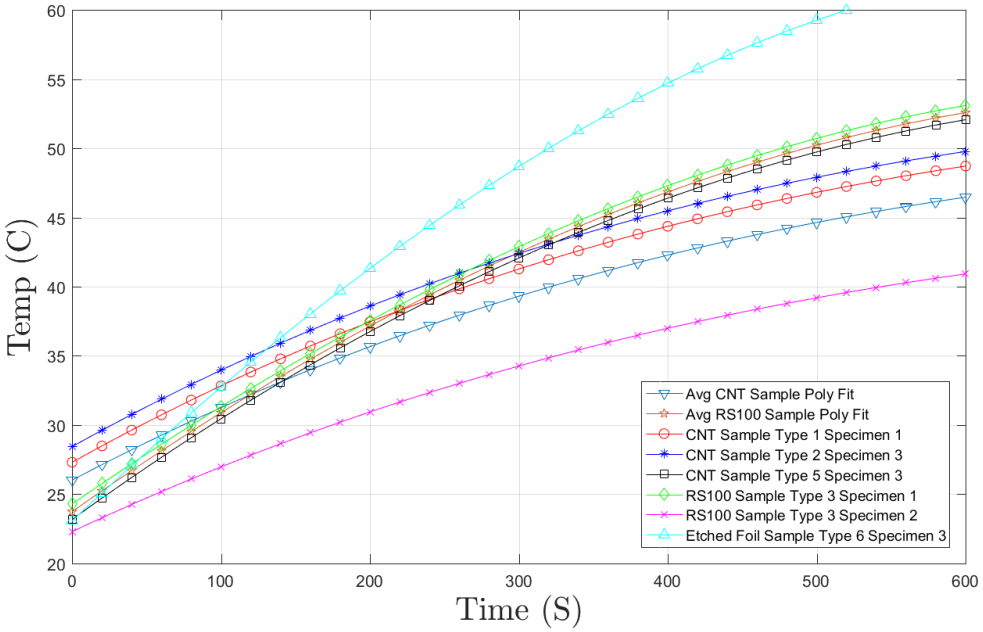

Figure B.39: 3rd order polynomial fit of all the ramp data and the trend line for the average of each specimen type

B.6 CNT Amperage Ramp Response Plots

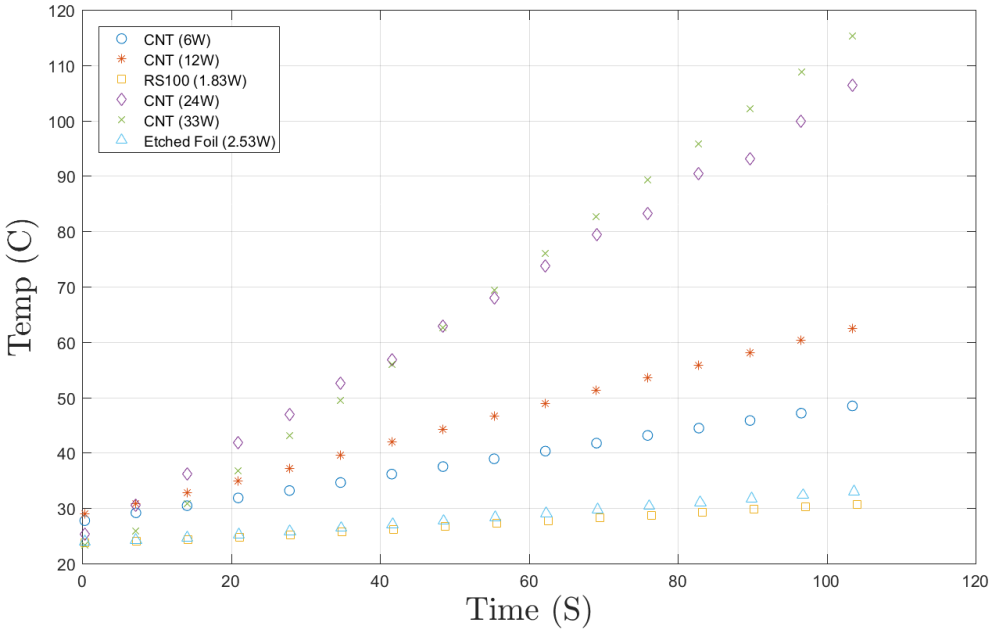

Figure B.40: High current ramp response data for the specimens

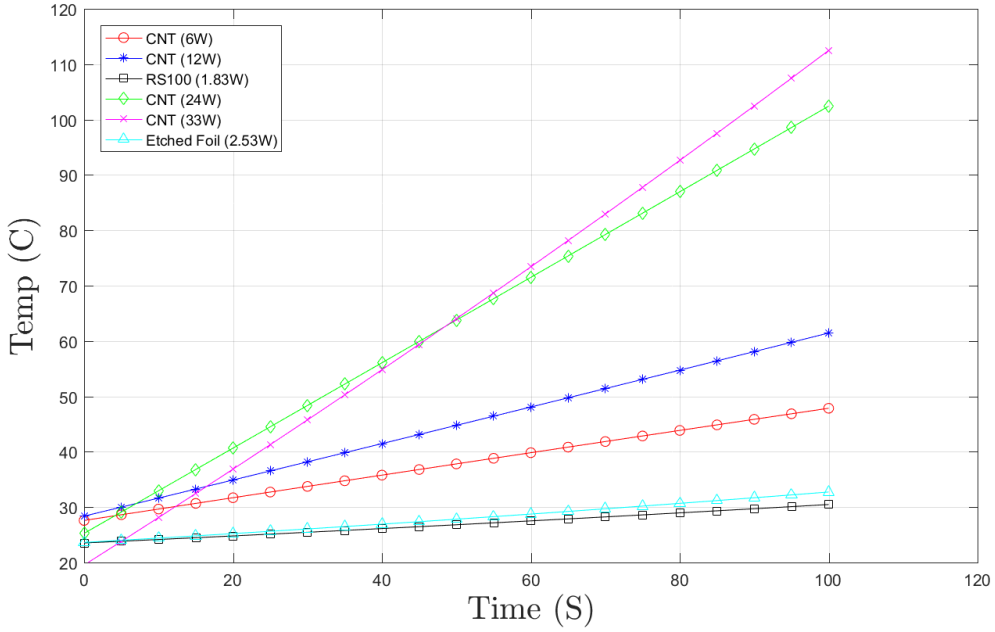

Figure B.41: Comparison plot of trend lines for the high current ramp responses

Appendix C. Arduino Shield Board Schematic and Code

C.1 Arduino Shield Board Schematic

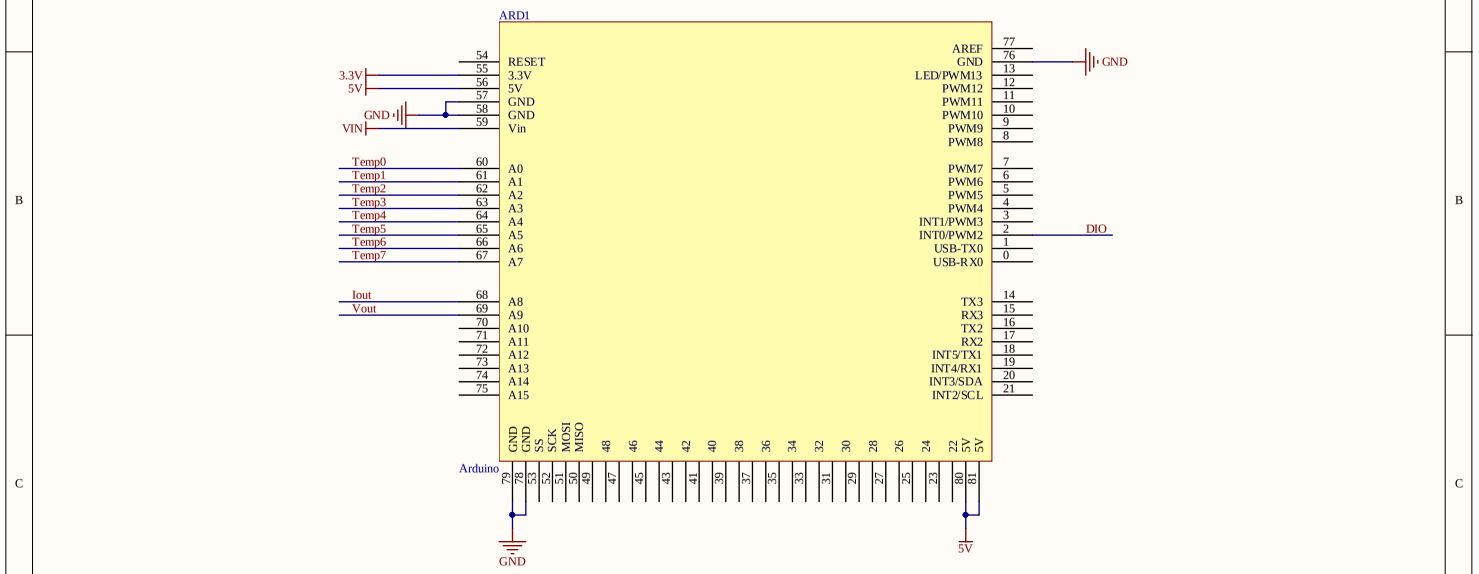

Title		
Size: Letter	Number	Revision
Date: 2/8/2018		Sheet of
File: C:\Files\..\Arduino_Headers.SchDoc		Drawn By:

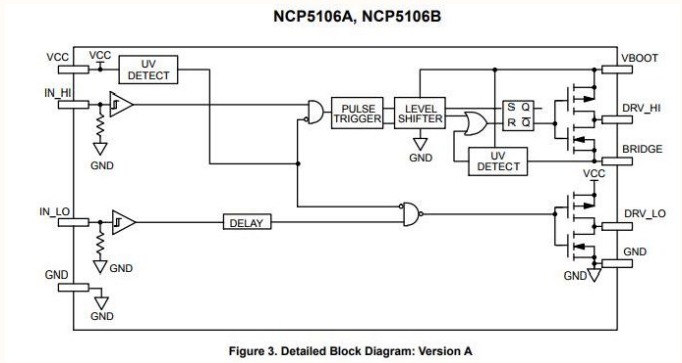

Figure 3. Detailed Block Diagram: Version A

Rs = 0.05
RL = 48.7k = 48,700

Vout = (Is * Rs * RL) / 1000
1000 * Vout = Is * 2435
Is = Vout * 0.41068

Offset:
LED 0.0147 A

Min Read = 0.0020041 A
Max Read = 2.0502012 A

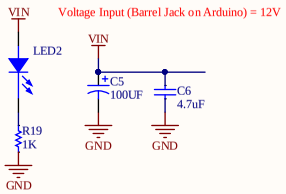

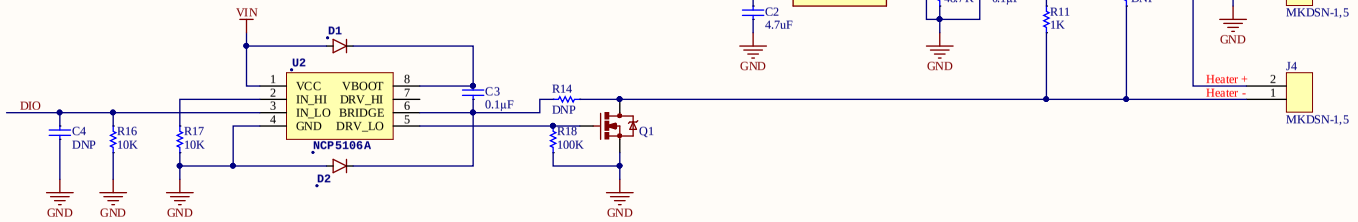

Title			
Size: Letter	Number		Revision
Date: 2/8/2018		Sheet of	
File: C:\Files\..\Heater_Patch_PWM_Control.SchDoc		Drawn By:	

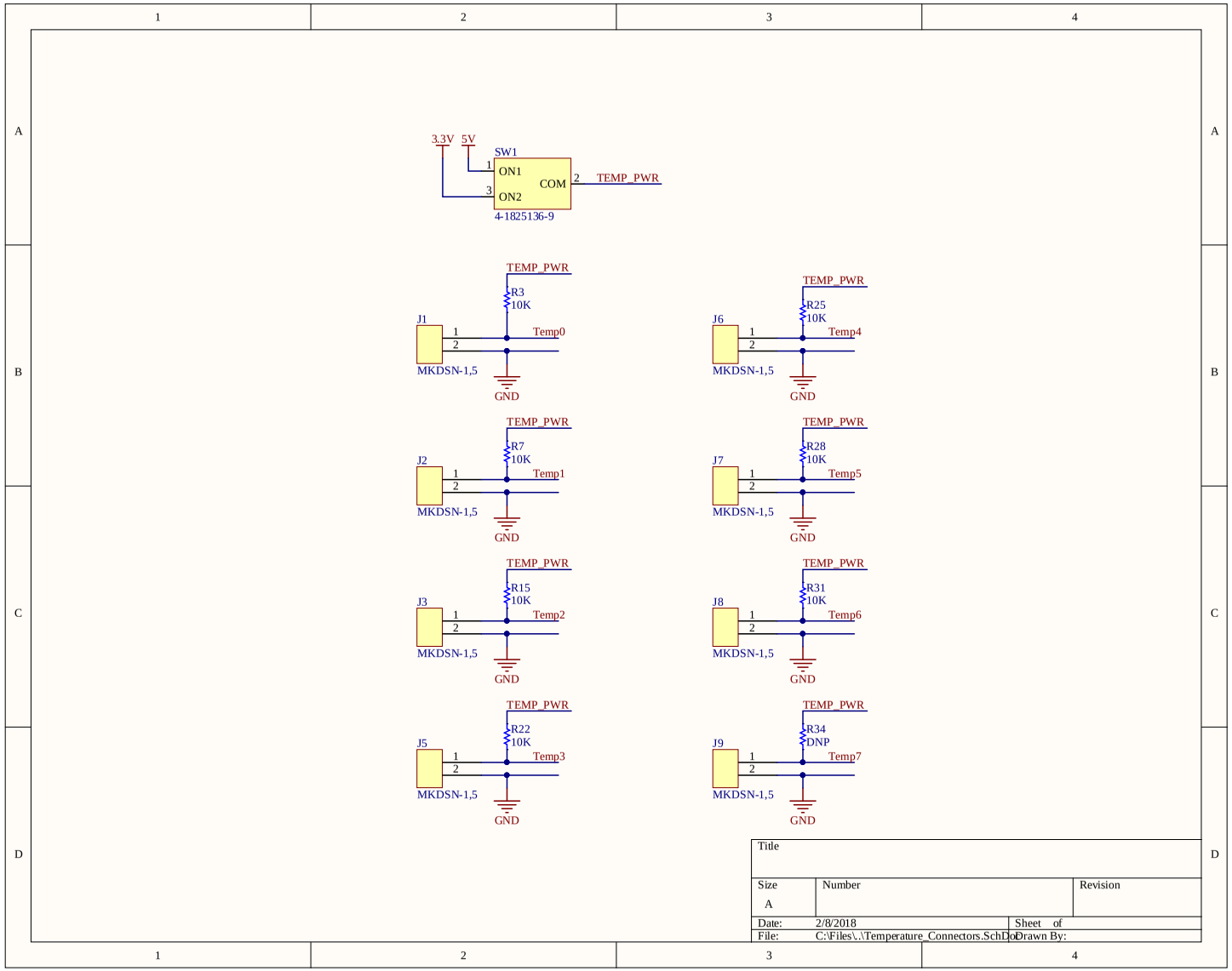
3.3V
5V
SW1
1
ON1
COM
2
TEMP_PWR
3
ON2
4-1825136-9
TEMP_PWR
R3
10K
J1
1
2
Temp0
MKDSN-1,5
GND
TEMP_PWR
R25
10K
J6
1
2
Temp4
MKDSN-1,5
GND
TEMP_PWR
R7
10K
J2
1
2
Temp1
MKDSN-1,5
GND
TEMP_PWR
R28
10K
J7
1
2
Temp5
MKDSN-1,5
GND
TEMP_PWR
R15
10K
J3
1
2
Temp2
MKDSN-1,5
GND
TEMP_PWR
R31
10K
J8
1
2
Temp6
MKDSN-1,5
GND
TEMP_PWR
R22
10K
J5
1
2
Temp3
MKDSN-1,5
GND
TEMP_PWR
R34
DNP
J9
1
2
Temp7
MKDSN-1,5
GND
Title
Size
A
Number
Revision
Date:
2/8/2018
Sheet of
File:
C:\Files\..\Temperature_Connectors.SchDo
Drawn By:

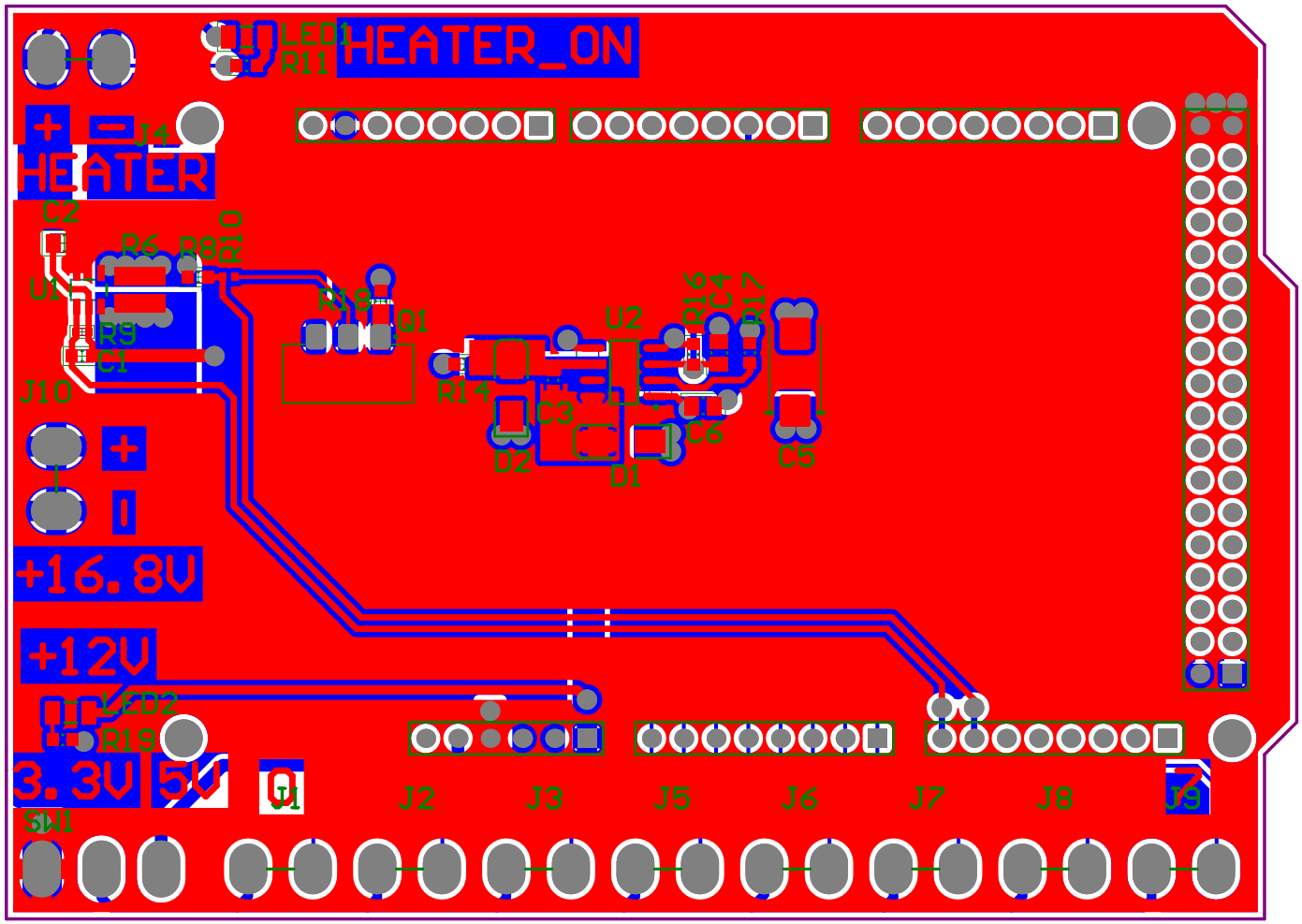
HEATER_ON
LED1
R11
J4
HEATER
C2
R6
R8
U1
R9
C1
J10
Q1
R14
U2
C3
C4
C6
C5
D2
D1
+16.8V
+12V
LED2
R19
3.3V
5V
J1
J2
J3
J5
J6
J7
J8
J9
SW1

C.2 Arduino Code

```
// Default is 0% duty cycle out of pin 2 (Atmega 2560).
int pwmPin = 2;

int interruptPin = 21;                 // Pin used for the
interrupt (Push button).
long debounceTime = 1000;              // Debouncing in milli
seconds
volatile unsigned long last_micros;

double dutyCycleValue = 0;  // 0 = Always off (0%), 255 = Always
on (100%)
float dutyCyclePercentage = 50.0;  // Used to calculate the
value from the percentage.
float increments;    // initial step increments for the pwm
float heaterohms;    // initial heater restistance
float BaseVoltage; // Voltage being supplied by powersupply
float increment = 0.0; // initial increment value
float thermistor_reading=0; // initial thermistor reading

// which analog pin to connect for ambient temperature readings
#define AMBIENTPIN_A0 A0
// which analog pin to connect for each thermistor
#define THERMISTORPIN_A1 A1
// resistance at 25 degrees C in Ohms
#define THERMISTORPIN_A2 A2
// resistance at 25 degrees C in Ohms
#define THERMISTORPIN_A3 A3
// resistance at 25 degrees C in Ohms
#define THERMISTORPIN_A4 A4
// resistance at 25 degrees C in Ohms
#define THERMISTORPIN_A5 A5
// resistance at 25 degrees C in Ohms
#define THERMISTORPIN_A6 A6
// resistance at 25 degrees C in Ohms



void setup(void) {
```

```
  Serial.begin(9600);
  analogReference(EXTERNAL);

  // Initialize all the variables in case of reset.
  dutyCycleValue = 0;
  dutyCyclePercentage = 0;
  increments = 0.0;
  heaterohms = 0.0;
  BaseVoltage = 0.0;
  increment = 0.0;
  thermistor_reading = 0.0;
  analogWrite(pwmPin, 0);       // sets the PWM setting to the
s0

  // Initializing interrupt for the killswitch.
  pinMode(interruptPin, INPUT_PULLUP);
 attachInterrupt(digitalPinToInterrupt(interruptPin),
debounceKillSwitch, FALLING);

  delay(200);

  // Set up the base voltage.
  Serial.print("Enter voltage from power supply: "); // Outputs
to the serial monitor a prompt asking for the voltage from the
power supply
  while (Serial.available() <= 0);
  BaseVoltage = Serial.parseFloat();
  Serial.print(BaseVoltage);
  Serial.println(" Volts from power supply");

    // Set up the increments for pwm stepping.
  Serial.print("Enter PWM step increments in %: "); // Outputs
to the serial monitor a prompt asking for the PWM stepping
increments
  while (Serial.available() <= 0);
  increment = Serial.parseFloat();
  Serial.print(increment);
  Serial.println("% increments");
```

```
    // Set up the patch heater resistance.
  Serial.print("Enter Patch heaters resistance in Ohms: "); //
Outputs to the serial monitor a prompt asking for the patch
heaters resistance.
  while (Serial.available() <=0);
  heaterohms = Serial.parseFloat();     // assigns inputed
value to a variable
 Serial.print(heaterohms,1);
  Serial.println(" Ohms selected");
  Serial.println("\r\nAmbient Temperature *C, Thermistor 1
Temperature *C, Thermistor 2 Temperature *C, Thermistor 3
Temperature *C, Thermistor 4 Temperature *C, Thermistor 5
Temperature *C, Thermistor 6 Temperature *C, Heater Resistance
(Ohms), Base voltage, PWM setting (%), Current (uA), Temp delta
(%), Elapsed time (s)");


}
/*---------------------------------------------------------------
---------------------*/

void loop(void) {

int g ;
for (g=1; g<=5 ;g++){

  float p=0.0; // PWM steps
  int t;  // time steps

  float average;
  float timedelay;
float Ambient;
float Therm_01;
float Therm_02;
float Therm_03;
float Therm_04;
float Therm_05;
```

```
float Therm_06;


  // Set PWM increment loop
  while (p<=(100.0-increment)){


          float current;
          float ElapsedTime = 0;
          unsigned long StartTime = micros();

    p += increment;
    dutyCyclePercentage = p;
    dutyCycleValue = dutyCyclePercentage * 2.55; // Converts
from percent to value used by Arduino.
    analogWrite(pwmPin, dutyCycleValue);       // sets the new
PWM setting to the specified pin
    // Run sampling code for 180 secs or 3 minutes
          int count = 0;
          float deltaper=999;
          float temp1=0;
          float temp2=0;

   while(abs(deltaper)>0.25){
         count = count+1;
          // temperature voltage calculations
          Ambient = TempCalc(AMBIENTPIN_A0);                //
temperature read from the ambient environment
          Therm_01 = TempCalc(THERMISTORPIN_A1);            //
temperature read from thermistor in pin A1
          Therm_02 = TempCalc(THERMISTORPIN_A2);            //
temperature read from thermistor in pin A2
          Therm_03 = TempCalc(THERMISTORPIN_A3);            //
temperature read from thermistor in pin A3
          Therm_04 = TempCalc(THERMISTORPIN_A4);            //
temperature read from thermistor in pin A4
          Therm_05 = TempCalc(THERMISTORPIN_A5);            //
temperature read from thermistor in pin A5
```

```
          Therm_06 = TempCalc(THERMISTORPIN_A6);             //
temperature read from thermistor in pin A6


          // current calculation
            // Current Measurement
          current = currentAverage();
//          Serial.print("Current: ");
//          Serial.print(current);
//          Serial.println(" uA");

         // steady state temperature loop
         if(count%10==0 && count>60){
          temp1 = temp2;
          temp2 = Therm_01;
          deltaper = ((temp2-temp1)/temp2)*100;
         }


          unsigned long CurrentTime = micros();
          float ElapsedTime = (CurrentTime - StartTime)/1000000.
0;

// print to CSV format
          Serial.print(Ambient);  // print the ambient
temperature from thermistor 0
          Serial.print(",");
          Serial.print(Therm_01);  // print the temperature from
thermistor 1
          Serial.print(",");
          Serial.print(Therm_02);  // print the temperature from
thermistor 2
          Serial.print(",");
          Serial.print(Therm_03);  // print the temperature from
thermistor 3
          Serial.print(",");
          Serial.print(Therm_04);  // print the temperature from
thermistor 4
```

```
         Serial.print(",");
         Serial.print(Therm_05);  // print the temperature from
thermistor 5
         Serial.print(",");
         Serial.print(Therm_06);  // print the temperature from
thermistor 6
         Serial.print(",");
         Serial.print(heaterohms); // print the resistance of
the patch heater
         Serial.print(",");
         Serial.print(BaseVoltage); // print base voltage
         Serial.print(",");
         Serial.print(p,1);    // print the pwm setting
         Serial.print(",");
         Serial.print(current,3);  // output the current value
         Serial.print(",");
         Serial.print(deltaper);    // print the % difference
between the last 5 samples
         Serial.print(",");
         Serial.println(ElapsedTime); // print elapsed time

         delay(1000); // delay 1 second after all readings are
complete
      }
         Serial.print("N/a");  // Placeholder for temperature
from ambient
         Serial.print(",");
         Serial.print("N/a");  // Placeholder for thermistor 1
         Serial.print(",");
         Serial.print("N/a");    // Placeholder for termistor 2
         Serial.print(",");
         Serial.print("N/a");    // Placeholder for termistor 3
         Serial.print(",");
         Serial.print("N/a");    // Placeholder for termistor 4
         Serial.print(",");
         Serial.print("N/a");    // Placeholder for termistor 5
         Serial.print(",");
         Serial.print("N/a");    // Placeholder for termistor 6
```

```
         Serial.print(",");
         Serial.print("N/a");    // Placeholder for heater
resistance
         Serial.print(",");
         Serial.print("N/a");    // Placeholder for base voltage
         Serial.print(",");
         Serial.print("N/a");    // Placeholder for PWM setting
         Serial.print(",");
         Serial.print("N/a");    // Placeholder for current
         Serial.print(",");
         Serial.print("N/a");    // Placeholder for delta
percent
         Serial.print(",");
         Serial.print("N/a\r\n");    // Placeholder for delta
time
      delay(15000); // delay 15 seconds to collect data

     }
     float off = 0.0;
     analogWrite(pwmPin, off);       // sets the PWM to 0 to
allow for cooldown to ambient temperature

    while(Therm_01>Ambient+0.50){
          Ambient = TempCalc(AMBIENTPIN_A0);                 //
temperature read from the ambient environment
          Therm_01 = TempCalc(THERMISTORPIN_A1);             //
temperature read from thermistor in pin A1
         unsigned long CurrentTime = micros();
         //float ElapsedTime = (CurrentTime -
StartTime)/1000000.0;
         Serial.print(Ambient);  // print the ambient
temperature from ambient
         Serial.print(",");
         Serial.print(Therm_01);  // print the temperature from
thermistor 1
         Serial.print(",");
         Serial.print("N/a");    // Placeholder for termistor 2
         Serial.print(",");
```

```
         Serial.print("N/a");    // Placeholder for termistor 3
         Serial.print(",");
         Serial.print("N/a");    // Placeholder for termistor 4
         Serial.print(",");
         Serial.print("N/a");    // Placeholder for termistor 5
         Serial.print(",");
         Serial.print("N/a");    // Placeholder for termistor 6
         Serial.print(",");
         Serial.print("N/a");    // Placeholder for heater
resistance
         Serial.print(",");
         Serial.print("N/a");    // Placeholder for base voltage
         Serial.print(",");
         Serial.print(off,1);    // Placeholder for PWM setting
         Serial.print(",");
         Serial.print("N/a");    // Placeholder for current
         Serial.print(",");
         Serial.print("N/a");    // Placeholder for delta
percent
         Serial.print(",");
         Serial.print("N/a\r\n"); // print elapsed time
         delay(5000);// delay 5 seconds
    }

}
   while(1){}  // force the loop to cycle through only once then
stop
}

/*-----------------------------------------------------------------
-----------------------------------------------------------------*/

float TempCalc(float thermistor_reading){
     #define THERMISTORNOMINAL 100000
     // temp. for nominal resistance (almost always 25 C)
     #define TEMPERATURENOMINAL 25
     // how many samples to take and average, more takes longer
     // but is more 'smooth'
```

```
     #define NUMSAMPLES 5
     // The beta coefficient of the thermistor (usually
3000-4000)
     #define BCOEFFICIENT 3950
     // the value of the 'other' resistor in Ohms
     #define SERIESRESISTOR 100000

     int samples[NUMSAMPLES]; // old code uint16_t

           // take N samples in a row, with a slight delay
           float THERMISTORPIN;
            int i;
           int timedelay;

           THERMISTORPIN = thermistor_reading;

          for (i=0; i< NUMSAMPLES; i++) {
              samples[i] = analogRead(THERMISTORPIN);
              timedelay = 10;  // delay 10 milliseconds
              delay(timedelay);
              }

          // average all the samples out
          float average = 0;

          for (i=0; i< NUMSAMPLES; i++) {
              average += samples[i];
              }
          average /= NUMSAMPLES;

          // convert the value to resistance
          average = 1023.0 / average - 1;
          average = SERIESRESISTOR / average;

          float steinhart;
          steinhart = average / THERMISTORNOMINAL;     // (R/Ro)
           steinhart = log(steinhart);                  //
ln(R/Ro)
```

```
          steinhart /= BCOEFFICIENT;                  // 1/B *
ln(R/Ro)
         steinhart += 1.0 / (TEMPERATURENOMINAL + 273.15); // +
(1/To)
          steinhart = 1.0 / steinhart;                // Invert
          steinhart -= 273.15;                        //
convert to C
          return steinhart;
}
/*-----------------------------------------------------------------
-----------------------------------------------------------------*/

/*  Debounce function for the Interrupt Service Routine.
 *  This function will be called whenever the Push button is
pressed.
 *
 */
void debounceKillSwitch()
{
  // Checks how long the button has been pressed.
  if ((long)(micros() - last_micros) >= debounceTime * 1000)
  {
    killSwitch();
    last_micros = micros();
  }
}

/*  Interrupt Service Routine (ISR)
 *  This function will be called whenever the Push button is
pressed, and jump to the beginning of the program (restarts).
 *
 */
void killSwitch()
{
  asm volatile (" jmp 0");
}

/*  Current Average
```

```
 *  This function will average the current readings.
 *
 */
float currentAverage()
{
  float tempCurrent = 0;

  for (int i = 0; i < 5; i++)
  {
    // IC parnt number INA169
//    tempCurrent = tempCurrent + (((4.88 * analogRead(8)) * 410.
68) - 14.7);
     tempCurrent = tempCurrent + ((analogRead(8) * (0.0049))*0.
411);
  }

  return (tempCurrent / 5);
}
```

C.3 Test Stand Mount Schematic

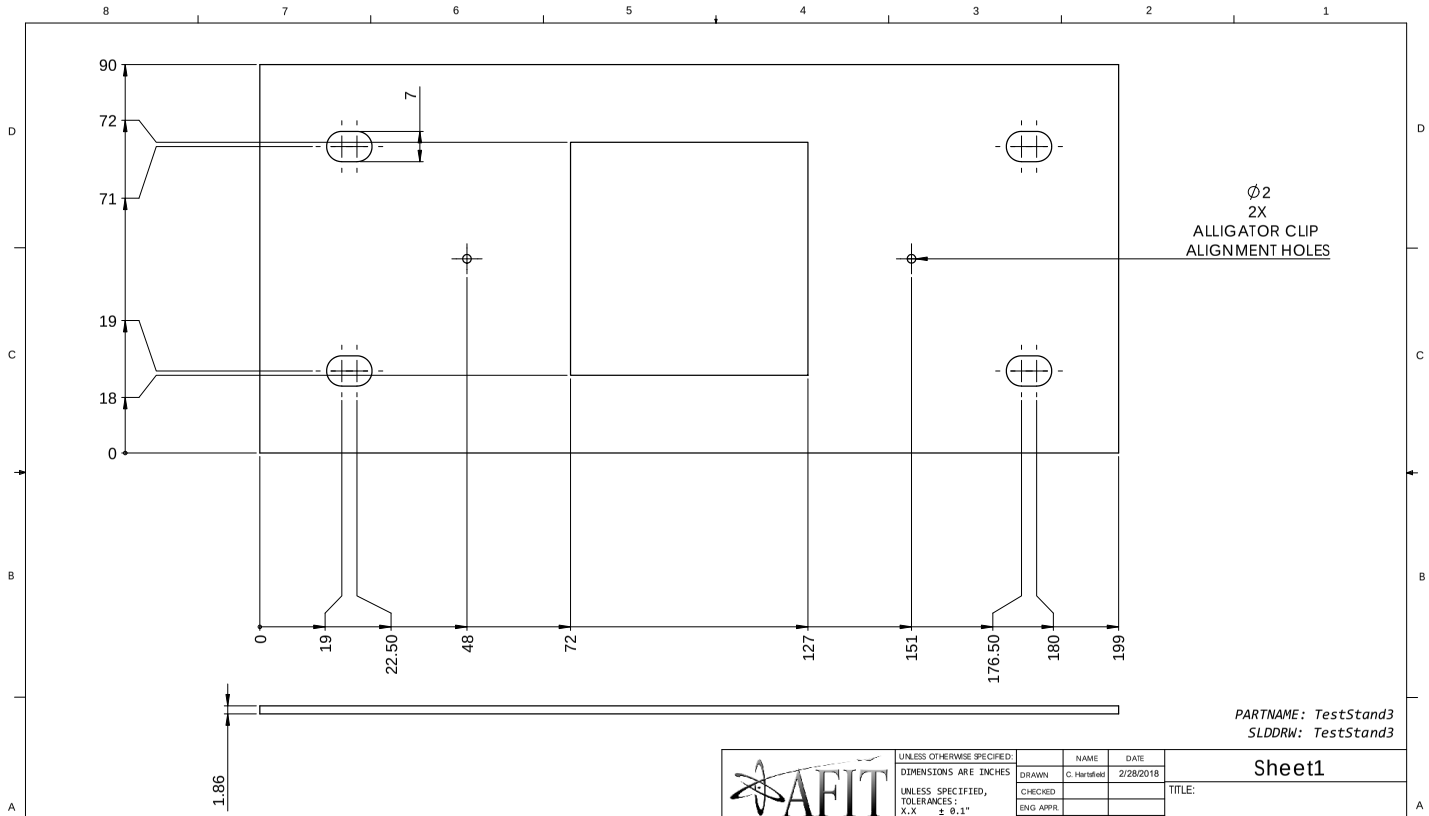

PARTNAME: TestStand3
SLDDRW: TestStand3

AFIT
Air Force Institute of Technology

WARNING: UNCLASSIFIED INFORMATION

THE INFORMATION CONTAINED IN THIS DRAWING IS PROPERTY OF AIR FORCE INSTITUTE OF TECHNOLOGY (AFIT).

ANY REPRODUCTION IN PART OR AS A WHOLE IS PROHIBITED BY ITAR CATEGORY *"XV SPACECRAFT SYSTEMS AND ASSOCIATED EQUIPMENT"*

UNLESS OTHERWISE SPECIFIED:
DIMENSIONS ARE INCHES
UNLESS SPECIFIED, TOLERANCES:
X.X ± 0.1"
X.XX ± 0.01"
X.XXX ± 0.005"
X.XXXX ± 0.0005"

MATERIAL: Printed Circuit Board
FINISH:
DO NOT SCALE DRAWING

	NAME	DATE
DRAWN	C. Hartsfield	2/28/2018
CHECKED		
ENG APPR.		
MFG APPR.		
Q.A.		

COMMENTS:

Sheet1

TITLE:

SIZE B | DWG. NO. | REV

SCALE: 1:2 | SHEET 1 OF 1

Appendix D. Material Specification Sheets

D.1 Miralon Carbon Nanotube Specification Sheet

Miralon® Sheets/Tape

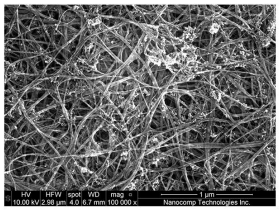

Miralon sheet and tape products are carbon nanotube (CNT) non-woven materials that can be used in a variety of applications to lightweight and enhance product or system performance. They are manufactured via chemical vapor deposition into the final product format, eliminating the need for binders or secondary processing steps.

Potential Applications:

- Honeycomb core structures
- Composites
- EMI & ESD protection
- Environmental protection (corrosion and UV resistance, thermal shielding, etc.)
- Ballistics
- Far infrared heating solutions
- Wire and cable shielding

Using a proprietary seaming process, Miralon sheets and tapes can be delivered in lengths up to 1000'. These products can also be post-processed for specific applications. Miralon sheets can be prepregged with a variety of resin systems or infiltrated with various polymer systems, all with industry standard equipment.

Typical Physical Properties*

Dimensional	Metric		Standard	
Bulk Density	0.3 - 0.5	g/cm^3	0.03	lbs/in^3
Areal Density	10 - 15	g/m^2	0.002	lbs/ft^2
Thickness (typ)	22	µm	0.001	in
Standard Widths	0.64 - 137	cm	0.25 - 54	inches
Porosity	70	%	70	%
Thermal				
Temperature Operating Range	-200 to + 250	°C	-328 to + 482	°F
Max Processing Temperature	350	°C	662	°F
Thermal Conductivity	30	W/m*K		
CTE	$-3x10^{-6}$	m/m-°C		
Electrical				
Surface Resistivity	1.5	(Ω/□)	1.5	(Ω/□)
Specific Conductivity	600	$S*cm^2/g$		
EMI Shielding Effectiveness	40	dB @ 2 GHz	40	dB @ 2 GHz
Temperature Coefficient of Resistivity	$7.40*10^{-7}$	Ω*cm/K		
Mechanical				
Specific Strength	0.07	$GPa/(g/cm^3)$	338	$ksi/(lbs/in^3)$

*Based on a solvent-condensed 10 - 15 gsm sheet. Other areal densities are available.

www.nanocomptech.com

D.2 Dupont RS Polyimide Film Data Sheet

DUPONT™ KAPTON® 200RS100

DESCRIPTION

DuPont™ Kapton® 200RS100 is a two layer polyimide film with an electrically conductive layer on one side and a dielectric insulator on the other side. The temperature is highly customizable based on distance between electrodes and can be designed for temperatures up to 240°C in continuous heating. Kapton® RS has proven performance in applications where a precisely controlled surface resistivity was needed. It provides a durable resistivity, which is only slightly affected by temperature and humidity changes. Kapton® RS film retains all the outstanding inertness, radiation and temperature resistance of other Kapton® polyimide films, which make them ideal for use in extreme environments.

Heating applications requiring thin, light-weight, uniform or high temperature performance would benefit from this all-polyimide conductive film. Given the low thermal mass, this material is a more efficient heater than other systems. The material is not limited by inputs such as current or voltage and can be designed for any output temperature desired. It can also be easily cut into various configurations and will continue to function even if it has been punctured. Due to its polyimide composition, it is resilient to high temperature, thin, and highly flexible.

CHARACTERISTICS

- High Tg
- Conductive side: black matte surface
- Dielectric side: shiny smooth surface
- Durable from -270°C to 240°C
- Thermally durable to 325°C in oxygen-free environments

APPLICATIONS

- Surface Deicing
- Automotive Interior Heating
- Aerospace Temperature Regulation
- Industrial Tube Heating
- Composite Curing
- Wearables
- Consumer Appliances

Table 1 Typical Properties of Kapton® 200RS100 Film

Property	Units	Value	Method, Comments
Key Properties			
Thickness	µm	50	
Surface resistivity	ohms/sq	100	Four-point probe measurement Range 92-104 ohm/square (MD, TD direction)
Surface resistivity – water bath	ohms/sq	+1.8	Immersion 20 hours, hand-dried. Four-point probe measurement.
Additional Properties			
Dielectric strength	V//25µm	>2,500	ASTM D-149 (60Hz, 0.25 inch electrodes, 500V/sec rise)
Tensile strength md/td	MPa	>100	ASTM D-882
Tensile modulus md/td	MPa	>2,750	ASTM D-882
Elongation to break md/td	%	>40	ASTM D-882
Initial tear strength md/td	N	>12	ASTM D-1004
MIT fold endurance md/td	cycles	>35,000	ASTM D-2176
Density	g/cc	1.46	ASTM D-1505
Light transmission		Opaque	
Flammability	rating	94V-0	UL-94
% Water uptake	%	1.9	Immersion 24 hours. % wt loss 30C –>150C

kapton.com

Appendix E. Materials & Equipment List

This study required the use of a variety of equipment/materials. To conduct the experiments that characterized the heating properties of the CNT the following equipment and materials is used:

Table E.1: List of Equipment Used

Infra in in-red (IR) camera (Optotherm, Inc. Infrasight MI320 or similar)
FLIR SC7000 camera and L0106 lens
Computer with IR camera software
Nanocomp Tech Inc. CNT sheets(Multi-walled) 0.038 mm thick
Kapton® MT+ sheets
Pyralux(r) FR 1500 sheet film adhesive
Dupont™ RS100 flexible dielectric material
Ultra-Violet laser cutter (LPKF ProtoLaser U)
Vacuum chamber
MultiPress S (LPKF)
Oven/furnace Megalux (LUF-3550) or similar
Arduino Mega 2560 board
Voltera V-One circuit printer
Voltera supplies: flexible conductive ink and 225 micron dispensing tips
11 gauge aluminum plate (2“x2” squares)
Etched foil heaters (Minco™ HK5369 R101L12A)
Printed Circuit Board (PCB) material
100k Ohm thermistors
Multimeter
Various electrical components (e.g. 20 ga. wire, copper strips, alligator clips, binder clips)

Bibliography

[1] G. Horvath *et al.*, "Battery characterization for CubeSat missions with battery tester application," *Proceedings of the Biennial Baltic Electronics Conference, BEC*, pp. 97–100, 2012.

[2] M. Zahran and A. Atef, "Electrical and thermal properties of NiCd battery for low earth orbit satellite's applications," *WSEAS Transactions on Electronics*, vol. 3, no. 6, pp. 340–348, 2006. [Online]. Available: http://www.scopus.com/inward/record.url?eid=2-s2.0-33751563841{\&}partnerID=tZOtx3y1

[3] BatteryUniversity, "Charging Batteries at High and Low Temperatures Battery University." [Online]. Available: http://batteryuniversity.com/learn/article/charging{_}at{_}high{_}and{_}low{_}temperatures

[4] "FoilHeaterlayer." [Online]. Available: http://cfnewsads.thomasnet.com/images/medium/548/548048.jpg

[5] "FoilRoll - Product HK6907." [Online]. Available: http://catalog.minco.com/catalog3/d/minco/?c=products{\&}cid=3{_}1-polyimide-thermofoil-heaters{\&}id=HK6907

[6] Villinger, "heat_vergleich." [Online]. Available: http://www.villinger.com/index.php?lang=1{\&}hID=4

[7] B. K. Kaushik and M. K. Majumder, "Carbon Nanotube Based VLSI Interconnects: Analysis and Design," *Carbon Nanotube Based VLSI Interconnects*, vol. 1, p. 86, 2014. [Online]. Available: https://books.google.com/books?id=BrkjBQAAQBAJ{\&}pgis=1

[8] D. G. Gilmore *et al.*, "Heaters," *Spacecraft Thermal Control Handbook Volume I : Fundamental Technologies*, pp. 223–245, 2002. [Online]. Available: http://matthewwturner.com/uah/IPT2008{_}summer/baselines/LOWFiles/Thermal/SpacecraftThermalControlHandbook/07.pdf

[9] D. Janas and K. K. Koziol, "Rapid electrothermal response of high-temperature carbon nanotube film heaters," *Carbon*, vol. 59, pp. 457–463, 2013. [Online]. Available: http://dx.doi.org/10.1016/j.carbon.2013.03.039

[10] R. D. Karam, *Satellite Thermal Control for Systems Engineers*, 1998.

[11] J. Meseguer *et al.*, "Heaters," *Spacecraft Thermal Control*, pp. 225–235, 2012. [Online]. Available: http://linkinghub.elsevier.com/retrieve/pii/B9781845699963500137

[12] T. A. Stuart and A. Hande, "HEV battery heating using AC currents," *Journal of Power Sources*, vol. 129, no. 2, pp. 368–378, 2004.

[13] M. Israel, "How do Satellites survive Hot and Cold Orbit Environments ?" pp. 1–5, 2017.

[14] Dupont, "Dupont Kapton 200RS100." [Online]. Available: http://www.dupont.com/content/dam/dupont/products-and-services/membranes-and-films/polyimde-films/documents/DEC-Kapton-RS-data-sheet.pdf

[15] Nanocomp Technologies Inc, "Miralon_Sheets_Tape.pd.pdf," 2016.

[16] C. Singh *et al.*, "Production of controlled architectures of aligned carbon nanotubes by an injection chemical vapour deposition method," *Carbon*, vol. 41, no. 2, pp. 359–368, 2003.

[17] M. LaSaint, "Creep Properties of Carbon Nanotube Sheets," Ph.D. dissertation, Air Force Institute of Technology, 2017.

[18] A. M. Marconnet *et al.*, "Thermal conduction phenomena in carbon nanotubes and related nanostructured materials," *Reviews of Modern Physics*, vol. 85, no. 3, pp. 1295–1326, 2013. [Online]. Available: https://nanoheat.stanford.edu/sites/default/files/publications/RevModPhysMarconnetetal..pdf

[19] K. H. Baloch *et al.*, "Remote Joule heating by a carbon nanotube," *Nature Nanotechnology*, vol. 7, no. 5, pp. 316–319, 2012. [Online]. Available: http://dx.doi.org/10.1038/nnano.2012.39

REPORT DOCUMENTATION PAGE

Form Approved
OMB No. 0704–0188

1. REPORT DATE *(DD–MM–YYYY)*	2. REPORT TYPE	3. DATES COVERED *(From — To)*
22-03-2018	Master's Thesis	Sep 2016 - Mar 2018

4. TITLE AND SUBTITLE

THE STUDY AND APPLICATION OF CARBON NANOTUBE FILM HEATERS FOR SPACE APPLICATIONS

5a. CONTRACT NUMBER

5b. GRANT NUMBER

5c. PROGRAM ELEMENT NUMBER

6. AUTHOR(S)

Captain Chris Rocker

5d. PROJECT NUMBER

5e. TASK NUMBER

5f. WORK UNIT NUMBER

7. PERFORMING ORGANIZATION NAME(S) AND ADDRESS(ES)

Air Force Institute of Technology
Graduate School of Engineering and Management (AFIT/EN)
2950 Hobson Way
WPAFB OH 45433-7765

8. PERFORMING ORGANIZATION REPORT NUMBER

AFIT-ENY-MS-18-M-290

9. SPONSORING / MONITORING AGENCY NAME(S) AND ADDRESS(ES)

10. SPONSOR/MONITOR'S ACRONYM(S)

11. SPONSOR/MONITOR'S REPORT NUMBER(S)

12. DISTRIBUTION / AVAILABILITY STATEMENT

DISTRIBUTION STATEMENT A:
APPROVED FOR PUBLIC RELEASE; DISTRIBUTION UNLIMITED.

13. SUPPLEMENTARY NOTES

14. ABSTRACT

"The purpose of this research was to examine the feasibility of using Carbon Nanotube (CNT) sheets as thin film heaters for space applications. Battery heaters are the focus of this research. CNT sheets have many beneficial properties and show potential in replacing the etched foil heater currently being used. In this study test specimens were created by forming laminate test articles comprised of CNT sheets and an adhesive Kapton substrate material. These test articles were subjected to a series of tests both in atmosphere and in vacuum. It was found that while the CNT articles were not as power efficient as the etched foil design, in the configurations tested, they offered a much higher maximum temperature with the available on-board power, a faster response time, and mitigated the potential for total heater failure. In conclusion, CNT thin film heaters proved to be a viable alternative to current battery heater technology."

15. SUBJECT TERMS

16. SECURITY CLASSIFICATION OF:			17. LIMITATION OF ABSTRACT	18. NUMBER OF PAGES	19a. NAME OF RESPONSIBLE PERSON
a. REPORT	b. ABSTRACT	c. THIS PAGE			Maj Ryan O'Hara, AFIT/ENY
U	U	U	UU	175	19b. TELEPHONE NUMBER *(include area code)* (937) 255-3636, x4542; ryan.ohara@afit.edu